Vol, 58 JUNE, 1954 No. 6

THE JOURNAL OF PHYSICAL CHEMISTRY

(Registered in U. S. Patent Office)

THE JOURNAL OF PHYSICAL CHEMISTRY

(Registered in U. S. Patent Office)

Published monthly by the American Chemical Society at 20th and Northampton Sts., Easton, Pa.

Entered as second-class matter at the Post Office at Easton, Pennsylvania.

The *Journal of Physical Chemistry* is devoted to the publication of selected symposia in the broad field of physical chemistry and to other contributed papers.

Manuscripts originating in the British Isles, Europe and Africa should be sent to F. C. Tompkins, The Faraday Society, 6 Gray's Inn Square, London W. C. 1, England.

Manuscripts originating elsewhere should be sent to W. Albert Noyes, Jr., Department of Chemistry, University of Rochester, Rochester 3, N. Y.

Correspondence regarding accepted copy, proofs and reprints should be directed to Assistant Editor, Allen D. Bliss, Department of Chemistry, Simmons College, 300 The Fenway, Boston 15, Mass.

Business Office: American Chemical Society, 1155 Sixteenth St. N. W., Washington 6, D. C.

Advertising Office: American Chemical Society, 332 West 42nd St., New York 36, N. Y.

Articles must be submitted in duplicate, typed and double spaced. They should have at the beginning a brief Abstract, in no case exceeding 300 words. Original drawings should accompany the manuscript. Lettering at the sides of graphs (black on white or blue) may be pencilled in, and will be typeset. Figures and tables should be held to a minimum consistent with adequate presentation of information. Photographs will not be printed on glossy paper except by special arrangement. All footnotes and references to the literature should be numbered consecutively and placed on the manuscript at the proper places. Initials of authors referred to in citations should be given. Nomenclature should conform to that used in *Chemical Abstracts*, mathematical characters marked for italic, Greek letters carefully made or annotated, and subscripts and superscripts clearly shown. Articles should be written as briefly as possible consistent with clarity, and should avoid historical background unnecessary for specialists.

Symposium papers should be sent in all cases to Secretaries of Divisions sponsoring the symposium, who will be responsible for their transmittal to the Editor. The Secretary of the Division by agreement with the Editor will specify a time after which symposium papers cannot be accepted. The Editor reserves the right to refuse to publish symposium articles, for valid scientific reasons. Each symposium paper may not exceed four printed pages (about sixteen double spaced typewritten pages) in length except by prior arrangement with the Editor.

Remittances and orders for subscriptions and for single copies, notices of changes of address and new professional connections, and claims for missing numbers should be sent to the American Chemical Society, 1155 Sixteenth St., N. W., Washington 6, D. C. Changes of address for the *Journal of Physical Chemistry* must be received on or before the 30th of the preceding month.

Claims for missing numbers will not be allowed (1) if received more than sixty days from date of issue (because of delivery hazards, no claims can be honored from subscribers in Central Europe, Asia, or Pacific Islands other than Hawaii), (2) if loss was due to failure of notice of change of address to be received before the date specified in the preceding paragraph, or (3) if the reason for the claim is "missing from files."

Subscription Rates: to members of the American Chemical Society, $8.00 for 1 year, $15.00 for 2 years, $22.00 for 3 years; to nonmembers, $10.00 for 1 year, $18.00 for 2 years, $26.00 for 3 years. Postage free to countries in the Pan American Union; Canada, $0.40; all other countries, $1.20. Single copies, $1.25; foreign postage, $0.15; Canadian postage $0.05. Back issue rates (starting with Vol. 56): nonmember, $1.50 per issue, foreign postage $0.15, Canadian postage $0.05; $12.50 per volume, foreign postage $1.20, Canadian postage $0.40; special rates for A.C.S. members supplied on request.

The American Chemical Society and the Editors of the *Journal of Physical Chemistry* assume no responsibility for the statements and opinions advanced by contributors to This Journal.

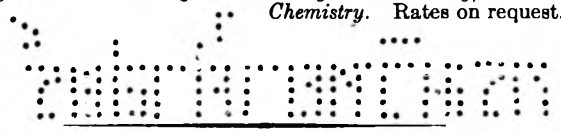

THE JOURNAL OF
PHYSICAL CHEMISTRY

(Registered in U. S. Patent Office) (Copyright, 1954, by the American Chemical Society)

VOLUME 58 JUNE 22, 1954 NUMBER 6

THE ADSORPTION OF *n*-NONADECANOIC ACID ON METAL SURFACES

BY HILTON A. SMITH AND KENNETH A. ALLEN

Contribution No. 126 from the Department of Chemistry, University of Tennessee, Knoxville, Tenn.

Received October 26, 1953

The adsorption of *n*-nonadecanoic acid from cyclohexane solutions on copper, nickel, iron and aluminum has been measured under various conditions of concentration and surface state of the metals. The amounts adsorbed on surfaces known to be coated with oxide increased indefinitely with time of exposure to the solutions. On surfaces prepared directly under the solutions in such a manner that initial freedom from oxide contamination was assured, the number of adsorbed molecules per unit area rapidly attained a certain maximum value which did not increase thereafter. This value was dependent on the metal substrate, decreasing in the order copper, nickel, iron and aluminum, with some doubt as to the relative positions of the last two metals. Both types of adsorbed layer were removed by cyclohexane at room temperature.

In much of the previous work on the adsorption of organic compounds on metals it has been realized that the surfaces were contaminated with oxide. Greenhill,[1] working with metal powders, found that the adsorption of stearic acid was increased when the powders had been treated with hydrogen at elevated temperatures. Daniel[2] concluded that this difference was sufficiently small that results obtained on the untreated metals could be considered reliable. The adsorption of palmitic acid on Raney nickel was interpreted by Smith and Fuzek[3] as indicating irreversible chemisorption, and the amounts adsorbed were related to the surface areas of the catalyst powders. Raney nickel is subjected to violent chemical treatment in its preparation, however, and it is doubtful that its surface corresponds to that of the pure metal. Beischer[4] deposited radioactive monolayers of stearic acid onto metal plates from a Langmuir trough, and found that the extent of subsequent chemical reaction between the acid and a copper sample was strongly dependent on the thickness of the oxide film.

In the present work the problem of oxide contamination was met by machining fresh surfaces on bulk samples of the metals. An early example of the use of such an approach was Millikan's "machine shop in a vacuum."[5] There was the possibility that traces of metal from the cutting tool might lead to errors. It has been shown by Shaw,[6] however, that in most machining processes the edge of the tool becomes faced with a layer of the metal being cut; contamination from this source could therefore be neglected.

The adsorption characteristics of fatty acids in the chain length range of from sixteen to twenty-two carbon atoms are very similar.[3,7] For the present study *n*-nonadecanoic acid was chosen as a typical representative of this group, and for analytical purposes the sample used was "tagged" with carbon fourteen at the carboxyl position. Cyclohexane was preferable to benzene as a solvent because of the well known lower solubility of oxygen in saturated hydrocarbons; it was also desirably volatile, inert and easily purified. For practical reasons these reagents were adhered to throughout the work.

Experimental

Materials.—Eastman White Label cyclohexane was passed through a bed of 100 mesh activated alumina. The freedom of the resulting solvent from polar impurities was checked periodically by the drop test.[8] For the preparation of the tagged acid a sample of octadecyl bromide was vacuum distilled, the fraction boiling from 174.4 to 174.8° at 1.35 mm. being collected for the Grignard reaction. The details of this synthesis are described elsewhere.[9] Radioactive barium carbonate obtained from the Atomic Energy Commission was diluted with J. T. Baker C.P. normal

(1) E. B. Greenhill, *Trans. Faraday Soc.*, **45**, 625 (1949).
(2) S. G. Daniel, *ibid.*, **47**, 1347 (1951).
(3) H. A. Smith and J. F. Fuzek, *J. Am. Chem. Soc.*, **68**, 229 (1946).
(4) D. E. Beischer, THIS JOURNAL, **57**, 134 (1953).
(5) R. A. Millikan, *Phys. Rev.*, **7**, 361 (1916).
(6) M. C. Shaw, *J. Appl. Phys.*, **18**, 683 (1947).
(7) I. Langmuir, *J. Am. Chem. Soc.*, **39**, 1848 (1917); W. C. Bigelow, D. L. Pickett and W. A. Zisman, *J. Colloid Sci.*, **1**, 513 (1946); W. C. Bigelow, E. Glass and W. A. Zisman, *ibid.*, **2**, 563 (1947).
(8) W. A. Zisman, *J. Chem. Phys.*, **9**, 534, 729 (1941).
(9) W. G. Dauben, J. C. Reid and P. E. Yankwich, *Anal. Chem.*, **19**, 828 (1947).

material to a final tagging of 1.44 atomic per cent. carbon fourteen. The recrystallized nonadecanoic acid melted at 67.2–68.2°, in fair agreement with the published value, 68.65°.[10] The metal samples were in the form of cylinders 1.5″ in diameter. The nickel was kindly donated by the International Nickel Co., Inc. The copper, aluminum and iron were samples of commercially available metals, the aluminum actually being a machinable magnesium alloy, and the iron, 1020 steel.[11]

Apparatus.—A standard metal-turning lathe bed was adapted to cut fresh surfaces on the metals. Cuts were made on the horizontal face of a sample, the cylinder axis being vertical in the holder, thus giving a machined surface of 11.5 cm.^{2} apparent area. The cylinders were provided with tapered brass rings on which cups could be fitted for machining under the solutions. An end window G. M. tube of window thickness 1.7 mg./cm.^{2} was used for counting the surfaces. This tube was provided with an aluminum shield which had a circular hole 5 cm.^{2} in area machined in its center. Thus, in order to obtain the maximum geometry consistent with the system under study, the metal surfaces could be pressed directly against the shield for counting, without touching the tube itself. Constant tension for this purpose was provided by a sponge rubber pad under the sample holders. Adsorptions with air exposure were carried out in magnetically stirred glass cups. Desorptions were run in similar cups provided with inlets and outlets for the circulation of freshly distilled cyclohexane.

Analyses.—A stock solution of the radioactive acid in cyclohexane was prepared by weighing an original quantity of the recrystallized product on a semi-microbalance. Standard solutions A and 8A, containing 2.63 and 21.04 mg., respectively, of total nonadecanoic acid per liter were made by diluting the stock. These solutions were standardized with respect to the metal samples by pipetting small amounts, usually 0.5 ml., directly onto a freshly cut surface whose background had already been determined. This operation was greatly facilitated by the fortunate circumstance that the sharp edges around the periphery of the metals effectively prevented liquid flow from the surfaces. The latter were covered and allowed to remain wet for about an hour, whereupon evaporation of the liquid generally left a surface free from visible inhomogeneities. It is felt that most of the acid in these standardization runs was actually adsorbed onto the metals in this process, in a manner entirely analogous to that found later for adsorption from the solutions. The standardization counts, background counts and adsorption measurements were all made under identical conditions of geometry.

Each flask for use with a given solution was previously equilibrated for at least one week, with frequent shaking, with a solution of *n*-nonadecanoic acid of the same strength. Similar treatment was accorded all other vessels used in this work, including both types of adsorption cups, all pipets, and other glassware with which the solutions were required to make contact.

Procedures.—For adsorption on an oxide-coated surface, a metal was simply machined in air, counted for background, and placed in contact with the required solution contained in an adsorption cup equipped with a magnetic stirrer. After a given time the metal was removed, tilted against the edge of the cup, and allowed to drain. A small amount of solution was always left to evaporate and, since this would lead to a high result, an estimate of this error was made by counting the acid deposited on a fresh surface during drainage after a rapid dip into a non-stirred solution. It was realized that a certain amount of adsorption could occur during the dips made for determination of drainage counts. By comparing surfaces wetted from a pipet with those lifted from the adsorption cups, it was estimated that the quantity of liquid which evaporated from the surfaces was approximately 0.04 ml. This quantity was known to contain the same amount of acid as the amount calculated from drainage counts. Furthermore, preliminary rate studies showed conclusively that in the time of a rapid dip, adsorption as such could occur only to a negligible extent.

The drainage counts, together with the background count, were subtracted from the total adsorption counts. A typical correction for both drainage count and background was 120 counts per minute. The usual results when studying adsorption showed 400–1000 c./min. with minimum and maximum values of 200 and 1500 c./min. Even with a value as low as 200 c./min., standard methods for computing errors in such counts showed that the 90% error (Reliable Error) in net adsorption was only ±10%.

An average time of one hour elapsed between machining and placing of the sample in the adsorption cups. At room temperature and atmospheric pressure a copper surface freshly exposed to the air forms an oxide layer 15 Å. thick in 30 minutes, and the other metals used behave similarly.[12]

Adsorption on surfaces initially free from oxide was studied by machining the metals under a layer of radioactive solution in the brass cups previously described. For some of these runs the solutions were flushed with argon and boiled vigorously immediately before use. After machining, the cups were covered and the sample holders placed on a shaker for a given time interval. All runs were made at room temperature, which varied from 25 to 30°.

For desorption the samples were dipped into the continuous extraction cups described above until no further decrease in the count could be obtained from longer immersion. Overnight washing was both convenient and sufficient for this purpose.

Results and Discussion

The standardizations indicated a linear relationship between counts per minute and molecules per unit of apparent area up to 18.6 molecules per 100 Å.^{2}. This is in agreement with the results of other work of a related nature,[4] in which it was found that self-adsorption was negligible for as many as nine monolayers of a tagged fatty acid on a metal surface. A backscattering correction was necessary for aluminum; however, this amounted to 15%, based on the factor calculated for iron, copper and nickel. The atomic numbers of the latter three metals are closely spaced, and differences in their standardization counts outside the range of statistical counting errors were neither expected nor found. The magnitude of the correction for aluminum is in agreement with that found by others[13] for various beta radiations. A statistical analysis of the standardization data indicated that the factors relating counts per minute with molecules per unit area could be reproduced to within ±5% by similar sets of data, nine times out of ten. This was considered sufficient precision for the present work, especially in view of the severe limitations on accuracy in the adsorption runs imposed by fluctuations in the drainage counts. The predominant cause of the latter error was uncontrollable local air currents, and its magnitude was such that for some of the low counts an unreliability of as much as 20% was introduced.

In Table I are listed the results obtained on machining the metals under solution A (2.63 mg. nonadecanoic acid per liter). For each of the values shown the sample was re-machined under a fresh batch of solution and allowed to equilibrate for the entire period of time given. The solutions were not boiled for these runs. It may be tenta-

(10) F. Francis and S. H. Piper, *J. Am. Chem. Soc.*, **61**, 577 (1939).

(11) Spectrographic analyses of these metals showed the following detectable percentages of impurities. Aluminum: Cr, 0.2; Cu, 0.04; Fe, 0.2; Mg, 2.0; Si, 0.6; Ti, 0.04. Copper: Hg, 0.04; Cr, 0.04; Fe, 0.04. Iron: Cr, 0.04; Cu, 0.08; Mn, 0.6; Ni, 0.1; Si, 0.2. Nickel: Cr, 0.3; Cu, 0.08; Fe, 0.04; Mg, 0.02; Mn, 0.1.

(12) G. Hess, *Z. anorg. Chem.*, **254**, 96 (1947); E. A. Gulbransen, *Ind. Eng. Chem.*, **41**, 1385 (1949); J. A. Allen, *Trans. Faraday Soc.*, **48**, 273 (1952); R. M. Dell, F. S. Stone and P. F. Tiley, *ibid.*, **49**, 195 (1953); F. Todt, R. Freier and W. Schwarz, *Z. Elektrochem.*, **53**, 132 (1949).

(13) D. Christian, W. W. Dunning and D. S. Martin, *Nucleonics*, **10**, No. 5, 41 (1952); B. P. Burtt, *ibid.*, **5**, No. 2, 28 (1949); D. E. Beischer, *Science*, **112**, 535 (1950).

TABLE I

RESULTS OF MACHINING UNDER SOLUTION A
(ADS. IN MOLECULES PER 100 Å.²)

Metal	Time, min.	Ads.	Metal	Time, min.	Ads.
Cu	15	4.11	Ni	20	2.64
	20	4.20		60	2.99
	45	4.56		150	3.16
	120	3.98		20 hr.	3.02
	120	4.42			
	24 hr.	4.11		av.	2.95
	24 hr.	4.45			
	av.	4.26			
Fe	20	1.63	Al	20	2.28
	30	1.80		60	2.11
	120	1.80		150	2.18
	120	1.92		24 hr.	1.87
	20 hr.	1.69			
				av.	2.11
	av.	1.77			

tively concluded that the amounts adsorbed do not tend to increase after the rapid attainment of a certain initial value, and that this value depends on the metal substrate. It is also apparent that in no case did the number of molecules per unit apparent area reach the accepted value for a monolayer (one acid molecule per 20.5 Å.²), with the possible exception of copper, even on the assumption of a roughness factor of unity.

Preliminary rate studies with the metals machined in air indicated a gradual increase in the amounts adsorbed after the completion of the rapid initial process. A more extensive series of runs with the more concentrated solution (8A, 21.04 mg./l.) was undertaken with the expectation that

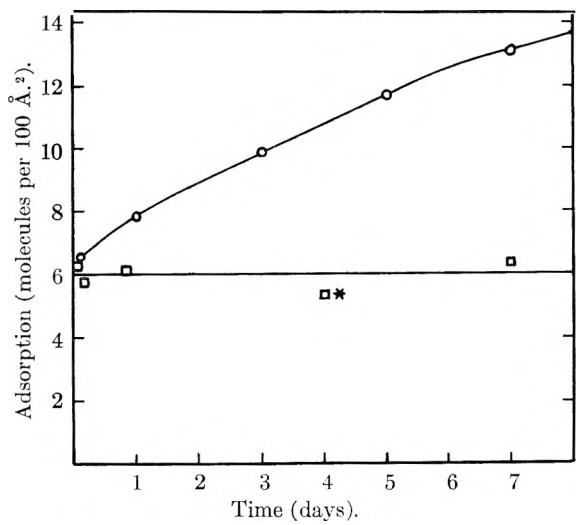

Fig. 1.—Adsorption of *n*-nonadecanoic acid by copper with (—○—) and without (--□—) an initial oxide layer.

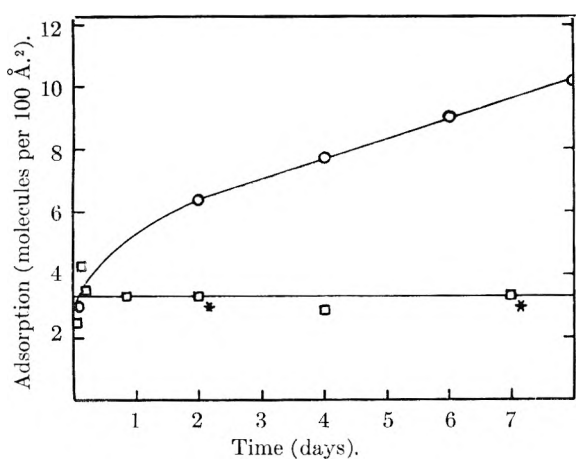

Fig. 2.—Adsorption of *n*-nonadecanoic acid by nickel with (—○—) and without (—□—) an initial oxide layer.

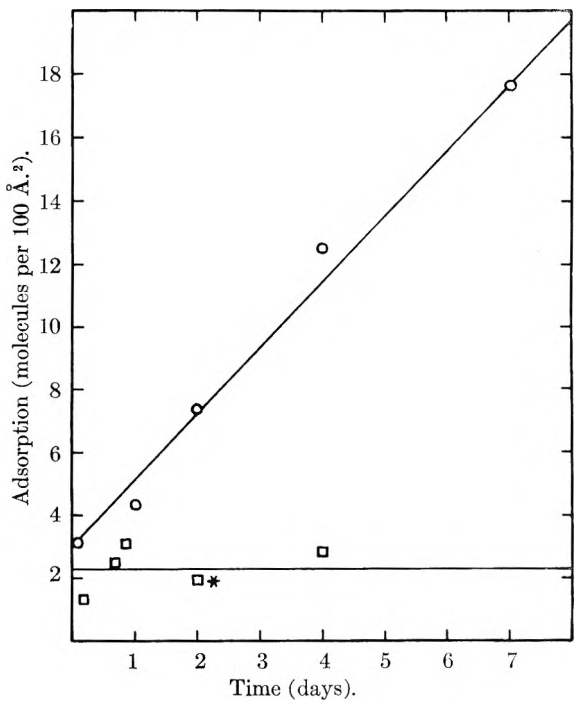

Fig. 3.—Adsorption of *n*-nonadecanoic acid by aluminum with (—○—) and without (—□—) an initial oxide layer.

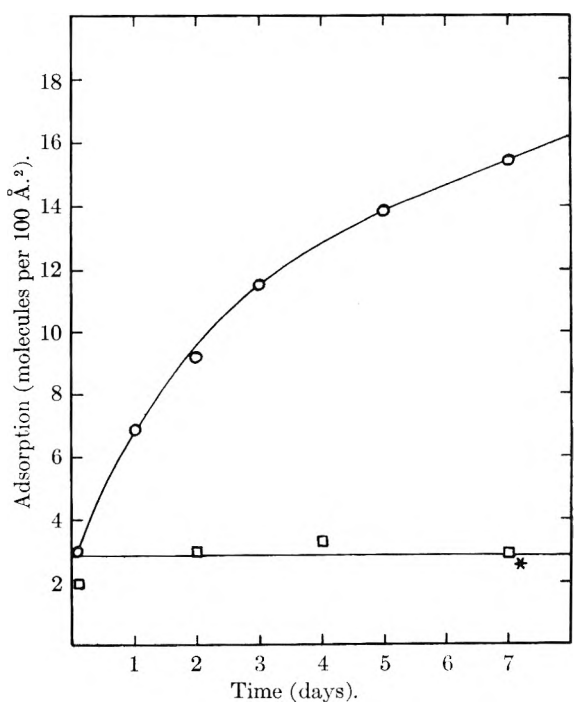

Fig. 4.—Adsorption of *n*-nonadecanoic acid by iron with (—○—) and without (—□—) an initial oxide layer.

this effect might become more pronounced. Figures 1–4 show that such was indeed the case. The points marked with circles on the rising curves were obtained by the described method, the metals simply being removed from the adsorption cups for periodic counting. For each of the square points a new surface was prepared under the solution as before, and in this series each fresh batch of solution was flushed with argon and boiled just before use, except at the points marked with an asterisk. The latter are in satisfactory accord with the other values, and it is to be remembered that for the results shown in Table I no attempt was made to remove dissolved gases from the solution. Also, even when the solution was boiled it was not feasible to maintain an inert atmosphere over the liquid surface during the machining process and the subsequent lengthy equilibrations, and it is therefore to be expected that the solutions soon became resaturated with atmospheric gases. It must be concluded that the latter played no very important part in the process leading to the observed effects.

The surfaces from several of these runs were subjected to desorption, and with a few exceptions essentially all of the adsorbed layer was removed. There were no differences from this standpoint either among the metals or with respect to their previous treatment. The exceptions noted were erratic, and the conditions leading to them were not reproducible. Even in these cases, however, the greater portion of the layer was desorbed; in no instance did the amount of tightly bound acid exceed a fraction of one molecule per 100 Å.^{2} of apparent area.

The increasing amounts "adsorbed" on the oxide-coated surfaces indicate the possibility of chemical reaction between the acid and the metal oxide. Such increases have been observed by others[1,2] in the case of copper powder. The values attained at the termination of these runs are such as to preclude the possibility of the gradual buildup of a monolayer, since this would require roughness factors much higher than indicated by oleophobic layers.

Oleophobic layers are considered to require close packed orientation.[14] Attempts to form oleophobic layers from hexadecane solution of the radioactive acid on these machined surfaces met with only partial success. The films would form on portions of the surface, but did not cover the entire area necessary for counting. A technique of forming the partial films, removing excess solution from the remainder of the metal surface by blotting with filter paper and determining the number of molecules on the surface by the counting method indicated a roughness factor for all metal surfaces of the order of one on the basis of one acid molecule per 20.5 Å.^{2}. A complete oleophobic layer was formed on a brass surface machined in the same manner, and the resulting counts again indicated a roughness factor close to unity. It is doubtful that the present surfaces are actually as smooth as this, however; the cutting tool was ground on an ordinary hone and might be expected to leave a surface similar to that obtained on grinding the metal itself. Profilometer tracings recorded by Abbott[15] indicate that the profile of a ground steel surface can be roughly approximated by a row of low triangles, which would lead to a roughness factor somewhat greater than unity. It is probable that the appropriate factor for the present surfaces is also somewhat greater than unity. The machining process was the same for all of the metals used; there were no visible differences in the surfaces, nor did the experiments with oleophobic layers indicate any variation.

The averages of the equilibrium values obtained on machining the copper, nickel, aluminum and iron under solution 8A are, respectively, 6.0, 3.3, 2.3 and 2.8 molecules per 100 Å.^{2} of apparent area. Comparison with the averages in Table I shows that an eightfold increase in the concentration of the solution resulted in only a small increase in the amounts adsorbed, and a reversal in the effect noted for iron and aluminum. It is probable that these two metals have an approximately equal affinity for the acid. On the basis of 20.5 Å.^{2} for the cross-section of the adsorbed acid molecule, copper is the only molecule which could be covered with a monolayer, and it would have a roughness factor of at least 1.2. It is apparent, however, that the molecular population on the other metal surfaces is much too sparse for the assumption of close packed orientation, and since there is no reason for assuming a different mechanism in the case of copper, it may be that close packing did not occur on this metal either. It is of interest to note that the affinities of the metal surfaces for the adsorption of the nonadecanoic acid is parallel to the stability of the complexes formed by their ions, which decreases in the same order, *i.e.*, copper, nickel, iron and aluminum.[16] It can be postulated that in the violent disruption of intermetallic bonds engendered by the machining process, valences exposed at certain locations are capable of forming hydrogen bonds with the carboxyl groups. Such bonds are typical of metal chelate compounds.

One could assume that each of the machined surfaces was covered with a complete film of adsorbed fatty acid molecules, and that the differences in the amounts adsorbed were due to variations in roughness. Since the minimum roughness factor is unity, one can calculate from the data found for adsorption by aluminum (2.1 molecules per 100 Å.^{2} of apparent area using solution A and 2.3 using solution 8A) that the effective area of the adsorbed fatty acid must be about 45 Å.^{2} on this basis. There does not appear to be any independent experimental basis for such a figure, although Zisman and co-workers did find an approximate value of 31 Å.^{2} for the adsorption of a long chain amine on platinum.

Acknowledgment.—The authors are grateful to the Office of Ordnance Research, United States Army, for the sponsorship of this research.

(14) W. C. Bigelow, D. L. Pickett and W. A. Zisman, *J. Colloid Sci.*, **1**, 513 (1946).

(15) E. J. Abbott, "The Tracer Method of Measuring Surface Irregularities," in "Surface Treatment of Metals," American Society for Metals, Cleveland, Ohio, 1941, pp. 392–411.

(16) A. E. Martell and M. Calvin, "Chemistry of the Metal Chelate Compounds," Prentice-Hall, Inc., New York, N. Y., 1952, p. 184.

THE SOLUBILITY OF AMORPHOUS SILICA IN WATER

BY G. B. ALEXANDER, W. M. HESTON AND R. K. ILER

Grasselli Chemicals Department, Experimental Station, E. I. du Pont de Nemours and Company, Inc., Wilmington, Delaware

Received November 9, 1953

The solubility of amorphous silica in water at 25° is shown to involve an equilibrium between the solid phase and a monomeric form of silica in solution, presumably $Si(OH)_4$. The same solubility (0.01 to 0.012%) was found using a suspension of finely divided amorphous silica powder and sols of colloidal particles of silica. The increase in total dissolved silica above *p*H 8 is shown to be due to the presence of $[H_3SiO_4]$ ion in addition to $Si(OH)_4$ in solution. The concentration of $Si(OH)_4$ in equilibrium with the solid phase apparently is not affected by *p*H.

Introduction.—Numerous studies of the solubility of silica in water have been reported[1-7] (Fig. 1) but it was not clear in most cases whether solubility-equilibrium was actually established. Also it was not determined whether the silica in apparent solution was present as monosilicic acid, polysilicic acid or colloidal silica particles. It is the purpose of this investigation to clarify these points.

In order to ensure that equilibrium was reached, we have approached the true value of the solubility at 25° from the unsaturated state by starting with suspensions of colloidal particles of amorphous silica in water, and from the supersaturated condition by starting with soluble silicic acid of low molecular weight, letting it polymerize to the colloidal state. In order to determine whether the silica in solution is monomeric or polymeric, we have employed a modification of previously described methods involving the formation of silicomolybic acid.[8-11] By this method it is possible to measure the concentration of monosilicic acid in the presence of other forms of silica, since the monomer reacts with molybdic acid very rapidly; polysilicic acids react more slowly and colloidal forms of silica scarcely at all. Monosilicic acid is known to result from the dissolution of silica gel[12] and in solution has been shown to be a hydrated form of SiO_2,[13] presumably $Si(OH)_4$. The solubility has already been shown to increase above *p*H 9.[14] It was another objective of our investigation to explain this behavior.

It is well known that amorphous silica is more soluble than crystalline silica (quartz) but it has not been demonstrated that the different forms of amorphous silica such as finely divided powder, wet silica gel and colloidal particles in the form of a sol, are soluble to the same extent. Accordingly, these different forms of silica were employed in this study. The fact that we find the solubilities of these different forms to be the same, indicates that the fundamental structure of amorphous silica in these various forms is identical. This agrees with the conclusions reached by other investigators,[15-18] who employed X-ray and electron diffraction methods. Morey[19] concluded that if there are any "crystals" in amorphous silica glass, they must be scarcely larger than one unit cell of cristobalite. The same appears to be true for silica sol and gel particles prepared in aqueous solutions. Morey points out that since a crystal is, by definition, a regular repetition of unit cells, it is artificial to call materials

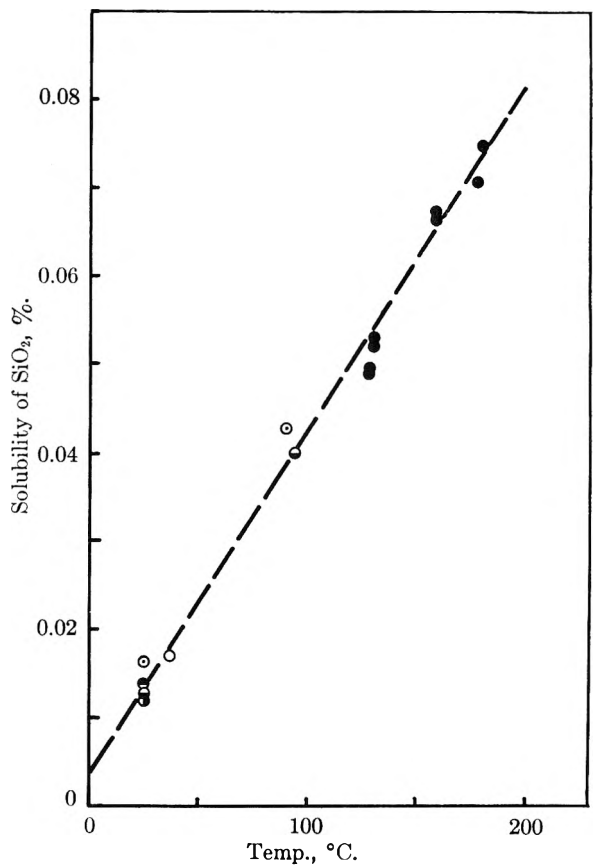

Fig. 1.—Solubility of amorphous silica: ◓, Struckman[2]; ◒, Gardner[5]; ◐, Spychalski[6]; ●, Hitchen[3]; ⊙, Lenher and Merrill[4]; ○, Jephcott and Johnson.[7]

(1) *FIAT Rev. Ger. Sci.*, Part 1, 265 (1939-1946 (Pub. 1948)).
(2) C. Struckman, *Liebigs Ann. Chem.*, **94**, 341 (1855).
(3) C. S. Hitchen, *Inst. of Mining and Met.*, 255 (1935).
(4) V. Lenher and H. B. Merrill, *J. Am. Chem. Soc.*, **39**, 2630 (1917).
(5) L. U. Gardner, Amer. Inst. of Metallurgical and Mining Engineers, Technical Publication No. 929, p. 7.
(6) R. Spychalski, *A. anorg. allgem. Chem.*, **239**, 317 (1938).
(7) C. M. Jephcott and J. H. Johnston, *Arch. Ind. Hyg. and Occupational Med.*, **1**, 323 (1950).
(8) F. Dienert and F. Wandenbulcke, *Compt. rend.*, **176**, 146 (1923).
(9) R. W. Harmon, THIS JOURNAL, **31**, 616 (1927).
(10) T. Okwia, *J. Chem. Soc. Japan, Pure Chem. Sect.*, **72**, 927 (1951); *C. A.*, **46**, 6995 (1952).
(11) E. Weitz, H. Franck and M. Schuchard, *Chem. Ztg.*, **74**, 256 (1950).
(12) G. Jander and K. F. Jahr, *Kolloid-Beih.*, **41**, 48-57 (1934).
(13) H. and W. Brintzinger, *Z. anorg. allgem. Chem.*, **196**, 44 (1931).
(14) G. Jander and W. Heukeshoven, *ibid.*, **201**, 301 (1931).
(15) O. E. Radczewski and H. Richter, *Kolloid Z.*, **96**, 1 (1941).
(16) L. Krejci and E. Ott, THIS JOURNAL, **35**, 2031 (1931).
(17) J. T. Randall, H. P. Rooksby and B. S. Cooper, *J. Soc. Glass Technol.*, **15**, 54 (1931).
(18) B. E. Warren, *J. Appl. Phys.*, **8**, 645 (1937); *Z. Krist.*, **86**, 349 (1933).
(19) G. W. Morey, "The Properties of Glass," A.C.S. Monograph Series No. 77, Reinhold Publishing Corp., New York, N. Y., 1938.

"crystalline" in which crystals are only one unit cell in size.

Experimental

The following experimental work was designed to determine the solubility of amorphous silica in the forms of (A) fine powder, (B) colloidal solution, and (C) freshly prepared silica gel, and to elucidate the nature of the soluble silica in acidic, neutral and basic aqueous solutions. It will be noted that the silica structures used in this study had very small particles (high surface area); this factor has been shown to be important if equilibrium conditions are to be achieved in a reasonable period of time.

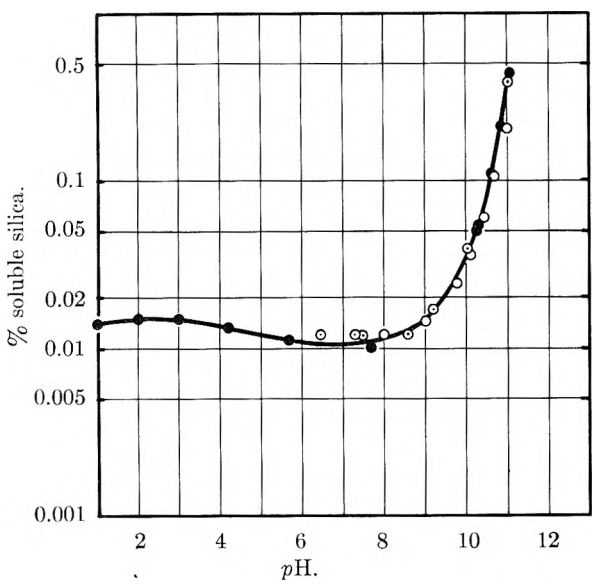

Fig. 2.—Solubility of silica in water: ⊙, sols by removal of Na^+ from sodium silicate solution; ●, suspensions of "Silica A," *p*H adjusted with HCl or NaOH; O, calculated from equation 1.

Method of Determining Soluble Silica.—It has been verified recently[20] that the observation of Weitz, Franck and Schuchard[11] is valid: monomeric silicic acid reacts very quickly with molybdic acid, while polysilicic acids react more slowly. Under the reaction conditions which were adopted for this study, at least 98% of the monosilicic acid in a solution reacts with molybdic acid within two minutes.[20]

The molybdate reagent is prepared as follows: 100 g. of $(NH_4)_6Mo_7O_{24}\cdot 4H_2O$ (J. T. Baker) is dissolved in distilled water and is diluted to one liter. Just prior to use, 40 ml. of this reagent is added to 860 ml. of distilled water and 100 ml. of 1 *N* sulfuric acid. This strength molybdate reagent is mixed with enough sample to result in a maximum soluble silica concentration of about one milligram per 50 ml. in the color developing solution. A Beckman Model DU photoelectric quartz spectrophotometer with a thermostatically controlled cell (25°) is used to follow the increase in optical density of the sample due to the formation of the yellow silicomolybdic acid complex. The optical density is measured at a wave length of 400 mμ with a slit width of 0.04 μ. Under these conditions, one milligram of silica per 50 ml. of solution produces an optical density of 0.720. As soon as the silica sample is mixed with the molybdate reagent, the color reading is noted at ½-minute intervals until a constant value is obtained.

(A) Solubility of Silica Powder.—As a typical silica powder, an amorphous silica, "Silica A," produced by combustion of silane vapors, was employed. This material contained 99.9% silicon dioxide and had a specific surface area of 240 square meters per gram. This material was suspended in boiled, freshly distilled water which had been previously adjusted to *p*H 5.6 with a trace of HCl, and kept in waxed bottles. Concentrations of the powder in suspension ranged from 0.03 to 1.0% by weight. Different concentrations of the suspensions from 0.03 to 1% SiO_2 were made to check the effect of the amount of silica in suspension on the equilibrium solubility. The concentration of soluble silica in the supernatant liquid in these suspensions was determined after 20, 39 and 62 days, and found to increase and become essentially constant after 20 days providing at least 0.3% SiO_2 was present in the suspension. The equilibrium solubility proved to be 0.014% SiO_2 in solution as monomeric silica.

The solubility of this silica was relatively independent of the amount of solid silica in the suspension, except when less than 0.1% silica powder is present in the dispersion.

In another set of experiments, the solubility of "Silica A" in water was measured at various *p*H values from 1 to 10.2. The *p*H was adjusted with HCl or NaOH, and 1% by weight of the silica powder was suspended in the water. The amount of silica in solution was determined after three weeks and six months at 25°. The final solubilities at different *p*H values are included in Fig. 2.

The color reaction of the soluble silica with molybdic acid was complete within two minutes at 25°, indicating that the soluble silica was monomeric.

Another series of suspensions of "Silica A" was aged for six months in more alkaline solutions. The results shown in Table I indicate that above about *p*H 10.6, the solution contains not only monosilicic acid but low molecular weight polymerized silica, presumably present as polysilicate anions.

TABLE I

SOLUBLE SILICA AND *p*H OF 1% SUSPENSION OF "SILICA A" IN NaOH SOLUTION AFTER 6 MONTHS AT 25°

Molar ratio, SiO_2/Na_2O	*p*H	As monomer, %	As "active" polymer,[a] %
33	10.28	0.053	0.00
16	10.60	.11	.00
8	10.85	.21	.05
3	11.04	.36	.36

[a] Low molecular weight polysilicate ions, which react with molybdic acid reagent within 10 minutes.

Rate of Reaction of Molybdate Reagent with "Silica A."—Two milliliters of a 1% suspension of "Silica A" aged six months in methanol was added to 100 ml. of the molybdic acid solution and the development of the color was followed at 25°.

Time, min.	Apparent % SiO_2 in methanol soln.
1	0.0007
40	0.0014

This not only shows that very little silica is dissolved in the methanol, but also that the "Silica A" is essentially not reactive with the molybdate reagent even after 40 minutes.

(B) "Soluble Silica" in Aged Sols.—Instead of approaching solubility equilibrium by suspending silica powder in water or dilute alkali, it is possible to start with a colloidal solution of silica particles or polysilicic acid and determine the concentration of monomeric silica in such colloidal solutions.

(1) Alkaline Sols.—Clear sols of colloidal silica were prepared by partial removal of sodium ions from a dilute solution of sodium silicate by means of an ion-exchange resin. At the outset, these sols were supersaturated with respect to monosilicic acid. Equilibrium was then approached by aging the sols for 6 months at 25°.

In this preparation a commercial sodium silicate (du Pont No. 9 Grade) containing a weight ratio of $SiO_2:Na_2O$ of 3.25:1.0, was diluted with distilled water to produce a solution containing 1.5 g. SiO_2 per 100 ml. Acid-regenerated "Nalcite" HCR resin, washed and then air-dried for two days, was added in weighed amount to a sample of the diluted silicate solution. The mixture was stirred for 3.0 minutes at 25°, and then filtered to remove resin. The amount of resin required to remove the desired amount of sodium in each experiment was predetermined in preliminary experiments. The final molar ratio of $SiO_2:Na_2O$ in the silica sol was then determined by analysis.

The diameter of the particles of colloidal silica after aging for six months is not known, but it was probably no greater than 5 or 10 mμ, since the sols were very clear. To deter-

(20) G. B. Alexander, *J. Am. Chem. Soc.*, **75**, 5655 (1953).

mine the concentration of monosilicic acid in these sols, aliquots of said sols were reacted with molybdic acid reagent. The rate and extent of reaction were used to identify the concentration of monosilicic acid. Because the size of the colloidal silica particles in the sols was very small, they did not interfere in the colorimetric reaction. It will be noted in Table II, that for $SiO_2:Na_2O$ ratios above 3, the "active" polymer concentration is higher than in Table I, indicating that true equilibrium solubility was not quite reached. However, at higher ratios (77 and 224) the concentration of monomer corresponds essentially to the solubility of amorphous silica.

TABLE II

% SILICA IN SOLUTION IN 1.5% SILICA SOL AFTER 6 MONTHS AT 25° AS DETERMINED BY THE SILICOMOLYBDATE METHOD

Molar ratio $SiO_2:Na_2O$	pH		Silica in soln. after 6 months, %	
	Initial	After 6 months	As monomer	As "active" polymer
3.25	10.95	11.03	0.32	0.34
25	8.73	9.2	.017	.03
77	7.30	8.6	.012	.03
224	6.45	7.5	.012	.02

It is significant that the 3.25 ratio solution shown in Table II contained about the same amount of sodium polysilicate ("active" polymer) as the 3 ratio sol in Table I. Also it will be noted that the amount of silica in true solution below *p*H 9 is comparable to that of "Silica A."

A plot of "soluble" silica, as indicated by the silica which reacts with the molybdate reagent within two minutes, *versus* *p*H, is shown in Fig. 2 for "Silica A" and for the sols of colloidal silica.

(2) **Acid Sols.**—A solution of silicic acid containing 1% SiO_2, prepared by ion-exchange from 3.25 ratio ($SiO_2:Na_2O$) sodium silicate and having a *p*H of 2.7 adjusted with H_2SO_4, was aged for 1 month at 25°. At the end of this time, polymerization had progressed to the point where the concentration of molybdate-reactive SiO_2 had dropped to 0.03%. Samples of this clear aged sol were then diluted with H_2SO_4 to give solutions containing 0.1% SiO_2 and ranging in *p*H from 2.1 to 4.0; the concentration of molybdate reactive silica was followed over a period of 12 days. The concentration of monosilicic acid in the diluted sols increased from an initial value of 0.003 to 0.010% in every case. While the solubility had probably not reached equilibrium after 12 days, it appeared to be approaching the range of 0.01 to 0.015 found for "Silica A" in aqueous solution.

(C) **Solubility of Silica Gel.**—In a concurrent study of the reaction of low molecular weight silicic acid with molybdic acid,[20] a silica gel was prepared by polymerizing a solution of silicic acid (1.0% SiO_2) at *p*H 2.7 and a room temperature of about 25° for two weeks. This gel was then dehydrated under vacuum at about 90° and slurried in distilled water. The solubility of silica was determined by the silicomolybdate method. A concentration of 0.02% SiO_2 was found in the supernatant solution. That this soluble silica was monomeric was shown by the fact that it reacted completely with molybdic acid within two minutes. Further evidence that the soluble silica was of low molecular weight was obtained by measuring the freezing point of the solution using a technique described previously by one of the authors.[21] The freezing point depression of this silica solution was 0.012° lower than the freezing point of a solution free from silica but containing a concentration of H_2SO_4 (0.001 *N*) equivalent to that in the silicic acid solution. The depression for 0.02% SiO_2 as monomer is calculated to be 0.005°; agreement is within the accuracy of the temperature measurement.

Discussion

Establishment of Equilibrium.—From the foregoing results, it is clear that *solubility equilibrium at 25° has been established.* This is shown by the fact that when amorphous silica powder ("Silica A") was suspended in water the concentration of monomeric silica increased to a value of 0.014% SiO_2, while in a solution of polysilicic acid supersaturated with monosilicic acid which was permitted to polymerize for six months (Table II), the concentration of monomer decreased until it was about the same value, *i.e.*, 0.012% SiO_2. The solubility of silica in these systems was relatively constant at about 0.012–0.014% in the *p*H range 5 to 8 (Fig. 2). At *p*H 2.1 to 2.7, the solubility of monomeric silica from polymerized polysilicic acid is approximately 0.010% SiO_2.

The Effect of *p*H on the Solubility of Silica.—The increase in the total "soluble" silica at high *p*H can be explained on the basis of the following equilibrium, assuming that the *concentration of $Si(OH)_4$ does not change with pH.*

$$Si(OH)_4 + (OH^-) = (HO)_3SiO^- + H_2O$$

Although silicon in the silicate ion is represented in the above equation to have a coördination number of four, it is believed that it may actually have a coördination number of six in accordance with the formula $Si(OH)_6^{-2}$, which would be analogous to the fluosilicate ion.

The equilibrium constant for the above equation can be calculated from data obtained by Roller and Ervin[22] in a study of the association of silicate ions in the $CaO/SiO_2/H_2O$ system. These authors found at 30°

$$\frac{[H^+][(HO)_3SiO^-]}{[Si(OH)_4]} = 10^{-9.8}$$

Let

S_t = total solubility of silica including monomeric silicic acid and silicate ions, in g. SiO_2 per 100 ml.

S_m = concn. of monosilicic acid in g. SiO_2 per 100 ml.

Whence

$$\frac{[H^+][S_t - S_m]}{[S_m]} = 10^{-9.8}$$

$$pH - \log\left[\frac{S_t - S_m}{S_m}\right] = 9.8 \qquad (1)$$

Taking $S_m = 0.012\%$, then the value of S_t for various *p*H values was calculated. As shown in Fig. 2, the values which were obtained experimentally are in reasonably good agreement with those calculated. This is evidence that the concentration of $Si(OH)_4$ in equilibrium with the solid phase is not affected by *p*H.

While it is certain that the solubility of silica increases at high *p*H because of the formation of silicate ion in addition to $Si(OH)_4$ in solution, it is also possible that at low *p*H the solubility may increase by reaction of $Si(OH)_4$ with acids, especially when a trace of fluoride ion is present, to form silicofluoride anions.

The possibility that acids other than hydrofluoric may promote the solution of silica is indicated by Jander and Henkeshoven,[14] who found that in acid solution the solubility of silica from silica gel was highest in 0.1 to 0.01 normal solutions of HCl or HNO_3, where a solubility of 1.5×10^{-3} molar solution (0.0009%) of silica was found. A combination of chloride ion with silicic acid is indicated by Sadek,[23] who measured *p*Cl with a silver chloride electrode and found that chloride ion is bound to the silicic acid in the proportion of one molecule of HCl per molecule of SiO_2.

(21) G. B. Alexander, *J. Am. Chem. Soc.*, **75**, 2887 (1953).

(22) P. S. Roller, Jr., and Guy Ervin, Jr., *ibid.*, **62**, 468 (1940).

(23) H. Sadek, *J. Ind. Chem. Soc.*, **29**, 507 (1952).

IONIC EQUILIBRIA AND SELF-DIFFUSION RATES IN DESULFONATED CATION EXCHANGERS[1]

By G. E. Boyd, B. A. Soldano and O. D. Bonner[2]

Oak Ridge National Laboratory, Oak Ridge, Tennessee

Received December 7, 1953

Sulfonated polystyrene–divinylbenzene type cation-exchangers of variable capacity were prepared by acid hydrolysis at 180–220°. Evidence for some rupture of divinylbenzene cross-links was found in an increased moisture absorption. Ionic selectivity coefficients measured for the sodium–hydrogen exchange decreased with decreasing capacity. Complete selectivity reversal at all exchanger compositions (*i.e.*, hydrogen preferred over sodium ion in the exchanger) was found for a 50% desulfonated nominal 16% DVB exchanger. In contrast, the uptake of silver ion in the silver–sodium exchange was increased by decreasing capacity. Self-diffusion coefficients for sodium, silver, zinc, yttrium and lanthanum ions showed initial increases with lowered exchange capacity, reflecting the breaking of cross-links. At still lower capacities, however, the self-diffusion coefficients decreased and the activation energies increased to large values.

Previous studies[3] of the influence of ion-exchange structure on ionic selectivity and exchange rate have been concerned with alterations brought about by varying the cross-linking of the polymeric network to which the exchange groups are covalently bonded. No reports have yet appeared which describe, or attempt to predict, the effect of varying the *number* of exchange groups holding all other factors unchanged. Accordingly, effort was devoted to the preparation of a number of sulfonated polystyrene type cation exchangers of varying capacity, and to the measurement of equilibrium selectivities and self-diffusion rates of various cations in them.

Experimental

The method to produce cation exchangers of varying capacity was based on the stability investigations of Bauman and Wheaton[4] which showed that Dowex-50 was desulfonated when its hydrogen form was heated in water in a closed vessel at temperatures above 180°. The thermal hydrolysis reaction leading to the splitting-off of sulfuric acid is believed to take place at random throughout the body of the exchanger, so that the remaining sulfonate groups are uniformly distributed.

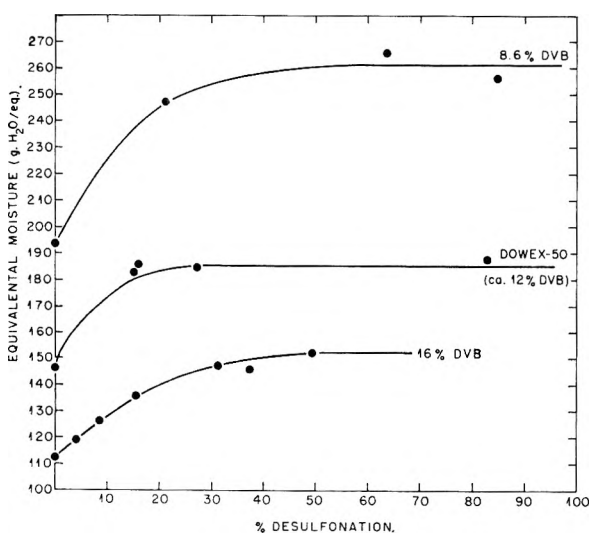

Fig. 1.—Equivalental moisture contents of hydrogen form of desulfonated cation exchangers.

Twenty- to thirty-gram amounts of acid exchanger together with approximately twice this quantity of pure water, freshly boiled to remove dissolved oxygen, were placed in a quartz tube which was sealed and then rocked in an autoclave at selected temperatures between 180 and 210°. Some difficulty was experienced in achieving a final desired capacity owing to the fact that hydrolysis took place fairly rapidly above an apparent threshold of about 180°. However, good use could be made of the known greater stability of the salt-forms; if only 50% desulfonation were desired, sufficient NaCl to convert one-half of the exchanger to the sodium-form was dissolved in the water, and then the temperature was increased to 200° where a rapid desulfonation of the remaining acid groups took place. Exchangers of nominal 8.6, 12 and 16% divinylbenzene (DVB) content were desulfonated to give preparations of varying capacity. The most weakly linked exchanger desulfonated the most rapidly, and showed after 8 and 23 hours capacity losses of 21 and 64%, respectively. Initial exchange capacities of the 8.6% DVB, the commercial Dowex-50 (*ca.* 12% DVB) and the 16% DVB preparations were 5.25, 5.14 and 5.10 meq./g. dry H-form, respectively, as determined by *p*H titration.

The desulfonated products were examined to determine changes other than a loss in capacity from the prolonged autoclaving. It was hoped that no changes in cross-linking might have occurred, as for example, if sulfonate groups were converted to sulfone linkages, or *vice versa*[5]; or, if there were appreciable depolymerization and/or a breaking of divinylbenzene cross-links. Equivalental moisture content, M_w, determinations (Fig. 1) revealed that the water uptake increased with desulfonation and then became constant. Equivalental moistures and volumes, V_e, of the wet-swollen desulfonated exchangers were measured for the sodium, silver and lanthanum salt forms of the 16% DVB preparation. These increased in a manner also suggesting that the polymer network was being ruptured. A comparison (Table I) was next made of the sulfur contents of several of these preparations estimated from *p*H titration data, assuming all acid to be nuclear sulfonic, with those found by direct analysis.[6] A collation of the results from these independent procedures suggests that sulfone linkages are probably not present in more than negligible amounts, and hence that their rupture cannot explain the observed increased equivalental moistures and volumes accompanying desulfonation. The presence of small amounts (2–4%) of weak acid capacity (carboxyl) in the undesulfonated and slightly desul-

(1) Presented before the Division of Colloid Chemistry, 120th National Meeting, American Chemical Society, Sept. 3-7, 1951, New York, N. Y.

(2) Summer Research Participant, 1951, Oak Ridge Institute for Nuclear Studies and the University of South Carolina, Columbia, S. C.

(3) For summaries see G. E. Boyd, *Ann. Rev. Phys. Chem.*, **2**, 309 (1951); W. C. Bauman, R. E. Anderson and R. M. Wheaton, *ibid.*, **3**, 109 (1952).

(4) W. C. Bauman and R. M. Wheaton, *Ind. Eng. Chem.*, **40**, 1350 (1948).

(5) W. C. Bauman and J. Eichhorn, *J. Am. Chem. Soc.*, **69**, 2830 (1947), report that approximately 6% of the total sulfur in Dowex-50 is probably combined in sulfone cross-links. Recent estimates on sulfonated styrene exchangers indicate 1–2% of the sulfur may be so combined.

(6) The exchangers were decomposed to give a homogeneous solution by a wet oxidation procedure employing perchloric acid, and sulfate determinations were performed on aliquots. The authors are indebted to J. M. Chilton of the Analytical Chemistry Division for these labors.

fonated exchangers may be inferred. However, the titratable capacity of the most extensively desulfonated preparation agreed within experimental error with the sulfur analysis, indicating that complete decarboxylation had occurred and that only sulfonic acid groups remained.

TABLE I

SULFUR CONTENTS OF DESULFONATED NOMINAL 16% DVB CATION EXCHANGERS

(Initial capacity = 5.10 meq./g. dry H-form)

Desulfonation, %	Titrated capacity (meq./g. air-dry H-form)	Sulfur from titrated capacity, %	Sulfur by chemical analysis, %
0	3.595	11.50 ± 0.05	11.20 ± 0.07
11.7	3.175	10.15 ± .05	9.72 ± .05
45.6	1.955	6.27 ± .03	6.33 ± .05

A further study was made to determine if temperatures of 180–220° were sufficient to depolymerize the hydrocarbon network of the exchanger. Divinylbenzene cross-linked polystyrene beads were heated in contact with pure water or dilute sulfuric acid solutions under conditions identical with those employed in the desulfonations. The copolymer was separated from the reaction mixture, washed with ethyl alcohol, dried at 80° in a vacuum oven and then immersed in toluene for several days. Toluene absorptions were estimated by weight loss on heating to 120° in a vacuum oven, and specific volumes were measured pycnometrically in liquid toluene (Table II). Small, but significant, decreases

TABLE II

TOLUENE ABSORPTION AND SPECIFIC VOLUMES OF HEAT TREATED POLYSTYRENE DIVINYLBENZENE COPOLYMER (16% DVB)

Treatment of copolymer	Toluene absorption (g. toluene/g. copolymer)	Specific vol. (ml./g. swollen copolymer)
Copolymer control, not heated	0.802	1.018
Heated in distilled water 20 hr. at 200°	.725	1.013± 0.002
Heated in dilute H_2SO_4 20 hr. at 200°	.666	0.997
Heated in distilled water 4 hr. at 250°	.469	0.973

in toluene absorption and specific volume were observed, suggesting that the net effect of heating was not to depolymerize and/or break cross-links, but rather the opposite. This finding contrasts markedly with the increased swelling initially accompanying desulfonation of cation exchangers based on this copolymer. The observation (Fig. 1) that the percentage swelling increase was greatest for the initially most highly cross-linked cation exchanger may also be of interest.[7]

Selectivity coefficient measurements for the sodium–hydrogen and sodium–silver exchange equilibria were performed using nominal 16% DVB cation exchangers showing titrated capacities of 2.52, 3.19, 4.29, 4.64, 4.89 and 5.10 meq./g. dry H-form. Approximately one milliequivalent of exchanger in the desired salt form was weighed and transferred to a 250-ml. ground glass stoppered erlenmeyer flask containing 25 ml. of 0.100 *M* aqueous solution. After shaking for a minimum of three hours, the exchanger was separated and washed with 100 ml. of demineralized water. Both supernatant solution plus washings and the exchanger were analyzed for both ions. Hydrogen ion was estimated volumetrically with standardized base, while partition ratios for sodium and silver ions between exchanger and equilibrium solution were estimated radiometrically using a 4π geometry, argon-filled ionization chamber. The reliability of the selectivity coefficient values was confirmed by material balances for both ions.

Ionic self-exchange rate measurements using radioactive tracers were conducted on the same 16% DVB preparations as above, as well as on variously desulfonated commercially available Dowex-50 (*ca.* 12% DVB) and on an 8.6% DVB exchanger. The experimental procedure, radioactivity assay method, particle diameter determinations, and the treatment of the rate data to estimate self-diffusion coefficients and activation energies were the same as in earlier studies.[8]

Experimental Results and Discussion

Large decreases in the selectivity coefficient, K_H^{Na}, for the sodium–hydrogen exchange (Fig. 2) on the one hand, and an increase in the coefficient, K_{Na}^{Ag}, for the silver–sodium exchange (Fig. 3) on the other were observed as the capacity of the 16% DVB exchanger was lowered. The possibility in the former system that the apparent increase in hydrogen ion selectivity resulted from the introduction of carboxyl groups into the exchanger during desulfonation could be excluded: (a) good agreement was demonstrated (Table I) between exchange capacities estimated from acidimetric titrations and from total sulfur analyses on the most extensively desulfonated preparation; (b) *p*H titration of this preparation using a variety of indicators gave no evidence of weak acid capacity, nor was there any drifting of the indicator end-points with time; (c) mass balances were obtained to better than one per cent. for the total ionic contents of the exchangers. These remained constant and equal to the titrated capacity.

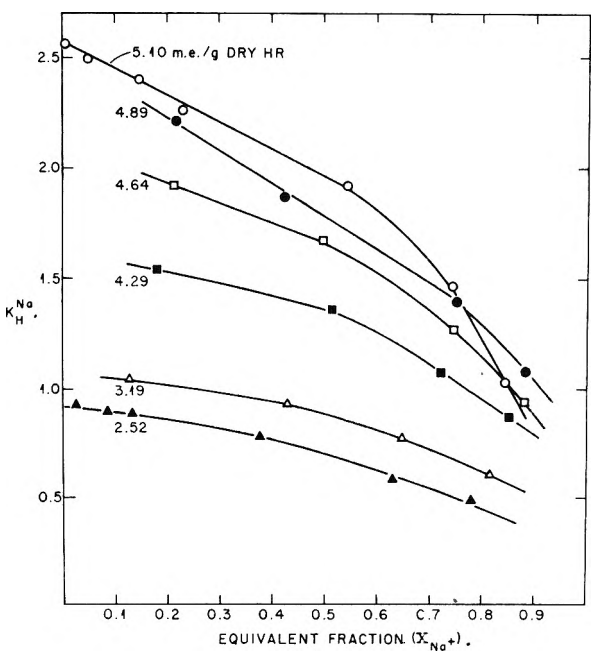

Fig. 2.—Dependence of the sodium–hydrogen exchange selectivity coefficient at 25° on exchanger composition and capacity (variously desulfonated nominal 16% DVB cation exchanger).

Part of the observed decrease in selectivity for sodium over hydrogen ion, however, may be attributed to the breaking of cross-links in the desulfonation. Thus, from swelling measurements (Fig. 1)

(7) It is not to be assumed that there were no side reactions. A strong, mercaptan-like odor, indicating some reduction of sulfonate, was frequently detected upon opening the quartz ampoule after autoclaving. Complete desulfonation was achieved in one instance by heating for seven days at 240°; however, complete breakdown of the polymer also seemed to occur for only a tarry mass remained.

(8) G. E. Boyd and B. A. Soldano, *J. Am. Chem. Soc.*, **75**, 6091 (1953).

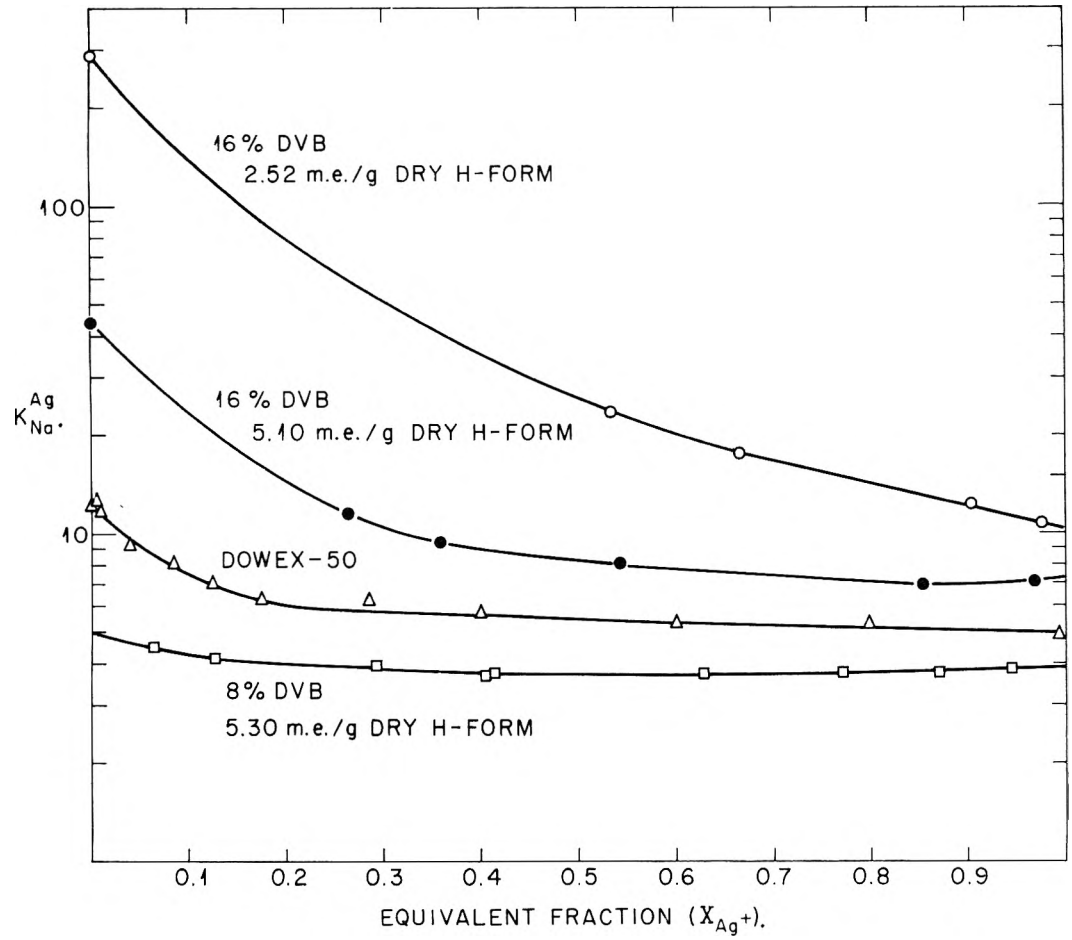

Fig. 3.—Dependence of selectivity coefficient of silver–sodium exchange at 25° on exchanger composition and capacity. (Data for undesulfonated nominal 8% DVB exchanger from O. D. Bonner and V. Rhett, This Journal, **57**, 254 (1953); data for Dowex-50 from E. Glueckauf, *Endeavour*, 10, 40 (1951)).

it may be estimated that the nominal 16% DVB cross-linked exchanger decreased to approximately 12% DVB when its capacity was reduced to roughly one-half. If the capacity had remained unchanged, this diminution in cross-linking would have caused K_H^{Na} to decrease from 2.32 to 1.79 at an equivalent fraction for sodium, X_{Na}, of 0.2. Only a small part of the observed selectivity lowering may therefore be attributed to the decreased cross-linking on desulfonation. The complete selectivity reversal found with the 51% desulfonated exchanger must be due almost entirely to a new effect, for even with exchangers of only nominal 1% DVB K_H^{Na} exceeds unity for all values of X_{Na}.

The silver–sodium behavior was the reverse of that for the sodium–hydrogen system in that the selectivity of the preferred ion (*i.e.*, Ag^+) was increased rather than decreased by desulfonation. Moreover, as may be seen in Fig. 3, the effect of reduced cross-linking which is to lower the relative affinity for silver ion seemed outweighed by an increased selectivity presumably caused by the capacity decrease.

The foregoing selectivity behavior of nuclear sulfonic acid cation exchangers of varying exchange capacity may be compared with a report[9] published after our work was completed on the selectivity of a polyacrylic acid exchanger (12% DVB) whose capacity was varied by partial esterification of the carboxyl exchange groups. Here, the higher the exchange capacity, the greater the selectivity for the preferred ion.

The coefficients, D, for the self-diffusion of sodium, silver, zinc, yttrium and lanthanum ions all showed (Table III) initial increases with decreasing exchange capacity as expected if a breakage in cross-linkage had accompanied the first stages of the desulfonation. Further, the activation energy, $E_{act.}$, for self-diffusion was found to decrease initially. At still smaller capacities, however, self-diffusion became progressively less rapid and the activation energy increased so that D appeared to reach a maximum and then decrease while $E_{act.}$ passed through a minimum. The apparent entropy of activation, $\Delta S^{\pm}$, computed from D and $E_{act.}$ by means of the absolute reaction rate equation

$$D\ (\text{cm.}^2\ \text{sec.}^{-1}) = d^2(ekT/h)\ \exp\ (\Delta S^{\pm}/R)\ \exp\ (-E_{act.}/RT) \quad (1)$$

assuming $d = 1.5$ Å., showed (Table III) a slight decrease for small degrees of desulfonation, and then increased again sometimes to large positive values indicating strong interaction between the diffusing ion and its environment. The effect of

(9) H. Deuel, K. Hutscheneker and J. Solms, *Z. Elektrochem.*, **57**, 172 (1953).

TABLE III

SELF-DIFFUSION OF CATIONS ON CROSS-LINKED SULFONATED POLYSTYRENE TYPE CATION EXCHANGERS OF VARYING CAPACITY

Capacity, meq./g. dry HR	Desulfonated, %	Diffusion coefficient, cm.²/sec. 0.3°	25°	Activation energy, cal./mole	Entropy of activation, e.u.
		Na^+ Ion:Nominal 8.6% DVB			
5.25	0	3.42×10^{-7}	9.44×10^{-7}	6500	5.3
4.14	21.2	4.34×10^{-7}	11.20×10^{-7}	6170	4.5
1.91	63.6	3.44×10^{-7}	8.44×10^{-7}	5180	−1.6
		Na^+ Ion:Dowex-50			
5.14	0	1.15×10^{-7}	2.88×10^{-7}	5980	1.3
4.36	15.2	2.96×10^{-7}	6.56×10^{-7}	5220	3.3
		Zn^{++} Ion:Dowex-50			
5.14	0	0.88×10^{-8}	2.89×10^{-8}	7790	2.8
4.36	15.2	3.77×10^{-8}	10.50×10^{-8}	6720	1.7
4.18	18.7	5.44×10^{-8}	13.50×10^{-8}	6000	−0.3
3.74	27.3	2.70×10^{-8}	7.25×10^{-8}	6420	0.0
0.88	82.9	1.23×10^{-8}	5.88×10^{-8}	10000	11.5
		Y^{+++} Ion:Dowex-50			
5.14	0	1.01×10^{-9}	3.18×10^{-9}	7500	−2.5
4.36	15.2	4.05×10^{-9}	12.70×10^{-9}	7500	0.0
		Na^+ Ion:Nominal 16% DVB			
5.10	0	6.58×10^{-8}	2.40×10^{-7}	(8400)	(8.8)
4.89	4.2	...	2.75×10^{-7}	...	...
4.64	9.0	1.04×10^{-7}	3.30×10^{-7}	7500	6.6
4.29	15.9	1.25×10^{-7}	3.86×10^{-7}	7340	6.3
3.19	37.4	1.43×10^{-7}	3.96×10^{-7}	6620	4.0
2.52	50.6	9.68×10^{-8}	3.01×10^{-7}	7280	5.6
		Ag^+ Ion:Nominal 16% DVB			
5.10	0	1.00×10^{-7}	2.75×10^{-7}	6590	3.1
4.29	15.9	1.23×10^{-7}	3.32×10^{-7}	6660	3.8
3.19	37.4	6.84×10^{-8}	1.90×10^{-7}	6650	2.6
2.52	50.6	2.24×10^{-8}	6.98×10^{-8}	8180	5.8
		Zn^{++} Ion:Nominal 16% DVB			
5.10	0	3.12×10^{-9}	1.16×10^{-8}	8520	3.7
2.52	50.6	3.46×10^{-9}	1.20×10^{-8}	8980	5.3
		La^{+++} Ion:Nominal 16% DVB			
5.10	0	1.53×10^{-10}	4.87×10^{-10}	7530	−6.4
4.29	15.9	2.81×10^{-10}	7.80×10^{-10}	6640	−8.0
3.19	37.4	2.87×10^{-10}	7.55×10^{-10}	6300	−10.8
2.52	50.6	1.42×10^{-10}	5.96×10^{-10}	9340	0.5

this interaction was to overcome partially the increased activation energy, and to cause the diffusion to occur somewhat more rapidly than would be the case if there were no interaction (*cf.* eq. 1). Previously, larger than expected cationic self-diffusion coefficients had been observed[8] in work with highly cross-linked preparations of relatively low exchange capacities.

In attempting to understand the unusual changes in ionic selectivity caused by desulfonation at least two factors need to be considered: (a) the increased interaction of a given ion with its surroundings; and (b) the decreased *charge density on the polymeric network* of the exchanger. The latter factor may be the more important one in determining the selectivity reversal found in the sodium–hydrogen exchange system, and the increased silver ion affinity in the silver–sodium exchange, for factor (a) is also the consequence of an increased cross-linking which gives a higher rather than a lower sodium ion selectivity. Since the ions in an exchanger would be expected to act less strongly on each other as the network charge density decreases, it may be that like ion–ion interactions are of appreciable importance in determining ion exchange selectivity. By reason of these implications, the results of this research should be confirmed and extended by additional measurements preferably with variable capacity exchangers prepared by other methods. While it does not appear possible by direct sulfonation to vary the exchange capacity and still obtain a homogeneous product, the recent reports of the synthesis and polymerization of *p*-vinylbenzenesulfonic acid[10] suggest that such cross-linked cation exchangers might be prepared by copolymerization of varying amounts of styrene, divinylbenzene and sulfostyrene with one another. Additional selectivity measurements with such materials are planned when they become available.

(10) R. H. Wiley, N. R. Smith and C. C. Ketterer, *J. Am. Chem. Soc.*, **76**, 720 (1954).

AN INTERPOLATIVE METHOD OF CALCULATING SOLUBILITIES OF MISSING MEMBERS OF HOMOLOGOUS SERIES[1]

BY EVALD L. SKAU AND RICHARD E. BOUCHER

Southern Regional Research Laboratory,[2] New Orleans, Louisiana

Received December 28, 1953

From the approximate freezing point lowering equation and the known empirical relationships between the number of carbon atoms, n, and the heats and entropies of fusion of the members of a homologous series the following linear equation has been derived: $\log N = a + bn$, in which N is the solubility of the homologs (expressed in mole fraction) in a given solvent at a given temperature and a and b are constants depending upon the temperature and the system involved. Log N *vs.* n isotherms have been plotted for 125 systems involving ten homologous series in 16 different solvents using the published data of Ralston, Harwood, Hoerr and co-workers. The results have been tabulated and show that only about one-third of the 584 isotherms were straight lines as required by the equation, the rest being smooth curves. The log N *vs.* n plots have a number of important applications in connection with data on the solubilities of members of homologous series. They can be used (1) to smooth out experimental solubility data, (2) to locate discrepancies caused by experimental error or by an impurity in one sample in the series, and (3) by graphical interpolation to predict the solubility of missing members of the series. In two cases it was shown experimentally that points which deviated from the log N *vs.* n isotherms were actually in error. The published solubility data for the symmetrical aliphatic secondary amines containing 16, 24, 26, 28, 30 and 36 carbon atoms were used to predict the solubility of those containing 18, 20, 22, 32, 34 and 38 carbon atoms at a number of temperatures in eight solvents. Similarly solubility tables have been constructed for myristanilide and N,N-diphenylmyristamide, each at a number of temperatures in thirteen solvents.

It has been shown[3–5] that for the higher members of homologous series the heat of fusion and the entropy of fusion are each essentially a linear function of the number of carbon atoms in the molecule. That is

$$\Delta H_f = a' + b'n \qquad (1)$$

and

$$\Delta H_f/T_0 = a'' + b''n \qquad (2)$$

where ΔH_f is the heat of fusion in calories per mole, T_0 is the freezing point of the pure compound in degrees absolute, n is the total number of carbon atoms in the molecule, and a', a'', b' and b'' are constants. These constants may have one set of values when n is even and another when n is odd.[3]

Since the solubility of a compound is a function of its heat of fusion, it should be possible to show a correlation between the number of carbon atoms and the solubilities of the members of a homologous series of compounds. The approximate equation for the lowering of the freezing point assuming ideal solutions may be written as

$$2.303 \log N = \frac{\Delta H_f}{R}\left(\frac{1}{T_0} - \frac{1}{T}\right) \qquad (3)$$

where N is the mole fraction of the compound with which the solution is saturated; T is the solubility temperature in degrees absolute for the given composition, *i.e.*, the primary freezing point of the solution; and R is the gas constant.

Rearranging gives

$$2.303 \log N = \frac{1}{R}\left(\frac{\Delta H_f}{T_0}\right) - \frac{1}{RT}(\Delta H_f) \qquad (4)$$

and by substitution from equations 1 and 2

$$2.303 \log N = \frac{1}{R}(a'' + b''n) - \frac{1}{RT}(a' + b'n) \qquad (5)$$

or

$$2.303 \log N = \left[-\frac{a'}{R}\left(\frac{1}{T}\right) + \frac{a''}{R}\right] + \left[-\frac{b'}{R}\left(\frac{1}{T}\right) + \frac{b''}{R}\right]n \qquad (6)$$

At a given temperature, the values within the brackets become constants and equation 6 becomes

$$\log N = a + bn \qquad (7)$$

Thus, assuming that equations 1, 2 and 3 are valid over the concentration range considered, a straight line would be obtained for each temperature by plotting the logarithms of the solubilities (expressed in mole fraction) of the members of a homologous series in the given solvent against the total number of carbon atoms (or against the molecular weight). Furthermore, the equation for this straight line could be precalculated, since, from equations 6 and 7

$$a = \frac{1}{2.303}\left[-\frac{a'}{R}\left(\frac{1}{T}\right) + \frac{a''}{R}\right] \qquad (8)$$

and

$$b = \frac{1}{2.303}\left[-\frac{b'}{R}\left(\frac{1}{T}\right) + \frac{b''}{R}\right] \qquad (9)$$

Actually equations 1, 2 and 3 are not strictly valid, the first two being empirical and the third being applicable as a first approximation and then only if the solutions involved are ideal. Therefore the experimental values would not ordinarily be expected to conform to the straight-line relationship of equation 7. However, since the deviations would in all probability vary regularly as the chain length increased in a homologous series the log N *vs.* n isotherms would be expected to be smooth curves.

An empirical linear relationship between the logarithm of the solubility and the number of carbon atoms has been reported by Sobotka and Kahn,[6] by Rehberg and co-workers[7] and more recently by Erichsen.[8] Only the latter author

(1) Presented at the Regional Conclave of the American Chemical Society, New Orleans, Louisiana, December 10–12, 1953.

(2) One of the laboratories of the Bureau of Agricultural and Industrial Chemistry, Agricultural Research Service, U. S. Department of Agriculture. Article not copyrighted.

(3) W. E. Garner, F. C. Madden and J. E. Rushbrooke, *J. Chem. Soc.*, 2491 (1926).

(4) W. E. Garner and A. M. King, *ibid.*, 1849 (1929).

(5) (a) M. L. Huggins, THIS JOURNAL, **43**, 1083 (1939); (b) *Record Chem. Prog., Kresge-Hooker Sci. Lib.*, **11**, 85 (1950).

(6) H. Sobotka and J. Kahn, *J. Am. Chem. Soc.*, **53**, 2935 (1931).

(7) C. E. Rehberg, M. B. Dixon and C. H. Fisher, *ibid.*, **69**, 2966 (1947); M. B. Dixon, C. E. Rehberg and C. H. Fisher, *ibid.*, **70**, 3733 (1948); C. E. Rehberg and M. B. Dixon, *ibid.*, **72**, 1918 (1950); C. E. Rehberg and M. B. Dixon, *J. Org. Chem.*, **15**, 565 (1950).

(8) L. V. Erichsen, *Naturwissenschaften*, **39**, 41, 189 (1952).

expressed the solubility in mole %. All of the homologs studied by these investigators were liquids and only dilute solutions in water at room temperature were involved. The present report pertains to the solubilities of solid homologs over the whole range of concentrations and temperature.

Application to Experimental Data

On the basis of equation 7, log N *vs.* n plots have been constructed from data published by Ralston, Harwood, Hoerr, *et al.*, who have made careful extensive studies of the solubility of the homologous fatty acids,[9,10] methyl esters of the fatty acids,[11] ketones,[12] alcohols,[13] amides,[14] anilides,[14] N,N-diphenylamides,[14] nitriles,[15] primary amines[16] and symmetrical secondary amines,[17] in such solvents as benzene, cyclohexane, carbon tetrachloride, chloroform, glacial acetic acid, ethyl ether, ethyl acetate, butyl acetate, acetone, butanone, methanol, 95% ethanol, isopropyl alcohol, 1-butanol, acetonitrile and nitroethane.

The data have been plotted on semi-logarithmic coördinates as solubility in mole % (100 N) against the total number of carbon atoms, usually at temperature intervals of 10°. Solubilities below 0.1% were not considered unless reported to a sufficient number of significant figures to ensure the desired precision. Smooth curves were obtained as expected except for the amides, which show anomalies in their melting points as well and which have therefore not been included. The solubility data for each homologous series in each solvent resulted in a family of curves (isotherms) as typified by Figs. 1, 2 and 3, which represent the solubilities of the fatty acids in butanone, methyl esters of the fatty acids in chloroform, and the anilides in anhydrous benzene, respectively.

It has long been known that some homologous series exhibit the phenomenon of alternation of melting point; *i.e.*, with each additional CH_2 alternately larger and smaller increases in the melting point are observed depending upon whether the number of carbon atoms in the chain is even or odd. This effect is very marked in the normal fatty acids and Garner[3,4] found that their heats of fusion also showed this alternation. As a result he showed that the constants a', a'', b' and b'' in equations 1 and 2 have one set of values for the even members of the series and another for the odd members. It follows from equations 8 and 9 that the same would be true of a and b in equation 7 and it is therefore not surprising that separate log N *vs.* n plots are obtained from the odd and the even members of the series as shown by the dotted curve in Fig. 1. It will be noted that this 20° isotherm for the odd fatty acids falls above that for the even acids in the range shown and has a different slope. Similarly, the solubility data reported for methyl tridecanoate in methanol, 95% ethanol, 1-butanol and acetonitrile fall above the isotherms for the methyl esters of the even fatty acids. With the exception of methyl tridecanoate in the above solvents, the fatty acids were the only homologous series for which solubility data of both the odd and the even members of the series were reported.

Plots of the available solubility data resulted in 125 charts similar to Figs. 1, 2 and 3, a total of 584 isotherms. These have been summarized in Table I. The numerals in this table indicate the shape of each isotherm over the range considered, designating one of the five types of curvature shown schematically in Fig. 4. If sufficient data were not available to establish the curvature of the isotherm, it was omitted from the table.

In 18.4% of the systems, or charts, all of the isotherms were of type 1 (straight lines) as in Fig. 1, the slopes usually becoming steeper for the lower temperatures. In 16.0% of the systems the isotherms were all of type 5, and in 12.0% they were all of type 2; *i.e.*, a total of 46.4% of the systems consisted entirely of either type 1, 2 or 5. If combinations of the above types of curves are included 64.8% of the systems are accounted for. Double curvature of the isotherm was in general comparatively rare, occurring principally in the homologous anilides, N,N-diphenylamides and primary alcohols, as shown in Table I. Thus of the 584 individual isotherms 31.7% were of type 1, 33.2% of type 2 and 18.5% of type 5—a total of 83.4%.

In all the systems consisting of more than one type of isotherm, the uppermost isotherm was almost always of type 1, 2 or 5 and the shapes changed gradually to one or more other types for the lower temperatures as illustrated by Figs. 2 and 3. The change must be consistent, however; if, for example, the 20 and 40° isotherms for a given system were both of a given type the 30° isotherm would not be expected to be of a different type.

The fact that one type of isotherm curvature is obtained for a homologous series of compounds in a given solvent is not necessarily an indication of the type of isotherm that can be expected using a different solvent. However, similar solvents like the individual lower alcohols, do seem to give similarly shaped isotherms for a given homologous series. This similarity would probably have been more pronounced if the original experimental solubility data had been smoothed with the log N *vs.* n isotherms. For example, the few differences in the shapes of the isotherms between the odd- and the even-membered fatty acid series in any given solvent (see Table I) could possibly be eliminated by this initial smoothing.

The irregularity of the solubility, double curvature of the isotherms, in a large number of the systems of anilides and N,N-diphenylamides may be caused by a slight carry-over from the n-aliphatic amides for which there is no regular change in solubility as the chain length increases.

(9) A. W. Ralston and C. W. Hoerr, *J. Org. Chem.*, **7**, 546 (1942).

(10) C. W. Hoerr and A. W. Ralston, *ibid.*, **9**, 329 (1944).

(11) R. S. Sedgwick, C. W. Hoerr and H. J. Harwood, *ibid.*, **17**, 327 (1952).

(12) F. M. Garland, C. W. Hoerr, W. O. Pool and A. W. Ralston, *ibid.*, **8**, 344 (1943).

(13) C. W. Hoerr, H. J. Harwood and A. W. Ralston, *ibid.*, **9**, 267 (1944).

(14) A. W. Ralston, C. W. Hoerr and W. O. Pool, *ibid.*, **8**, 473 (1943).

(15) C. W. Hoerr, E. F. Binkerd, W. O. Pool and A. W. Ralston, *ibid.*, **9**, 68 (1944).

(16) A. W. Ralston, C. W. Hoerr, W. O. Pool and H. J. Harwood, *ibid.*, **9**, 102 (1944).

(17) C. W. Hoerr, H. J. Harwood and A. W. Ralston, *ibid.*, **9**, 201 (1944).

TABLE I

TYPES[a] OF CURVES OBTAINED FOR SEVERAL HOMOLOGOUS SERIES OF COMPOUNDS BY PLOTTING LOG OF SOLUBILITY (MOLE %) *vs.* TOTAL NO. OF CARBON ATOMS AT VARIOUS TEMPERATURES

Solvent	Temp., °C.	−50	−40	−30	−20	−10	0	10	20	30	40	50	60	70	80
Fatty acids, n = 8, 10, 12, 14, 16 and 18															
Benzene								3	3	2	1	1	1		
Cyclohexane								2	2	2	1	1	1		
Carbon tetrachloride							2	2	2	2	2	1	1		
Chloroform							2	2	2	2	1	1	1		
Glacial acetic acid									3	3	2	2	2		
Ethyl acetate							1	1	1	1	1	1	1		
Butyl acetate							2	2	2	2	2	1	1		
Acetone							1	1	1	1	1				
Butanone							1	1	1	1	1	1	1		
Methanol							2	2	2	2	2	2	2		
95% Ethanol							2	2	2	2	2	2	2		
Isopropyl alcohol							2	2	2	2	1	1	1		
1-Butanol							2	2	2	2	1	1	1		
Nitroethane							2	4	4	4	4	4	5		
Acetonitrile							3	4	5	5	5	5	5		
Fatty acids, n = 9, 11, 13, 15 and 17															
Benzene								2	2	1	1	1			
Cyclohexane								2	2	1	1	1			
Carbon tetrachloride							2	2	2	2	1	1			
Chloroform							3	3	3	1	1	1			
Ethyl acetate							2	2	1	1	1	1			
Butyl acetate							2	2	2	2	2	2			
Acetone							1	1	1	1	1				
Butanone							1	1	1	1	1	1			
Methanol							3	3	3	2	2	2			
95% Ethanol							2	2	2	2	2	1			
Isopropyl alcohol							2	2	2	1	1	1			
1-Butanol							2	2	1	1	1	1			
Aliphatic primary amines, n = 10, 12, 14, 16 and 18															
Benzene								1	1	1	1				
Cyclohexane								1	1	1	1				
Carbon tetrachloride					2		2		2	2	2				
Chloroform		1			1		1		1	1	1				
Ethyl ether					2		2		2	2					
Ethyl acetate					1		1		1	1	1				
Butyl acetate					2		2		1	1	1				
Butanone					2		2		2	2	2				
Methanol		2			2		2		2	2	2				
95% Ethanol		2			2		2		2	2	2				
Isopropyl alcohol		2			2		2		2	1	1				
1-Butanol		2			2		2		2	1	1				
Methyl esters of fatty acids (saturated), n = 13, 15, 17 and 19															
Benzene								1	1						
Cyclohexane								1	1						
Carbon tetrachloride					4	4	2	2	2						
Chloroform		2	2	2	1	5	5	5	5						
Ethyl acetate		1	1	1	1	1	1	1	1						
Butyl acetate		1	1	1	1	1	1	1	1						
Acetone						5	5	5	5						
95% Ethanol							5	5	5						
1-Butanol						5	5	5	5						

It is noteworthy that not only does the homologous series of nitriles have double curvature of the isotherms in many of its systems, but also when acetonitrile is the solvent for the other homologous series most of the systems have double curvature of at least some of the isotherms. Like acetonitrile, nitroethane as the solvent gave double curvature to at least some of the isotherms of most of the systems. Conversely, while ethyl ether was used with only four of the homologous series, straight line or only single curved isotherms are representative of all four systems.

The fact that the log N *vs.* n plots are straight lines as required by equation 7 does not imply that

TABLE I (*Continued*)

Solvent	Temp., °C.	−50	−40	−30	−20	−10	0	10	20	30	40	50	60	70	80
Symmetrical normal aliphatic ketones, n = 19, 23, 27, 31 and 35															
Benzene								1		1		1			1
Cyclohexane								1		1		1			1
Carbon tetrachloride								1		1		1		1[b]	
Ethyl acetate												1			
Butyl acetate										1		1			
Acetone												5[c]			
Butanone												1			
95% Ethanol													5[d]		
Isopropyl alcohol												5	5[d]		
1-Butanol															
Nitroethane												5	5		
Aliphatic primary alcohols, n = 10, 12, 14, 16 and 18															
Benzene								3	3	1	1				
Cyclohexane								3	3	2	2				
Carbon tetrachloride				3		3		3	3	2	2				
Chloroform		1		1		2			2	2	2				
Ethyl ether		1		1		1			1	1					
Ethyl acetate				5		5		5	5	5	5				
Butyl acetate				3		4		5	5	5	5				
Acetone				5		5		5	5	5	5				
Butanone				2		4		4	1	1	1				
Methanol				2		2			2	2	2				
95% Ethanol		2		2		3			3	3	2				
Isopropyl alcohol		2		2		3			3	3	2				
1-Butanol		1		1		1			1	1	1				
Symmetrical aliphatic secondary amines, n = 16, 24, 26, 28, 30 and 36															
Benzene								5	5	5	5	5	5		
Cyclohexane								1	1	1	5	5	5		
Carbon tetrachloride						2		4	5	5	5	5			
Chloroform						2		2	1	1	1	5			
Ethyl ether								2	2	2					
Ethyl acetate										1	2	2	2		
Butyl acetate									2	2	2	2	2		
Butanone											3	3	2		
95% Ethanol											2	2	2		
Isopropyl alcohol										2	2	2	2		
1-Butanol								2		2	2	2			
Aliphatic nitriles, n = 10, 12, 14, 16 and 18															
Benzene								5	5	5					
Cyclohexane								1	1	1					
Carbon tetrachloride				1		1		1	1	1					
Chloroform		2		2		5		5	5	5					
Ethyl ether		2		1		5		5	5	5					
Ethyl acetate		3		3		1		2	2	2					
Butyl acetate		3		4		1		1	1	1					
Acetone		5		3		2		2							
Butanone		1		2		1		1	1	1					
Methanol		5		5		5									
95% Ethanol		5		4		5		5	5						
Isopropyl alcohol		4		4		5		5	5						
1-Butanol		4		4		5		5	5						
Nitroethane		2		4		4		5							
Acetonitrile				5		5									

the systems in question are ideal or that equations 1, 2 and 3 are applicable to the particular homologous series and solvent involved. For the homologous even-membered fatty acids, for example, for which adequate experimental data are available to test this point, the solubilities of the individual acids in acetone, butanone and ethyl acetate at various temperatures show wide deviation from equation 3 and still give straight-line isotherms for the log N *vs.* n plots for the series $n = 8$ to $n = 18$ over the whole temperature range. It is not surprising therefore that for these systems the constants a and b in equation 7 cannot be calculated from a', a'', b' and b'' by substitution in linear equations 8 and

TABLE I (*Continued*)

Solvent	Temp., °C. −50	−40	−30	−20	−10	0	10	20	30	40	50	60	70	80
Aliphatic anilides, n = 10, 12, 16 and 18[a]														
Benzene							4		3		3	2	2	
Cyclohexane							4		4		3	2	2	
Carbon tetrachloride							5		3		2	2	1	
Ethyl acetate							3		3		3	2	1	
Butyl acetate							3		2		2		1	
Acetone							5		3		3			
Butanone							2		2		2	2	1	
Methanol											2	2		
95% Ethanol									3		3	3	2	
Isopropyl alcohol							3		3		3	3	5	
1-Butanol							2		3		3		2	
Nitroethane							3		3		5		4	
Acetonitrile											3	3	3	
N,N-Diphenylamides, n = 10, 12, 16 and 18[c]														
Benzene							1		5		5	5		
Cyclohexane							5		5		5	5		
Carbon tetrachloride							4		3		5	5		
Ethyl acetate							4		3		3			
Butyl acetate							5		3		3			
Acetone							2		4		1			
Butanone							4		4		2			
Methanol							3		3		2			
95% Ethanol									5		5	5		
Isopropyl alcohol							5		5		5			
1-Butanol							5		5		5			
Nitroethane							4		3		2			
Acetonitrile							3		3		3			

[a] The numerals in the table refer to the types of curve as designated in Fig. 4. [b] 76.0°. [c] 56.5°. [d] 65.0°. [e] Not counting carbons in the benzene nuclei.

9, a fact which is proved by Fig. 5. The dotted curves in this figure show the change of a and of b with the reciprocal of the absolute temperature as calculated from Garner's values[3,4] for the constants in equations 1 and 2 for the homologous fatty acids containing an even number of carbon atoms; namely, $a' = -3610$, $a'' = -4.3$, $b' = 1030$, and $b'' = 2.652$. The full lines show the corresponding values of a and b obtained from the log N *vs.* n plots of the solubilities of this series ($n = 8$ to $n = 18$) in acetone, butanone and ethyl acetate.

Applications of log N *vs.* n Plots

Because they are known to consist of smooth curves, log N *vs.* n plots have a number of important applications in connection with data on the solubilities of members of a homologous series. They can be used to smooth out experimental solubility data, to locate discrepancies caused by experimental error or by an impurity in one sample in the series, and to predict the solubility of missing members of the series.

Smoothing of Experimental Solubility Data.—The solubility data considered above were obtained by Ralston, *et al.*, by the typical procedure of determining the solubility temperatures of a limited number of compositions, drawing a curve through the experimental points, and then tabulating the solubilities at selected temperatures (in this case at ten-degree intervals) as read by graphical interpolation from this solubility curve. Even with perfect data the accuracy of these interpolated solubilities is limited; the experimental points do not define the solubility curve precisely, especially if they are far apart and if there is much curvature. Here the log N *vs.* n plots can be used to advantage as a guide. The solubility curves for the individual members of the series should be smoothed or adjusted so that in addition to satisfying the experimental solubilities for the individual compounds they also result in smooth log N *vs.* n isotherms for the whole series. Unfortunately this procedure cannot be demonstrated with the solubility data here considered; only the interpolated values at ten-degree intervals have been reported, the original experimental data being represented only graphically on small-scale plots.

Detecting Discrepancies.—In some cases it may be found that one or two points in a system of log N *vs.* n isotherms fall considerably above or below the curves established by the other points. Consider, for example, the point representing the solubility of myristic acid ($n = 14$) in butanone, at 20°, which falls below the 20° isotherm in Fig. 1. Since all of the other isotherms in this system are straight lines the 20° isotherm would certainly be expected to be straight and is defined by the four other points as plotted. It seemed probable therefore that the solubility of myristic acid in butanone at 20° should be about 6.7 instead of 5.5 mole % as reported. This was confirmed by determining the solubility temperature, by the static method,[18] of a

(18) F. C. Magne and E. L. Skau, *J. Am. Chem. Soc.*, **74**, 2628 (1952).

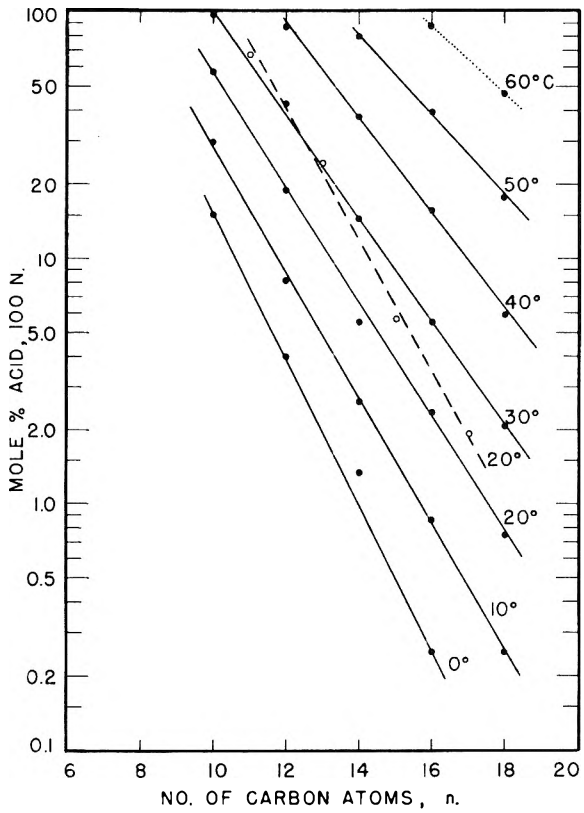

Fig. 1.—Effect of chain length upon the solubility of the normal saturated fatty acids ($C_{n-1}H_{2n-1}COOH$) in butanone at various temperatures: ——, even number of carbon atoms; - - - - -, odd number of carbon atoms.

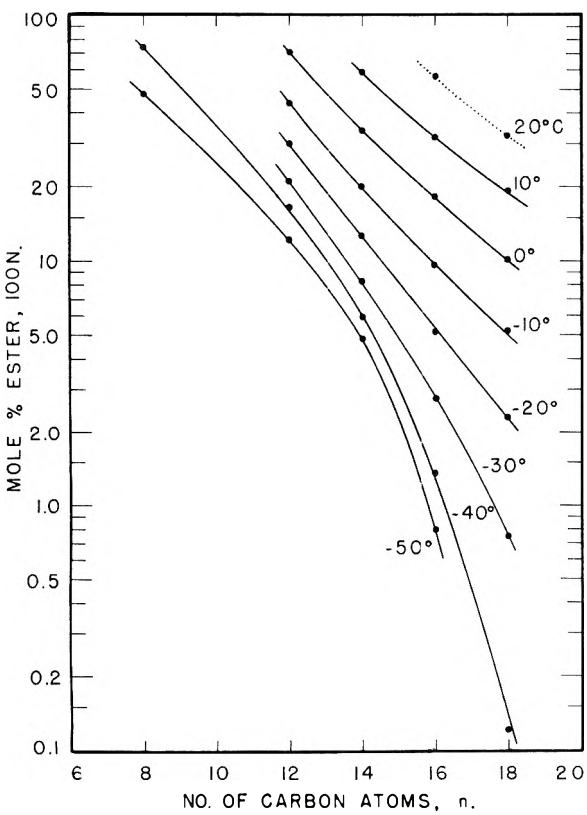

Fig. 2.—Effect of chain length upon the solubility of the methyl esters of the normal saturated fatty acids ($C_{n-2}H_{2n-3}COOCH_3$) in chloroform at various temperatures.

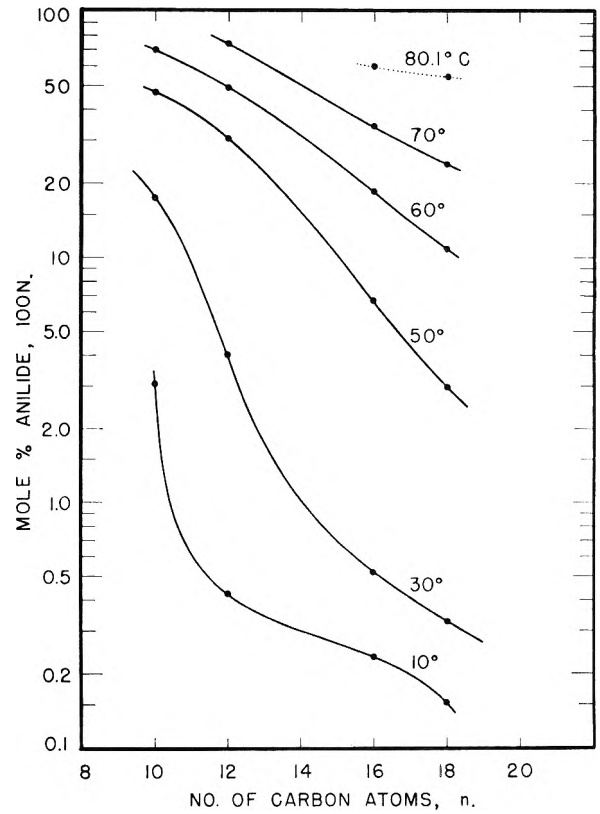

Fig. 3.—Effect of chain length upon the solubility of the normal aliphatic anilides ($C_{n-1}H_{2n-1}CONHC_6H_5$) in anhydrous benzene at various temperatures.

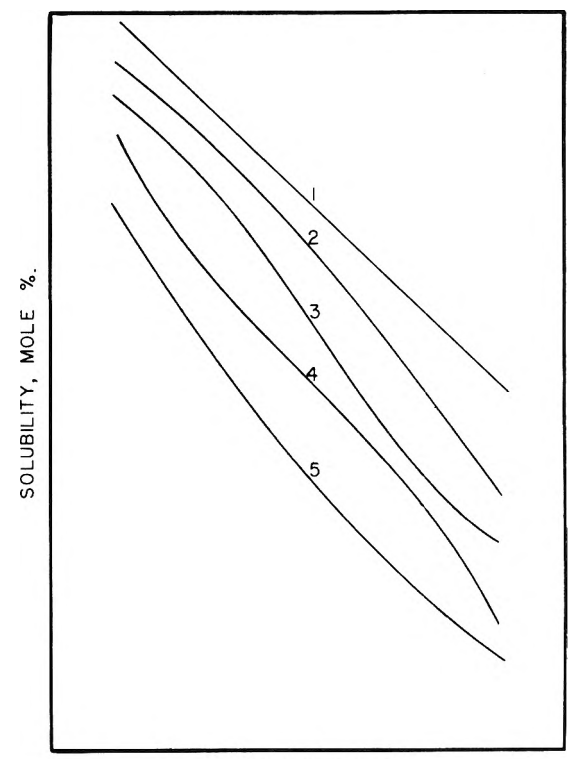

Fig. 4.—Types of isotherm curvature obtained from log *N vs. n* plots.

63.1 mole % mixture of pure myristic acid (f. p. 53.88°) and purified butanone. The acid was com-

TABLE II

PREDICTED SOLUBILITIES[a] IN MOLE PER CENT. OF SYMMETRICAL NORMAL ALIPHATIC SECONDARY AMINES (FROM LOG N *vs.* n CURVES)

Carbon atoms	Temp., °C. −10	0	10	20	30	40	50	60
				Solubility				
				In benzene				
18			10	28	(80)			
20			3.9	13	(37)			
22			1.6	6.1	(19)	(50)		
32				(0.28)	(1.2)	5.4	17	47
34					(0.74)	3.6	13	34
38						(1.7)	(7.3)	(19)
				In cyclohexane				
18			11	31				
20			3.9	14	(40)			
22			1.4	6.2	(19)	(52)		
32				(0.14)	(0.81)	4.7	16	48
34					(0.44)	3.1	12	35
38						(1.4)	(7.6)	(19)
				In carbon tetrachloride				
18	2.6		17	34				
20	1.3		9.1	18	(33)			
22	0.65		4.9	10	(20)	(44)		
32			(0.28)	0.90	2.8	7.5	17	
34				0.56	1.9	5.7	13	
38				(0.23)	(0.94)	(3.3)	(8.7)	
				In chloroform				
18	7.8		27	44				
20	4.9		17	28	(42)			
22	2.9		11	18	(28)	(52)		
32			0.48	1.7	4.6	10	21	
34			0.23	1.0	3.2	7.5	16	
38				(0.39)	(1.5)	(4.2)	(9.5)	
				In butyl acetate				
18				32				
20				15	(50)			
22				6.2	(22)	(68)		
32						(0.14)	3.9	57
34							1.4	30
38							(0.15)	
				In 95% ethanol				
					(30)			
22					(9.0)	(50)		
32							(1)	(30)
34								(6)
				In isopropyl alcohol				
18			(18)					
20			(6.8)					
22			(1.9)		(25)	(60)		
32							2.4	39
34							0.6	13
				In 1-butanol				
18			20		(85)			
20			7.6		(57)			
22			2.5		(30)	(70)		
32						(0.6)	6.3	41
34							2.3	20
38							(0.22)	(2.6)

[a] Values in parentheses less accurate (see text).

pletely dissolved at 18.9 ± 0.2°. Similarly the solubility of myristic acid in absolute methanol was determined and found to be 2.99 mole % at 20.4 ± 0.2° which is in better agreement with the smoothed

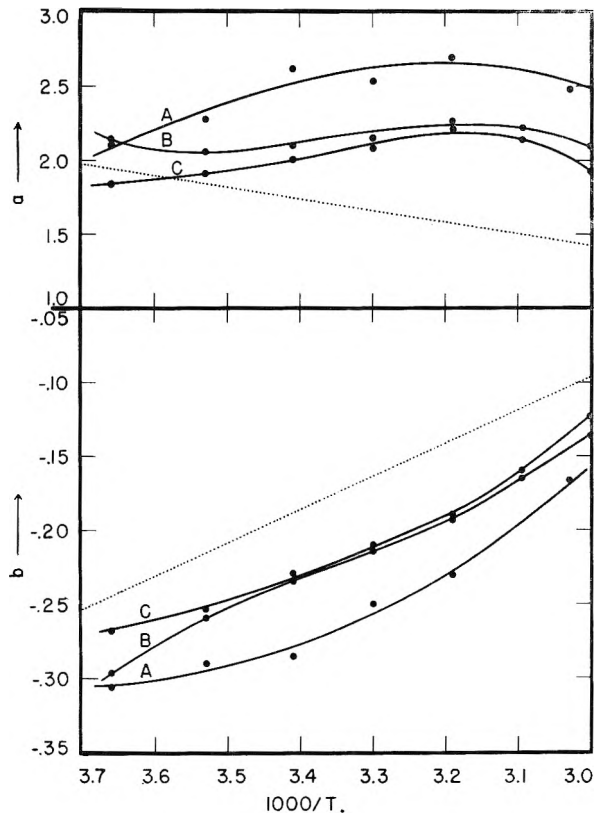

Fig. 5.—The change of the constants a and b with the reciprocal of the absolute temperature for the even-membered fatty acids: ...., as calculated by equations 8 and 9 using Garner's[3,4] values; ——, from the log N *vs.* n plots of the fatty acids (n = 8 to 18) in (A) acetone, (B) butanone and (C) ethyl acetate.

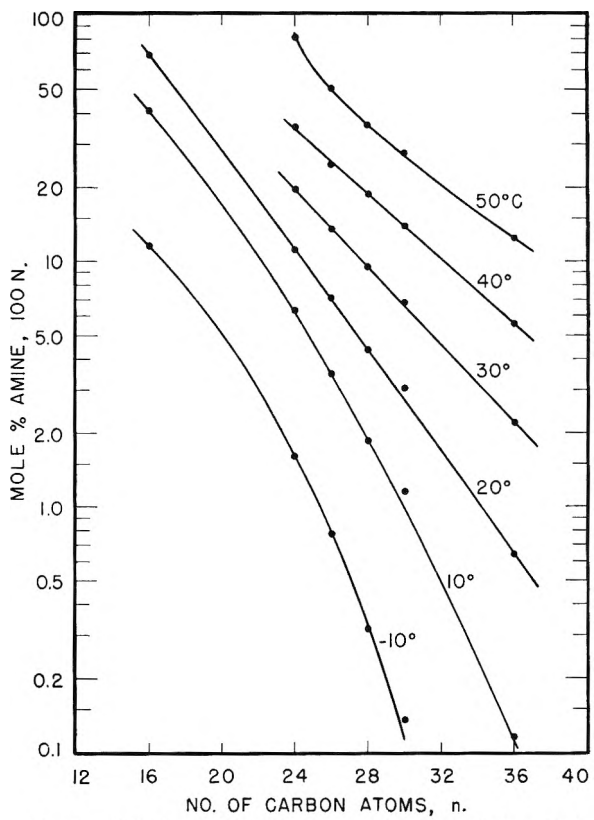

Fig. 6.—Effect of chain length upon the solubility of the symmetrical aliphatic secondary amines in chloroform at various temperatures (n = total no. of carbon atoms).

isotherm for the system then the reported value of 2.37 mole % at 20°.

Judging from the isotherms for the primary alcohols in butyl acetate the solubility of *n*-hexadecanol should be 2.6 instead of 3.3 mole % at −20°, and 0.64 instead of 1.0 mole % at 0°. Similarly the isotherms for the fatty acid series in ethyl acetate indicate that the solubility of lauric acid in this solvent at 30° should be about 38 instead of 53 mole % as reported.

Predicting Solubilities of Missing Members of a Homologous Series.—The log N *vs.* n plots can be used to estimate with some precision the solubilities of missing members of a homologous series, the precision depending upon the accuracy and consistency of the original data, and upon the amount and type of curvature of the isotherms. Thus, the published solubility data for the homologous symmetrical aliphatic secondary amines included only the members having the following total number of carbon atoms: 16, 24, 26, 28, 30 and 36. From the smooth log N *vs.* n isotherms (see, for example, Fig. 6) it was possible by graphical interpolation to read off the solubilities of the missing members of the series at each temperature and for each solvent; *i.e.*, those members containing 18, 20, 22, 32 and 34 carbon atoms. By extrapolation the solubilities for the C_{38} member can also be estimated but with an accuracy which is much less certain.

The solubilities of the missing members so obtained for a number of temperatures in eight different solvents are given in Table II. The values which were obtained by extrapolation or which

TABLE III

PREDICTED SOLUBILITIES[a] IN MOLE PER CENT. OF THE SUBSTITUTED NORMAL ALIPHATIC AMIDES: MYRISTANILIDE [$C_{13}H_{27}CONH(C_6H_5)$] AND N,N-DIPHENYLMYRISTAMIDE [$C_{13}H_{27}CON(C_6H_5)_2$] (FROM LOG N *vs.* n CURVES)

Temp., °C. / Solvent	10	30	50	60	70
	Solubility of myristanilide				
Benzene	0.3	1.0	15	31	50
Cyclohexane	0.12	0.19	6.0	26	47
Carbon tetrachloride	1.3	1.9	22	47	66
Ethyl acetate	0.59	1.8	10	26	49
Butyl acetate	1.3	3.6	13		47
Acetone	0.4	1.1	11	21[b]	
Butanone	1.4	3.7	15	29	49
Methanol			3.8	10	
95% Ethanol		0.8	5.2	16	42
Isopropyl alcohol	0.34	1.1	6.9	15	37
1-Butanol	1.3	2.6	11		44
Nitroethane	0.39	0.54	1.8		16
Acetonitrile		(0.13)	0.66	7.6	17
	Solubility of N,N-Diphenylmyristamide				
Benzene	6.2	19	47	(77)	
Cyclohexane	3.2	13	45	(76)	
Carbon tetrachloride	8.8	24	62	(93)	
Ethyl acetate	3	11	46	(86)	
Butyl acetate	4.0	12	46		
Acetone	3.5	12	44	67[b]	
Butanone	4.3	15	48	(78)	
Methanol	(0.24)	1.7	19	(56)	
95% Ethanol	(0.3)	1.5	16	(73)	
Isopropyl alcohol	1.7	5.3	26	(70)	
1-Butanol	2.5	7.0	31		
Nitroethane	4.0	9.6	4.3		
Acetonitrile	(0.4)	2.0	23	(65)	

[a] Values in parentheses less accurate (see text). [b] At 56.5°.

could be read with less accuracy because of the curvature of the isotherms are enclosed in parentheses.

It should be noted incidentally that the solubilities for the C_{36} member of the series tend to be more or less consistently higher than expected from the smooth isotherms (see Fig. 6). This could be explained by the presence of impurity in this particular sample. Since the published solubility data for the anilides and the N,N-diphenylamides[14] included only the capric, lauric, palmitic and stearic acid derivatives, it was possible to estimate the probable solubilities of the missing member of each of these series, myristanilide and N,N-diphenylmyristamide, over a range of temperatures in thirteen solvents as given in Table III.

As mentioned before it is known that alternation occurs in the melting point and heat of fusion in the fatty acid series and that therefore, as would be expected, the log N *vs.* n isotherms for the odd-membered acids are quite distinct from those for the even acids. It is thus impossible to estimate the solubility of the odd acids by interpolation in the isotherms for the even acids and *vice versa*. The same is probably true for any homologous series showing alternation of melting point. Only the solubility data for methyl tridecanoate ($n = 14$) in four different solvents are available to test this point and in every instance the points fail to fall on the log N *vs.* n isotherms for the members of the series for which n is odd. It seems reasonable to assume that for a homologous series such as the primary alcohols, which shows no alternating effect in the melting point,[19] the isotherms for the odd and even members would coincide and therefore it should be possible to predict the solubilities of the missing (odd) members by interpolation in the log N *vs.* n plots of this alcohol series for the solvents listed in Table I. The basic assumption should, however, first be confirmed by determining at least one solubilty curve for one of the missing members of the homologous series in question.

(19) R. T. Holman, W. O. Lindberg and T. Malkin, "Progress in the Chemistry of Fats and Other Lipids," Vol. I, Pergamon Press, Ltd., London, 1952, pp. 14–15.

THE HEAT OF ADSORPTION OF METHANOL ON CARBON ADSORBENTS AT 0°

BY B. MILLARD,[1] R. A. BEEBE AND J. CYNARSKI

Department of Chemistry, Amherst College, Amherst, Mass.

Received December 31, 1953

Heats of adsorption have been measured in an isothermal calorimeter at 0° for methanol on several carbon adsorbents previously studied. The results are compared and contrasted with those obtained in similar previous experiments on the same adsorbents but with the elementary gases, argon and nitrogen, as adsorbates. The calorimetric heats on the homogeneous surface of Graphon carbon, like the isosteric heats of Pierce and Smith for methanol–graphite, give no indication that the net heat of adsorption is negative in the region of low coverage where the isotherms are convex to the pressure axis.

Introduction

In an earlier publication we have reported the calorimetric heats of adsorption of nitrogen and argon on a number of porous and non-porous carbon adsorbents.[1] The following points were of special interest in the above work: (1) maxima were observed in the heat-coverage curves for argon–Graphon indicating a stepwise adsorption on the homogeneous carbon surface, (2) a correlation was shown to exist between the magnitude of the heats and pore diameters in two Saran charcoals and (3) the heat measurements indicated that wear dust carbon was more heterogeneous than had been anticipated.

In the present paper we give the results of heat measurements with methanol adsorbate on three of the carbon adsorbents used in the nitrogen and argon experiments; these adsorbents are Graphon, S84 Saran charcoal and carbon wear dust. As far as a comparison of these three adsorbing surfaces is concerned, the results of the measurements with methanol are in general consistent with the results of the earlier work in which the elementary gases were used as adsorbates. However, as might have been anticipated because of the polar character of the methanol molecule and possibly because of hydrogen bond formation, we find certain differences in comparing the heat curves for methanol and the elementary gas adsorbates on any one surface.

Pierce and Smith[2] have reported that the isotherm for methanol on NC-1 graphite was of an unusual form which they designated as Type VI. This isotherm like Types III and IV of the BDDT classification[3] is convex to the pressure axis at low coverage but behaves like a type II isotherm at higher coverage. They found a similar isotherm for the methanol–Graphon system. Contrary to the predictions of the theory of Brunauer, *et al.*,[3] Pierce and Smith have found that the isosteric heats of adsorption for methanol–graphite at low coverage are considerably higher than the heat of vaporization.

Our calorimetric studies for methanol–Graphon confirm the observations of Pierce and Smith. Like the latter authors, with methanol–graphite, we find that the net heat of adsorption is definitely positive even for the early increments where the isotherm is convex to the pressure axis.

(1) R. A. Beebe, B. Millard and J. Cynarski, *J. Am. Chem. Soc.*, **75**, 839 (1953).

(2) C. Pierce and R. N. Smith, Jr., THIS JOURNAL, **54**, 354 (1950).

(3) S. Brunauer, L. S. Deming, W. E. Deming and E. Teller, *J. Am. Chem. Soc.*, **62**, 1723 (1940).

Experimental

Carbon Adsorbents.—The Graphon, carbon wear dust and S84 samples were identical with those described in an earlier publication.[1] The wear dust was the sample number 2 of the earlier work and was kindly supplied by Mr. R. H. Savage. S84 was a Saran charcoal of high adsorptive capacity described by Pierce, Wiley and Smith.[4] NC-1 graphite, supplied through the courtesy of Professor Pierce, was taken from the same master batch as was the sample used by Pierce, *et al.*

Outgassing temperatures before each adsorption experiment were as follows: Graphon and wear dust, 200°; S84 charcoal, 260°.

Methanol.—Dry methanol was prepared by refluxing U.S.P. grade methanol with magnesium turnings for a total of four hours. The final product was then fractionally distilled in an all-glass apparatus, in an atmosphere of dry nitrogen. The middle fraction, boiling at 64.7°, was delivered directly through a stopcock into a 20-ml. bulb. After collection of the sample, the stopcock was closed, and the bulb sealed directly into a vacuum line which was then pumped out up to the stopcock. Removal of gases was effected by bulb-to-bulb distillation, cooling in liquid nitrogen, and evacuation until a constant vapor pressure was attained. In this process it was found better not to freeze the methanol before evacuation of the system, but rather to cool only sufficiently to reduce the vapor pressure of the liquid to a few mm. before outgassing. To facilitate the removal of dissolved gas the liquid was agitated during evacuation by a magnetically operated stirrer.[5]

Apparatus.—In some experiments the methanol was measured in the form of vapor in the gas buret which had been used for the elementary gases. However, it seemed desirable to test the possibility of error through condensation of methanol vapor in the gas buret. To do this, the methanol was measured by means of a weight buret equipped with a stopcock and the male part of a standard taper ground glass joint. Thus the buret could be connected to the adsorption system by means of the ground glass joint and a stopcock which protected the adsorption system from contact with the air while the ground glass joint was open. As successive increments of methanol were introduced, any vapor in the connecting tube, which did not get into the calorimeter, was frozen back into the weight buret by means of liquid nitrogen. Thus weighing the buret before and after each increment gave directly the weight admitted. Isotherms measured by the above volumetric and gravimetric techniques checked each other very well. This indicated that the gas buret method was sound in handling the methanol as vapor. Since methanol is not appreciably dissolved in Apiezon grease, it was found possible to use the latter on the stopcocks.

Except for the temperature of operation, the calorimetric procedure was identical with that described in the previous work on these adsorbents.[1] A constant temperature medium at 0° was achieved by surrounding the calorimeter with cracked ice. By our procedure we are measuring the isothermal calorimetric heat of adsorption as defined by Kington and Aston.[6] In no case during the present work was the isothermal heat of compression greater than 15 cal./mole of methanol. The calorimetrically measured values given in Fig. 3 are therefore identical, within experimental error, with the isosteric heats (q_{st}).

(4) C. Pierce, J. W. Wiley and R. N. Smith, Jr., THIS JOURNAL, **53**, 669 (1949).

(5) Dissolved gases, probably consisting largely of nitrogen, offered stubborn resistance to removal even after several bulb-to-bulb distillations. In some preliminary experiments, adsorption isotherms were obtained which might be described as having spurious hysteresis loops, the adsorption points falling well below and to the right of the desorption points. It was even possible to obtain an apparent scanning effect by alternating adsorption and desorption increments. The effect was doubtless caused by a buildup of pressure due to unadsorbed nitrogen during adsorption and by a more or less complete flushing out of this unadsorbed nitrogen from the space over the carbon adsorbent during desorption.

When the dissolved gases were completely removed, as was indicated by the agreement of the vapor pressure of the methanol with the accepted value (3.07 cm. at 0°), the above spurious hysteresis effect entirely disappeared.

(6) G. L. Kington and J. G. Aston, *J. Am. Chem. Soc.*, **73**, 1929 (1951).

Results

The experimental results for the adsorption of methanol at 0° on Graphon, carbon wear dust and S84 Saran charcoal are presented in Figs 1, 2 and 3.[7]

In the heat-coverage plots for Graphon and for wear dust (Fig. 3) the factor W/W_m represents the fraction of a monolayer of adsorbed methanol. W_m, the weight required to complete a monolayer, was calculated from the specific surface areas (80.0 and 770 m.²/g., respectively, for Graphon and wear dust) was determined by nitrogen adsorption. In calculating W_m for methanol from these areas it was assumed that the methanol molecule would occupy 16.2 A.²/g. in a close-packed monolayer.

It was shown in the earlier publication that it was not practicable to apply the B.E.T. method to adsorption data for the system argon–S84 as a means of determining V_m.[2] The same difficulties arise with the methanol adsorbent. We have therefore estimated W_s, the saturation weight of the adsorbed layer, by extrapolation of the methanol–S84 isotherm of Fig. 2 to $p/p_0 = 1$ and we have plotted W/W_s in Fig. 3 for the system methanol–S84. Since it is necessary to use values of W/W_s as abscissas in the case of S84 charcoal it is impossible to make a direct comparison of the heats on this adsorbent with those on the other adsorbents. However, the S84 curve is included to show that the heats are nearly constant and consistently high for all coverages.

To avoid confusion in presenting the data, the experimental points have been omitted in curves 2 and 3 of Fig. 3. Curve 2 is based on 19 adsorption points and 19 desorption points; curve 3 is based on 24 adsorption points and 6 desorption points. Because of the nature of the isotherm for the methanol–Graphon system in particular, it was possible to remove desorption increments and to measure the corresponding heats of desorption down to a coverage of less than 0.05 W/W_m.[8] For comparison, we have included curve 4 which is the heat curve calculated by means of the Clapeyron–Clausius equation by Pierce and Smith[2] from their adsorption data on the system methanol–Graphon.

Discussion

Graphon.—The isotherm of Fig. 1 for methanol–Graphon is in agreement with that previously reported by Pierce and Smith, having the form of Type VI.[2] Figure 3 shows that the calorimetrically measured heats of adsorption for this system exceed the heat of vaporization (E_L) for all degrees of coverage. Thus there is no evidence for a nega-

(7) For comparison with the isosteric heats of Pierce and Smith[2] we have attempted to obtain calorimetric heats at 0° for methanol on a sample of NC-1 graphite supplied by the above authors, although we were aware that the sensitivity of our calorimeter was too low to obtain accurate heat data for an adsorbent of such low specific surface area as the NC-1 graphite (4.0 m.²/g.).

In these measurements we obtained 12 kcal./mole for each of two successive increments at $V/V_m = 0.1$ and 0.4, and in a duplicate run we obtained 12, 11 and 10 for increments at $V/V_m = 0.4$, 0.8 and 1.0, respectively.

Although these values must be taken as only semiquantitative we have no indication for negative net heats for the system methanol–Graphon, thus tending to confirm the data of Pierce and Smith.

(8) Detailed experimental data for the methanol–Graphon system are available in our Technical Report Number 1 to the Office of Naval Research.

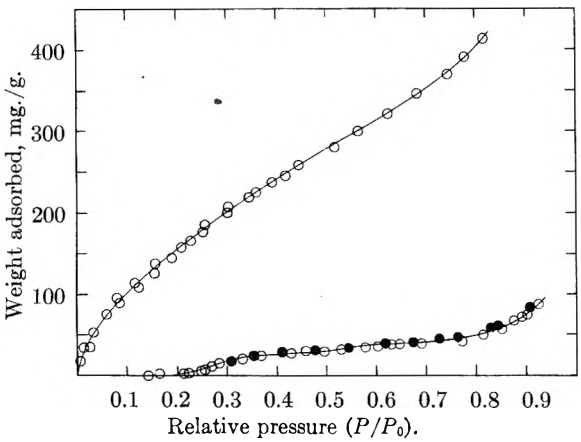

Fig. 1.—Isotherms, methanol on carbon adsorbents at 0°: upper curve, wear dust; lower curve, Graphon; adsorption, ○; desorption, ●.

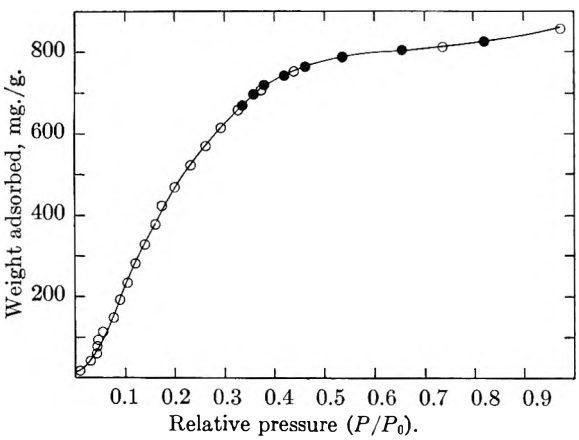

Fig. 2.—Isotherm, methanol on S84 charcoal at 0°; adsorption, ○; desorption, ●.

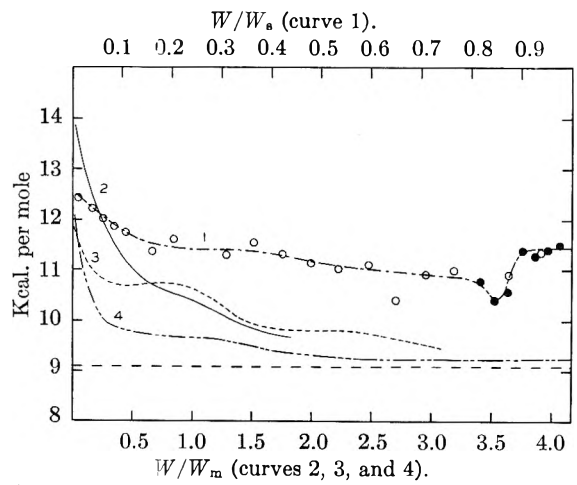

Fig. 3.—Heats of adsorption of methanol on carbon adsorbents at 0°: curve 1, —·—·—·—·—, S84 charcoal; curve 2, ————, wear dust; curve 3, - - - - - - - - - - - -, Graphon; curve 4, —··— ·—·—··—, graphite (Pierce, *et al.*), adsorption, ○; desorption, ●.

tive net heat of adsorption. In particular we see that, in the early increments up to about $0.2W_m$, the heats of adsorption exceed the heat of vaporization by one to two kcal./mole. This means that in the region where the isotherm is starting off like a Type III isotherm, and is convex to the pressure axis, we are definitely finding positive net heats. Thus the results of our experiments on Graphon are in agreement with those of Pierce and Smith on NC-1 graphite and lend strength to their contention that some modification is required for the theory of Brunauer, Deming, Deming and Teller[3] which in its present form would predict negative net heats at low coverage when the isotherm is convex to the pressure axis.

We are aware of course that the water–graphite and water–Graphon isotherms, reported by Pierce, *et al.*,[9] present an extreme Type III form, being convex to the pressure axis all the way up to saturation. It was obvious that calorimetric data on a system such as water–Graphon would be of great interest because in this case, if in any, we might expect to find negative net heats. Unfortunately, we have not been successful with our experimental method in obtaining calorimetric data for this system. It is interesting that in a recent publication Bartell and Suggitt[10] have reported negative net heats for the system water–graphite. These investigators employed a highly sensitive heat of wetting technique somewhat similar to that used by Harkins and Jura.[11]

The heat-coverage curves for nitrogen, argon and ethyl chloride on Graphon are all characterized by an increase in the heat values in the region V/V_m = 0.4 to 1.0. This effect has been attributed to lateral interaction in the adsorbed layer on the homogeneous surface of the adsorbent. There is no such increase in the heats for the system methanol–Graphon. It seems quite probable that the tendency toward hydrogen bond formation in methanol may result in less favorable conditions for observing the effect of interaction. Thus hydrogen bonding may well cause a smearing out of any sharp separation between adsorbed layers.

Wear Dust.—The wear dust isotherm in Fig. 1 has the form of Type II with a low C value (C = 2.6 for the B.E.T. treatment). Earlier heat experiments[1] with nitrogen and argon on this adsorbent had indicated that there was a considerable amount of adsorbing surface producing heats well above the value of approximately 3.0 kcal./mole found on a homogeneous surface like Graphon. This led to the conclusion that the surface was in general heterogeneous although some earlier work of Savage[12] suggested the possibility of a homogeneous surface.

From Fig. 3 it is seen that, on wear dust, methanol behaves in a way similar to argon and nitrogen, although the step in the heat coverage curves, which is present with the elementary gases, is virtually absent with methanol. The heat data at low coverage for methanol provide further support for the conclusion that the surface of this adsorbent is heterogeneous, since the values fall continuously for successive increments. Savage[13] has reported evidence for the chemisorption of oxygen on wear dust which led, as might be expected, to considerably enhanced water adsorption. It may be that our

(9) C. Pierce, R. N. Smith, Jr., J. W. Wiley and H. Cordes, *J. Am. Chem. Soc.*, **73**, 4551 (1951).
(10) F. E. Bartell and R. M. Suggitt, *ibid.*, **58**, 36 (1954).
(11) W. D. Harkins and G. Jura, *ibid.*, **66**, 1362 (1944).
(12) R. H. Savage, *J. Appl. Phys.*, **19**, 1 (1948).
(13) R. H. Savage, *Ann. N. Y. Acad. Sci.*, **53**, 862 (1951).

wear dust samples had adsorbed some oxygen during exposure to air and that this might account in part for the high heats of adsorption of methanol, a polar substance. However, because of the similarity in the heat curves for methanol, a polar adsorbate, and for argon which is non-polar we believe that the effect of chemisorbed oxygen is of less importance here, than the effect of physical heterogeneity of surface, in accounting for the data of Fig. 3.

S84 Saran Charcoal.—In comparing the heat-coverage curve for methanol on S84 charcoal with those on the other two adsorbents, it is important to remember that the S84 is a porous material whereas the Graphon and wear dust are essentially non-porous.[1,12] Hence as was suggested in the interpretation of the heat data for argon and nitrogen on these adsorbents, we believe that the sustained high level of the heat curve on S84 even at high coverage may be attributed to a coöperative effect of the opposite walls of the capillaries. With the non-porous adsorbents this coöperative effect of the walls would of course be absent.

Finally, attention should be called to the irregular hump in the heat curve for methanol–S84 of Fig. 3 in the region beyond 0.8 W_m. We have reported a similar hump for the system argon–S84.[1] As with the argon experiments, the hump of Fig. 3 is confirmed by both adsorption and desorption points.[14] It is interesting that Kington[15] and his co-workers have found a hump in their heat curves above 0.8 W_m for both argon and oxygen on chabazite at −183°. These investigators have suggested that some sort of exothermic rearrangement of the adsorbed phase may occur as the equilibrium pressure approaches saturation. Whatever the true explanation, it seems probable that the same explanation would be applicable to the cases of the artificially porous Saran charcoal and the naturally porous chabazite.

Acknowledgment.—Our thanks are due to the Office of Naval Research for support of this investigation.

(14) Because of the very high total adsorptive capacity of the S84 charcoal, it was possible to employ a high ratio of metal to adsorbent in the calorimeter. This produced very favorable conditions for rapid heat distribution and as a result we have especially high confidence in this particular heat run on S84. It seems to us therefore that the final maximum in Fig. 3 is real and not due to some artifact in the apparatus.

(15) G. L. Kington, Aberdeen University, Aberdeen, Scotland, private communication.

DIFFUSION AND REACTION RATE IN POROUS SYNTHETIC AMMONIA CATALYSTS

By C. Bokhoven and W. van Raayen

Staatsmijnen in Limburg, Centraal Laboratorium, Geleen, Holland

Received January 11, 1954

The effective diffusion constant of oxygen in nitrogen through tablets of a synthetic ammonia catalyst was measured at room temperature and atmospheric pressure. From the diffusion rate of oxygen the value of the effective diffusion constant of ammonia under reaction conditions was calculated. The activity of catalyst particles of different mesh-size was measured at 1 and 30 atm. and at different temperatures. A clear difference in activity between the small and large particles was found. Moreover, a plot of the logarithm of the rate constant against the reciprocal absolute temperature showed a decreasing slope at increasing temperature, except for the small particle size at 30 atm. These results could be quantitatively accounted for by the retardation of the reaction rate due to the restricted diffusion rate of ammonia through the pores of the catalyst particles.

1. Introduction.—In porous catalyst particles the reactants have to move by diffusion to the internal surface in order to react. It is well-known that under certain conditions (high temperature, large particle size), the diffusion rate may be insufficient to maintain an equal concentration inside and outside the catalyst particle.

As a result, the reaction rate will be smaller than would correspond with the intrinsic activity of the catalyst surface. The degree of retardation can be expressed in the effectiveness factor E, the ratio of the experimental and the true reaction rate constant. The retardation manifests itself among other things in the following phenomena: (a) the activity of the catalyst decreases with increasing particle size; (b) a plot of the logarithm of the rate constant against the reciprocal absolute temperature, which according to the Arrhenius relation is normally a straight line, shows a decreasing slope at increasing temperature. This corresponds with an apparent decrease (of maximal a factor 2) in the activation energy at increasing temperature.[1]

It is generally accepted that the reaction rate of the ammonia synthesis is too slow to be retarded by the restricted diffusion rate. This view is supported by the results of some activity measurements by Larson and Tour[2] at 100 atm. and 475°. Under these conditions no influence of the particle size on the reaction rate was observed. However, from estimations which Wagner[3] and Wheeler[4] have made of the diffusion rate inside the porous catalyst particles it appeared that under technical conditions a retardation of the reaction rate may be expected. For lack of reliable data, these estimations must be considered as rather rough. In view

(1) E. Wicke, *Angew. Chem.*, **B19**, 57 (1947); J. B. Zeldowitsch, *Acta Physicochim. (U.S.S.R.)*, **10**, 583 (1939).

(2) A. T. Larson and R. S. Tour, *Chem. and Met. Eng.*, **26**, 647 (1922)

(3) C. Wagner, *Z. physik. Chem.*, **A193**, 1 (1943).

(4) A. Wheeler, *Advances in Catalysis*, **3**, 249 (1951).

of this discrepancy Wagner pointed out that at high pressure, transport of adsorbed molecules or radicals by surface migration might contribute considerably to the diffusion rate. Some evidence for the phenomenon of surface migration is given by the exchange experiments between N_2^{30} and N_2^{28} over iron–synthetic ammonia catalysts.[5]

2. Scope of this Investigation.—A number of activity measurements at different temperatures and pressures were carried out with an iron catalyst of the normal type (catalyst A, promoted with 2.9% Al_2O_3 and 1.1% K_2O), using two different particle sizes. Obviously the results of these activity measurements had to be interpreted in terms of diffusional retardation.

For this reason information was obtained about the effective diffusion constant under reaction conditions by means of a method, devised by Dr. Hoogschagen[6] of this Laboratory, by which the diffusion constant of oxygen in nitrogen through large cylindrical tablets (ten by ten mm.) of the same catalyst is determined.

However, it appeared that after reduction at 450°, tablets of catalyst A were obtained with a surface area (5 m.²/g.) much smaller than the normal value (10–15 m.²/g.). This result is not a matter for surprise, for it was also found in this Laboratory that for this type of catalyst the surface area after reduction depends on the particle size.[7] Under the same reduction conditions large particles show a lower reduction rate and a smaller surface area than small particles. Thus it is clear that the results of the diffusion rate measurements for this catalyst are not representative for the conditions of the activity measurements.

The above mentioned particle size effect is much less pronounced with a catalyst promoted with MgO. After reduction of tablets of a catalyst promoted with 4.3% MgO and 0.55% SiO_2 (catalyst B) we succeeded in getting a tablet with a surface area of 11.6 m.²/g. The various properties of the catalysts A and B are summarized in Table I.

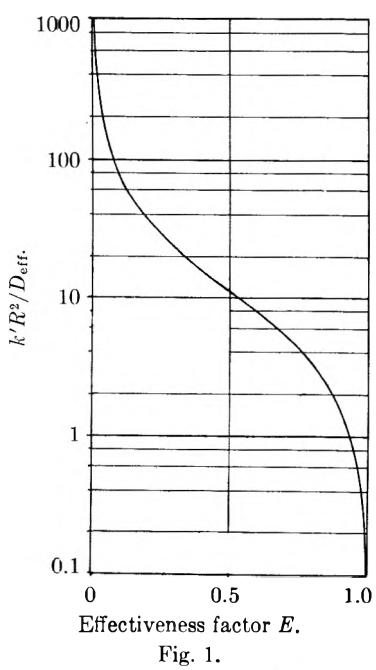

Fig. 1.

TABLE I

PROPERTIES OF SYNTHETIC AMMONIA–IRON CATALYSTS A AND B

Catalyst	Surface area, m.²/g.	Porosity	Mean pore radius, Å. From pore vol. and surface area	Mean pore radius, Å. From mercury penetration
A (2.9% Al_2O_3 + 1.1% K_2O)	13.1	0.52	177	151
B (4.3% MgO + 0.55% SiO_2)	11.6	0.52	202	...

As catalyst B has about the same surface area and porosity as catalyst A, it was considered reasonable to use the diffusion data obtained with catalyst B for the interpretation of the activity measurements with catalyst A.

From measurements of the pore size distribution of catalyst A carried out by P. Zwietering and H. L. T. Koks[8] of this Laboratory, it finally appeared that the mean pore radius calculated from the pore size distribution differs relatively little from the value calculated from the pore volume and pore surface.

We will give now a full account of both the diffusion and the activity measurements.[9]

3. The Effectiveness Factor.—Wagner[2] has shown that for a first-order reaction and a spherical catalyst particle the effectiveness factor E depends on the value of a dimensionless number

$$k'R^2/D_{eff}$$

where

k' = exptl. first-order rate constant
R = radius of the catalyst particle
D_{eff} = effective diffusion constant

The relation between E and the modulus $k'R^2/D_{eff}$ is given in Fig. 1, which has been taken from Wagner's paper. In order to calculate the effectiveness factor E, both the first-order rate constant k' and the value of D_{eff} under reaction conditions must be known.

Wagner showed that the same relation for the effectiveness factor is also valid for reactions whose rate is proportional to the concentration difference of one of the reactants with regard to the concentration at equilibrium

$$\frac{dc}{d\tau} = -k'(c - c_{equil}), \text{ or } \frac{d\eta}{d\tau} = k'(1 - \eta) \qquad (1)$$

By integration

$$k' = \frac{1}{\tau(1 - \epsilon)} \ln (1 - \eta) \qquad (2)$$

where

η = efficiency (c/c_{equil})
τ = contact time calcd. for the empty reactor
ϵ = intra-particle porosity.

(5) J. T. Kummer and P. H. Emmett, *J. Chem. Phys.*, **19**, 289 (1951).

(6) C. Bokhoven and J. Hoogschagen, *ibid.*, **21**, 159 (1953).

(7) For the particle sizes used in the activity measurements this effect is negligible.

(8) P. Zwietering and H. L. T. Koks, *Nature.*, **173**, 683 (1954).

(9) The results of these measurements were already communicated by one of the authors at the XIIIth International Congress for Pure and Applied Chemistry (Stockholm, 1953).

However the kinetics of the ammonia synthesis can only reasonably be described by the Temkin–Pyzhev[10] equation

$$\frac{dP_{NH_3}}{d\tau} = k_1 \frac{P_{N_2}P_{H_2}^{1.5}}{P_{NH_3}} - k_2 \frac{P_{NH_3}}{P_{H_2}^{1.5}} \qquad (3)$$

Neglecting the decrease in volume during reaction, the relation between the rate constant k_2, the contact time τ and the efficiency η can be found by integration

$$k_2 = -1/2(3/4)^{1.5}\frac{P^{1.5}}{\tau} \ln (1 - \eta^2) \qquad (4)$$

where

$\eta = P_{NH_3}/P_{NH_3\ equil}$
P = total pressure

Near equilibrium ($\eta \sim 1$) equation 4 is equivalent to equation 2. Therefore it will be clear that as a first approximation the Wagner method can also be applied to the ammonia synthesis. As will appear from our results this is allowed for experiments at high efficiencies with low effectiveness factors.

Finally it should be remarked that a rigorous solution meets with serious mathematical difficulties.

4. Effective Diffusion Constant.—Wagner, following Wicke and Kallenbach,[11] formally defined D_{eff} by Fick's relation

$$\dot{n} = D_{eff} S \times \text{grad } c \qquad (5)$$

where

$\dot{n}$ = rate of transport by diffusion
S = cross-sectional area of the porous substance
grad C = the concn. gradient in the gas phase in the direction of transport

According to this definition D_{eff} can be determined experimentally without making any assumption as to the structure of the pore system.

When the ammonia synthesis is carried out at not too high pressures, the relative change in the ammonia concentration is much greater than in the hydrogen and nitrogen concentrations. Consequently, the degree of retardation by diffusion is determined by the diffusion rate of ammonia through the hydrogen–nitrogen mixture. As it is very difficult to measure the effective diffusion constant of ammonia under reaction conditions, the diffusion constant of oxygen in nitrogen through catalyst tablets at room temperature and atmospheric pressure was measured. From the results of these measurements the effective diffusion constant of ammonia was calculated.

These measurements were carried out by a simple method which was devised by Dr. Hoogschagen[12] (Fig. 2). Atmospheric oxygen diffuses through the porous tablet connected to the apparatus by means of a piece of rubber tubing. By heating the widened part of the closed circuit, where active copper particles absorb the oxygen completely, a circulation flow is established. From the weight gain of the apparatus, the effective diffusion constant can be easily calculated.

The effective diffusion constant for oxygen in nitrogen through reduced tablets of catalyst B was determined at room temperature and atmospheric pressure. For this catalyst a value of 0.0078 cm.²/sec. (mean value of 0.0074 and 0.0082) for $D^{O_2\text{-}N_2}$ was found.

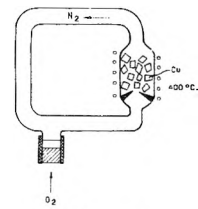

Fig. 2

In order to calculate the effective diffusion constant of ammonia under reaction conditions from the diffusion rate of oxygen, the following assumptions were made

(a) The diffusion constant D inside the pores of the catalyst can be calculated from the well-known formulas for Knudsen and normal gas diffusion

$$D_k = \frac{2r}{3}\sqrt{\frac{8RT}{\pi M}} \qquad (6)$$

$$D_b(\text{T.P.}) = \frac{D_b(P = 1,\ T = 300°\text{K.})}{P}\left(\frac{T}{300}\right)^{1.75} \qquad (7)$$

and from the formula Wheeler[4] has given for the transition region between pure Knudsen and bulk diffusion.

$$D = D_b(1 - e^{-D_k/D_b}) \qquad (8)$$

where

D = diffusion constant inside the pores
D_k = Knudsen diffusion constant
D_b = bulk diffusion constant
R = gas constant
r = mean pore radius
M = molecular weight
T = absolute temp.

(b) The ratio D_{eff}/D of the effective diffusion constant D_{eff} and the actual diffusion constant D inside the pores is a constant, which only depends on the porosity of the catalyst and the tortuosity of the pores, and is the same for Knudsen and bulk diffusion. This ratio will be calculated from the experimental value of 0.0078 cm.²/sec.

(c) The pore size distribution is homogeneous.

(d) The ratio mentioned in (b) is the same for catalyst B used in the diffusion experiments and for catalyst A used for the activity measurements. The mean pore radius of the former amounts to 202 Å., of the latter to 177 Å.

The diffusion constant of oxygen in nitrogen inside pores of 202 Å. radius at 1 atm. and room temperature can be calculated from formulas 6 and 8 after substituting the value 0.21 cm.²/sec. for the bulk diffusion constant of oxygen in nitrogen. In this way a value of 0.054 cm.²/sec. is found. In consequence the ratio D_{eff}/D mentioned in (b) equals the reasonable value of 0.0078/0.054 = 0.14.

From the formulas 6, 7 and 8, the value 0.14 for D_{eff}/D and from the mean pore radius of 177 Å. for catalyst A, the effective diffusion constant of ammonia for the conditions of the activity measurements can now be calculated. The required value of

$$D_b^{NH_3}(P = 1,\ T = 300°\text{K.})$$

was calculated by means of a formula which Buddenberg and Wilke[13] have given for the diffusion constant in multicomponent gas mixtures

$$D_b^{HN_3} = \frac{1 - x_{NH_3}}{x_{H_2}/D_{NH_3\text{-}H_2} + x_{N_2}/D_{NH_3\text{-}N_2}}$$

(10) M. Temkin and V. Pyzhev, *Acta Physicochim.* (*U.S.S.R.*), **12**, 327 (1940).

(11) E. Wicke and R. Kallenbach, *Kolloid-Z.*, **97**, 135 (1941).

(12) A detailed account of the diffusion measurements will be given elsewhere by Dr. Hoogschagen.

(13) J. W. Buddenberg and C. R. Wilke, *Ind. Eng. Chem.*, **41**, 1345 (1949).

where x = the mole fraction. After substitution of the values $D_{NH_3 \cdot H_2} = 0.68$ cm.^{2}/sec. and $D_{NH_3 \cdot N_2} = 0.19$ cm.^{2}/sec., given by Andrussow,[14] for a $3H_2$: $1N_2$ mixture a value of 0.41 cm.^{2}/sec. for $D_b^{NH_3}$ ($P = 1$, $T = 300°K.$) is obtained.

The calculated values of $D_{eff}^{NH_3}$ are shown in Fig. 3, as a function of pressure and at different temperatures. At low pressure the effective diffusion constant is nearly independent of pressure (Knudsen diffusion), whereas at high pressure D_{eff} decreases in inverse proportion to pressure (bulk diffusion).

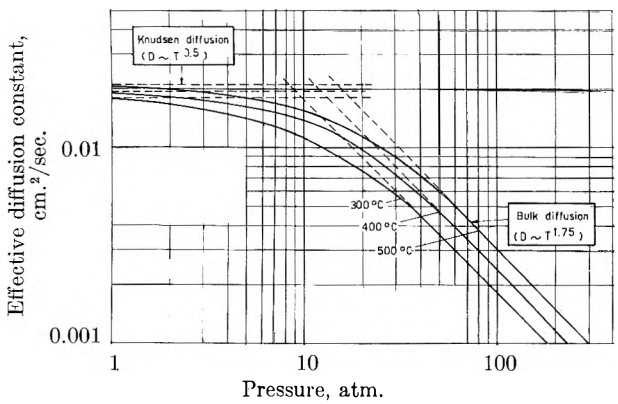

Fig. 3.

5. **Activity Measurements.**—The activity measurements were carried out with catalyst particles of different size, which had been reduced under identical conditions (1 atm., 450°, space velocity 10,000 hr.$^{-1}$). The activity was measured at 1 and 30 atm. and at different temperatures. Frequent cross checks were made to be sure that the catalytic activity did not change during the experiments. Points were measured both from lower to higher temperature and back again.

The apparatus used for the activity measurements is shown in Fig. 4. Commercial hydrogen and nitrogen in the ratio 3:1 were pressed into an ordinary 150-atm. cylinder. From this cylinder the gas mixture was passed over a purification train consisting of: (a) a vessel filled with activated carbon soaked in a solution of $ZnCl_2$ for the removal of traces of ammonia; (b) a converter filled with a reduced copper catalyst for the removal of oxygen at 330°; (c) a converter filled with a nickel catalyst of the pumice-supported type for the hydrogenation of trace quantities of carbon monoxide into methane at a temperature of 275°; (d) a vessel filled with sodium hydroxide for the removal of trace quantities of carbon dioxide; (e) two vessels filled with activated alumina for the elimination of water.

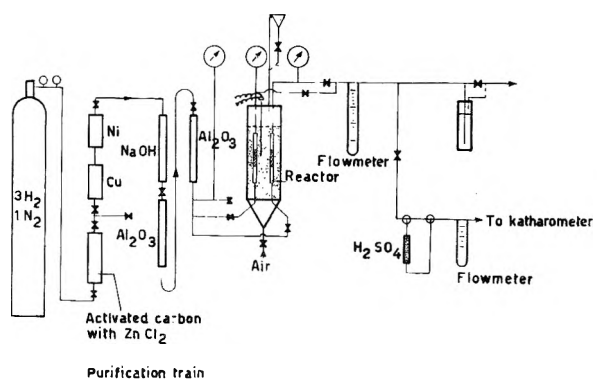

Fig. 4.—Apparatus for activity measurements.

From the purification train the gas mixture can be led to two parallel tubular reactors (6 mm. dia.). The reactors were filled with a supporting bed of glass spheres, a layer of catalyst particles topped by another layer of glass spheres. The reactor was heated by means of a fluid bed of carborundum powder (particle size 100 μ), using air as fluidizing gas. The temperature of the fluid bed was kept constant within 1° by means of a relay system controlled by a resistance thermometer in a Wheatstone bridge circuit. The pressure of the gas mixture leaving the reactor was reduced to 1 atmosphere, after which the flow rate was measured with a glass capillary flowmeter. In the high pressure measurements, the ammonia content was determined by means of thermal conductivity cells (katharometer), whereas the small concentrations in the measurements made at 1 atm. were determined by titration after absorption in a 0.1 N sulfuric acid solution. The katharometer consisted of an air-filled reference cell and a measuring cell. This cell assembly was immersed in a thermostated bath. The sensitivity of the system amounts to 0.793% NH_3 per millivolt, while a stability of about 0.02 millivolt could be obtained. This corresponds with an accuracy of 0.015% NH_3. The katharometer was calibrated both with H_2–N_2 and H_2–N_2–NH_3 mixtures. For the determination of the H_2/N_2 ratio and the ammonia content the gas mixture was led through the measuring cell both before and after ammonia removal.

The results of the activity measurements are given in Table II and in Figs. 5 and 6, where the activity, expressed as the reaction rate constant calculated according to the Temkin theory,[10] is plotted against the reciprocal absolute temperature.

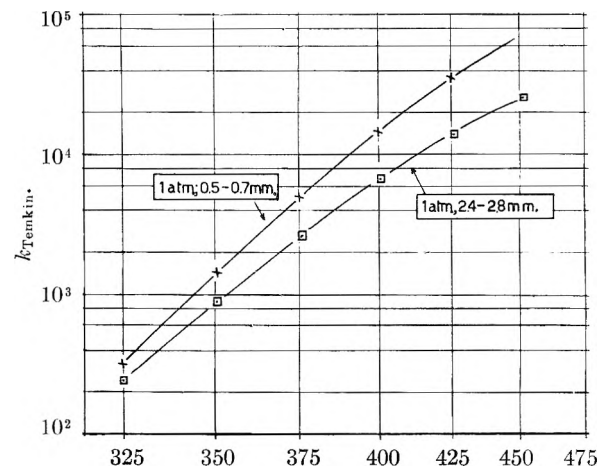

Fig. 5.

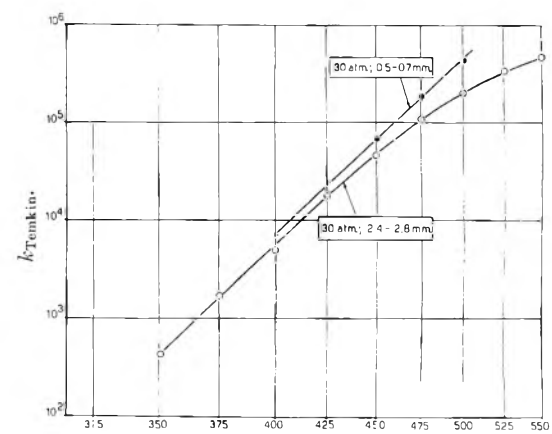

Fig. 6.

For the measurements at 1 atmosphere the rate constants were calculated according to equa-

(14) L. Andrussow, *Z. Elektrochem.*, **54**, 566 (1950).

TABLE II

RESULTS OF ACTIVITY MEASUREMENTS

Run	Part size, mm.	Press., atm.	Temp., °C.	Space vel. {cm.³ (NTP)}/ cm.³ cat. hr.	Efficiency $P_{NH_3(outlet)}/P_{NH_3(equil)}$	k_{Temkin} (before cor.)	Effectiveness factor
1	0.5–0.7	1	325	10880	0.238	319	0.995
2			350	19380	.366	1440	.955
3			374.5	19860	.607	4600	.90
4			400.5	42750	.700	14500	.75
5			424.5	62750	.816	34900	.55
6			450	98200	.876	72900	.36
7	2.4–2.8	1	325.5	11320	.201	236	.78
8			350.5	17800	.300	850	.53
9			375.5	32500	.372	2450	.29
10			399.5	33700	.556	6300	.17
11			425.5	56350	.617	13500	.08
12			450	82850	.668	25200	.05
13	0.5–0.7	30	400	14120	.472	7380	1.0
14			425	41800	.507	24600	0.995
15			450	49750	.692	69700	.985
16			476	82600	.804	196000	.95
17			500	146800	.849	444000	.89
18	2.4–2.8	30	351	6830	.213	444	.995
19			375	8260	.359	1740	.975
20			400	10620	.483	5010	.95
21			425	16000	.655	17800	.87
22			450	31150	.712	47400	.76
23			475.5	57800	.754	110700	.55
24			500	92500	.774	199000	.40
25			525	106400	.843	324000	.32
26			549.5	124500	.883	475000	.25

tion 4, which was rearranged to

$$k = -1/2P^{1/2}V_0 \ln (1 - \gamma^2)$$

where V_0 = entering space velocity {cm.³ gas (N.T.P.)}/(cm.³ cat. hour).

For the high pressure experiments the slightly modified expression of Emmett and Kummer[15] was used

$$k = P^{1/2}V_0 \int_0^z \frac{z(1 - z)^{1.5}dz}{(1 + z)^3[L^2(1 - z)^4 - z^2]}$$

where

z = mole fraction of ammonia = P_{NH_3}/P_{total}

$$L^2 = \frac{z^2_{equil}}{(1 - z_{equil})^4}$$

The calculated Temkin rate constants were corrected for retardation by diffusion in the following way:

(a) The pseudo first-order rate constant k' is calculated according to equation 2

$$k' = \frac{\text{space velocity}}{3600} \times \frac{1}{P} \frac{T}{273} \frac{1}{1 - \epsilon} \ln (1 - \eta)$$

(b) $D^{NH_3}_{eff}$ under reaction conditions is taken from Fig. 3.

(c) From the value of the modulus $k'R^2/D^{NH_3}_{eff}$ the effectiveness factor is taken from Fig. 1.

(d) The true rate constants are obtained after multiplying the Temkin rate constant by $1/E$.

6. Discussion of the Results.—The results of the activity measurements on particles of two different sizes (resp., 0.5–0.7 and 2.4–2.8 mm.) carried out at 1 and at 30 atm. are given in Figs. 5 and 6 and in Table II. We notice a clear difference in activity between the small and the large particles, especially at 1 atm. Moreover all curves, except the one for the smaller particles at 30 atm., show a decreasing slope at increasing temperature. These results are in full agreement with the assumption that the reaction rate is retarded by restricted diffusion.

In Fig. 7 the rate constants, corrected for the restricted diffusion, are plotted. All curves have become straight lines, three of them having the same slope. The values of the apparent activation energy are also mentioned in Fig. 7. There is a fair correspondence between these values, which are also in agreement with the value of 46.5 kcal./mole predicted by the Temkin theory. The less favorable result of the correction procedure for the measurements on the larger particles at 1 atm. is not a

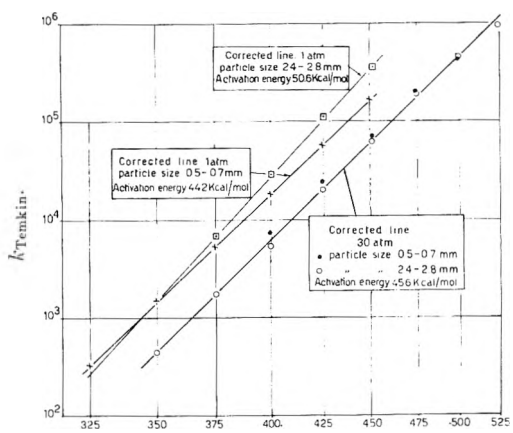

Fig. 7.

(15) P. H. Emmett and J. T. Kummer, *Ind. Eng. Chem.*, **35**, 677 (1943).

matter for surprise. In this case very high correction factors were found; *e.g.*, at 450° (run 12) the effectiveness factor E was only 5%, so that the correction factor amounts to about 20. It is clear that for such a strong retardation the simple correction method applied here is no longer reliable. Taking it all together, the results of our correction procedure provide a definite proof that the results given in Figs. 5 and 6 must be interpreted by diffusional retardation. Moreover, we may conclude that the values of the effective diffusion constant (Fig. 3) are approximately right.

For the calculation of the effective diffusion constants the phenomenon of surface migration suggested by Wagner was not taken into account. From the results obtained it is clear, however, that at pressures of up to 30 atm. this surface migration cannot contribute appreciably to the effective diffusion constant, since otherwise the rate constants would be overcompensated.

Finally, it should be remarked that the Temkin rate constants at 1 and 30 atm. differ by a factor of about 2, which is in contradiction with the Temkin theory. These and other kinetic results will be discussed in a separate paper.

7. Measurements by Larson and Tour.—It is interesting now to return to the measurements by Larson and Tour mentioned before. These authors did not find any influence of the particle size on the activity at 100 atm. Larson and Tour also carried out activity measurements at lower pressure. Since, especially at low pressures, an influence of the retardation by diffusion must be expected,[8] we calculated from their measurements at different temperatures the Temkin rate constants and from these the value of the apparent activation energy. Moreover, the effectiveness factor was calculated.[16] The results are given in Table III.

TABLE III

APPARENT ACTIVATION ENERGY AND EFFECTIVENESS FACTOR CALCULATED FROM MEASUREMENTS BY LARSON AND TOUR

Particle size, mm.	Pressure, atm.	Activation energy, kcal./mole	$E_{450°}$
1.4–2.4	1	23 (400–450°)	0.20
...[a]	10	29 (400–450°)	...
...[a]	31.6	37 (400–450°)	...
2.4–3.3[b]	100	50 (425–450°)	0.80

[a] For these measurements the particle size is not mentioned. [b] Largest particle size mentioned by the authors.

It appears that the activation energy increases by a factor 2, when going from low to high pressure. This is a clear indication that these measurements were affected by diffusional retardation.

In full agreement with this conclusion are the calculated values of the effectiveness factor. At 100 atm. the diffusional retardation, for the particle sizes used, is too small to be observed. Measurements at lower pressures would undoubtedly have shown a clear particle size effect.

8. Estimation of the Degree of Retardation under Industrial Conditions.—To estimate the degree of retardation at high pressures, the dependence of the modulus $k'R^2/D^{NH_3}_{eff}$ on the pressure must be examined. At high pressures D_{eff} decreases as $1/P$ (Fig. 3), while according to the Temkin relation the pseudo first-order rate constant decreases as $1/P^{1.5}$. Consequently k'/D_{eff} decreases as $1/P^{0.5}$, so that the retardation effect decreases at increasing pressure. However, it can be shown that for the particle sizes used in industrial practice, the reaction rate may still be retarded at pressures as high as 300 atm.

In order to estimate the effectiveness factor E under these conditions, we make use of the activity measurements by Nielsen,[17] which are the only high pressure activity measurements for which the particle size is given. From the results of Nielsen the pseudo first-order rate constant can be calculated, while the effective diffusion constant can be taken from Fig. 3. Table IV shows the effectiveness factor for the particle size used by Nielsen as well as the extrapolated values for a particle size of 5 and 10 mm.

From the results it appears that even at 330 atm. there may be a considerable retardation of the reaction rate if the catalyst particles are larger than 3 mm.

As long as there is no evidence that surface migration contributes to the diffusion rate, which seems to be true at pressures up to 30 atm., it must be expected that under technical conditions (300 atm., 450°, particle size 5–10 mm.) the restricted diffusion rate of ammonia through the pores of the catalyst particles will retard the reaction rate.

TABLE IV

EFFECTIVENESS FACTOR CALCULATED FROM MEASUREMENTS OF NIELSEN
(CATALYST E, PARTICLE SIZE 1.2–2.3 MM.)

Press., atm.	Temp., °C.	Space vel. cm.³ (NTP)/ cm.³ cat. hr.	Efficiency	E	E (5 mm.)	E (10 mm.)
330	450	15500	0.56	0.96	0.74	0.38
330	450	71000	.43	.89	.41	.15
330	480	30000	.57	.93	.59	.23
360	450	15000	.54	.98	.76	.40

Acknowledgment.—We wish to thank Dr. C. van Heerden for the helpful discussions in the course of this work. Thanks are also due to Prof. D. W. van Krevelen and Prof. J. H. de Boer for their interest shown in this investigation.

(16) For this calculation the values of $D^{NH_3}_{eff}$ from Fig. 3 were used. These values are considered reasonably representative for normal iron catalysts.

(17) A. Nielsen, "An Investigation on Promoted Iron Catalysts for the Synthesis of Ammonia," Copenhagen, 1950.

ELECTRICAL PROPERTIES OF SOLIDS. XVIII. POLARIZATION IN POLYELECTROLYTES[1]

By Michael Yamin[2] and Raymond M. Fuoss

Contribution No. 1212 from the Sterling Chemistry Laboratory of Yale University, New Haven, Conn.

Received January 12, 1954

Conducting polymeric systems can be made by quaternizing poly-4-vinylpyridine with alkyl halides such as methyl bromide. Conductance is increased by plasticizing with dibutyl tartrate. By using bromidized silver foil electrodes and a highly conducting paste (polyelectrolyte plus plasticizer, or polyvinyl chloride, tricresyl phosphate and a quaternary bromide) to eliminate the air film between the electrodes and the plastic, values of d.c. conductance are observed which are substantially independent of time and voltage. This result is in marked contrast with measurements made using ASTM foil-vaseline contacts; the large changes of apparent resistance with the latter contacts are ascribed to electrode polarization. The quaternized polymer possesses the ability to store charge; the corresponding dielectric constant increment exhibits a dispersion in the power and audio-frequency range. A broad spread of relaxation times appears.

Introduction

Previous work on polymeric systems which have a moderate ionic conductance includes data for plasticized polyvinyl chloride containing tetrabutylammonium picrate[3] and plasticized poly-4-vinylpyridinium picrate.[4] In the former case, aquadag was used to eliminate the air film between sample and cell electrodes; in the latter, a thin vaseline film was used. In both cases, the d.c. conductance decreased with time when a fixed voltage was applied to the cell; furthermore, different values of apparent conductance were obtained at different voltages. The field strengths were far below those at which a Wien effect might be expected, and it was easy to show that the resistance changes were not the trivial consequence of temperature changes in the sample produced by the flow of bridge current during measurement. The a.c. properties showed an excess dielectric constant and loss factor ($\Delta\epsilon'$ and $\Delta\epsilon''$) which were superimposed on the background values of the non-electrolytic solvent–polymer; both $\Delta\epsilon'$ and $\Delta\epsilon''$ varied approximately inversely as the square root of the frequency of the applied field.

Properties such as those just described could be the consequence of polarization arising from the inherent irreversibility of the electrode surfaces with respect to the ions in the polymeric medium. The purpose of this paper is to present experimental evidence which supports this hypothesis, and to describe a method which eliminates most of the uncertainty due to phenomena at the interface between sample and electrode for the case of plastics containing bromide ions. Briefly described, the method consists in using bromidized silver foil as the electrodes, and using a thin film of a highly conducting electrolytic paste to displace the air film between the sample and the electrode. When surface effects are thus eliminated (or at least, very much reduced), d.c. conductance is found to be independent of time and voltage. The a.c. properties which were linear in $f^{-1/2}$ are also eliminated; instead, a dielectric constant term appears which shows a sigmoid dispersion, and is accompanied by a dielectric loss which has a maximum. The data show that a distribution of relaxation times is needed to describe these ionic terms in the a.c. properties.

Experimental

Materials.—Poly-4-vinylpyridine was prepared by E. B. FitzGerald by emulsion polymerization.[5] The polymer was partially quaternized in dimethylformamide solution by the addition of predetermined amounts of methyl bromide. To 500 ml. of solvent, 50 g. of polymer was added and dissolved by rolling the mixture for 24–48 hr. A weighed portion of the viscous solution was cooled to 5° by standing in the cold room and then methyl bromide (condensed from a cylinder) was added from a pipet held under the surface of the solution. The mixture was allowed to warm to room temperature and was rolled another 18 hr. The final solution was usually amber in color; occasionally it was green, presumably as a consequence of a sequence of reactions (pyridinium salt → pyridinium hydroxide → pyridol → pyridone → dyestuff) initiated by dimethylamine which was in turn a hydrolysis product of the solvent. The polysalt was precipitated by pouring the reaction mixture dropwise (not over 5 ml./min.) into 10 volumes of dry dioxane, with violent stirring. The granular precipitate was washed 5–10 times on a büchner funnel with dioxane and dried under vacuum at 40°. The salts were analyzed by potentiometric titration in 50–50 methanol–water against 0.01 *N* silver nitrate solution, using a glass electrode as reference and a lightly bromidized silver wire as sensitive electrode. The titration solution was acidified (*ca.* 0.03 *N*) with nitric acid in order to stabilize the glass electrode. The products are copolymers of 4-vinylpyridine and 4-vinyl-N-methylpyridinium bromide; the percentage q of total nitrogens quaternized can be calculated readily from the bromide analyses.

Several of the salts were plasticized with dibutyl tartrate[4] by dissolving the desired amount of plasticizer in petroleum ether and adding the solution to a weighed portion of salt. The slurry was stirred until the solvent had evaporated; the resulting damp powder was heated for about 10 min. at 120° to allow the plasticizer to strike in, and then the last traces of petroleum ether were removed by several hours heating at 40° under vacuum. The plasticized materials were then again analyzed for bromide; the ratio of bromide contents before and after plasticizing gave an accurate figure for the amount of copolymer and of plasticizer in the final sample. Errors due to plasticizer evaporation were thereby avoided.

Discs for electrical measurements (5 cm. diameter, initially 2–3 mm. thick) were pressed as described in the previous paper of this series, except that lower press temperatures (140–150°) and longer times (7–10 min.) were used. The copolymers of low electrolyte content molded readily; with increasing extent of quaternization, the plastics became more brittle and showed a tendency to liquefy suddenly rather than to become softer on heating. This behavior resembles that of ordinary salts which of course have sharp melting points. Furthermore, plasticization did not pro-

(1) Project No. 051-002 of the Office of Naval Research, Paper No. 42.

(2) This paper is abstracted from a thesis presented by Michael Yamin to the Graduate School of Yale University in partial fulfillment of the requirements for the Degree of Doctor of Philosophy, June, 1952.

(3) D. J. Mead and R. M. Fuoss, *J. Am. Chem. Soc.*, **67**, 1566 (1945).

(4) W. N. Maclay and R. M. Fuoss, *ibid.*, **73**, 4065 (1951).

(5) E. B. FitzGerald and R. M. Fuoss, *Ind. Eng. Chem.*, **42**, 160 (1950).

duce elastomers: a sample (13% quaternized) containing 33% dibutyl tartrate felt and cut like ordinary polystyrene.

A minute amount of Dow-Corning silicone grease wiped onto the dies served as a satisfactory mold release. For brittle materials, discs of tin foil with a film of silicone grease between the molding powder and the top and bottom dies were used in order to avoid cracking the samples.

Table I summarizes the various compositions which were measured electrically. In order to simplify reference to them, a two-figure code is used, in which the first gives q, the approximate per cent. quaternization and the second p, the approximate per cent. plasticization; for example, sample 8-24 has 8.43% of the nitrogen atoms quaternized, and the material contains 24.2 weight % dibutyl phthalate. Densities (ρ in Table I) were determined from the weights and dimensions of the discs.

TABLE I

COMPOSITION OF POLYELECTROLYTE SAMPLES

No.	q	p	ρ	Q
0-0	0.00	0.0	1.130	..
8-0	8.25	.0	1.202	27
14-0	13.70	.0	...	26
27-0	26.75	.0	1.271	20
8-16	7.50	16.1	1.198	33
8-24	8.43	24.2	1.182	47
13-18	12.95	17.9	1.212	39
13-30	12.95	30.5	1.189	41

Electrodes.—The discs were measured in the guarded copper cell with platinum electrodes.[6] In order to obtain good (a.c.) electrical contact with the samples without an intervening air film,[7,8] tin foil electrodes were initially used, with a thin film of Vaseline as adhesive. We anticipated electrical difficulties with these conventional[9] electrodes when applied to conducting materials and as our results show, we were not disappointed. In order to obtain a low resistance adhesive, two different mixtures were used: (1) 85 parts dibutyl tartrate and 15 parts polyelectrolyte and (2) 100 parts tetrabutylammonium bromide, 500 parts tricresyl phosphate and 75 parts polyvinyl chloride. The latter was a deep purple: presumably Hofmann degradation of the quaternary salt produced tributylamine, which in turn dehydrochlorinated the polyvinyl chloride, producing long sequences of conjugated double bonds in the polymer. The tricresyl phosphate grease is preferable for work with polyvinylpyridine derivatives, because tricresyl phosphate is not a plasticizer; on long standing, dibutyl tartrate probably slowly diffuses into the samples. Also, instead of tin foil, bromidized silver foil was used with the above conducting grease, with the intention of obtaining reversible electrodes. The foil was 0.001 inch thick; it was bromidized in 1.0 M potassium bromide–0.05 M nitric acid solution by 15-minute electrolysis at a current density of 5 milliamp./in.^{2}. To simplify description, the following coding will be used in discussion: (V, Sn) = measurements with tin foil–Vaseline contacts, (PVC, Ag) = measurements with bromidized silver foil and the conducting polyvinyl chloride and (PS, Ag) = measurements with bromidized silver foil and the highly plasticized polyelectrolyte. Measurements were also made on some samples at various thicknesses; these will be designated as (PS, Ag)′, (PS, Ag)″, etc. The first thickness measured was that of the molded disc; then the disc was mounted in a split step-chuck and turned down on a lathe to a thinner disc. Cuts were made on both faces. A template was used to mount the (accurately cut) foil electrodes on the samples to permit accurate centering of the test electrode; care was taken to remove conducting grease from the test-guard interspace and from the edge of the sample, in order to avoid test-guard or high-guard shorts. The cell-sample assembly was wrapped with several turns of No. 33 electrical tape to prevent relative motion of the parts after the cell was placed in the thermostat. The tape also kept thermostat oil from seeping between the sample and the electrodes.

(6) R. M. Fuoss, *J. Am. Chem. Soc.*, **63**, 369 (1941).

(7) R. M. Fuoss, *ibid.*, **59**, 1703 (1937).

(8) R. M. Fuoss *Trans. Electrochem. Soc.*, **74**, 91 (1938).

(9) A.S.T.M. Standards on Electrical Insulating Materials, March, 1953, Edition, p. 945.

Apparatus.—Some changes were made in the bridges.[10,11] A synchronizing circuit was added to the oscillator, to permit accurate locking of the variable frequency source at 60 cycles and at 120 cycles to the 60-cycle mains; this device eliminated exasperating beat notes which had previously appeared when the bridge was operated at a frequency which was not precisely set. Frequencies of 30, 60, 120, 240 and 480 cycles were determined by checking the oscilloscope pattern against 60 cycles; 1, 2 and 4 kilocycles were checked against a tuning fork circuit in the same way (General Radio Type 723-C).

The d.c. bridge is a wheatstone circuit with a guard.[11] The power source is a General Electric Type PS5 Regulated Power Supply which will deliver 150 to 1500 volts (maximum current, 0.125 amp.). A General Radio Type 654 A Voltage Divider was used to obtain voltages less than 150. Polarity to the bridge (one terminal of which is grounded) can be reversed; by means of relays which are also actuated by the bridge on-off switch, one of two a.c. clocks can be started simultaneously with bridge current. The latter permit accurate timing of the duration of current flow through the sample in either direction. Bridge balance is indicated by a vacuum tube voltmeter across the midpoints of the bridge; the voltmeter is built around two 6AK5 pentodes, with a microammeter (range -10 to $+10$ μa.) as the indicating instrument. The maximum sensitivity is one microampere for 0.7 millivolt bridge unbalance. Appropriate switches permit the zero of the voltmeter to be checked without interrupting the flow of bridge current.

Results and Discussion

Similar to other conducting polymeric systems,[3,4] the apparent resistance of the materials listed in Table I also changes with the voltage applied to the cell, and in general increased with increasing duration of current flow, when (V, Sn) contacts are used. A typical example is shown in Figs. 1 and 2 for sample 27-0. On application of 50 volts in an arbitrarily defined positive direction (top electrode positive with respect to ground) to the sample at 25°, the conductance κ dropped from 4.1×10^{-12} ohm^{-1} cm.$^{-1}$ to 2.9×10^{-12} in 5 min. On reversal of polarity, the conductance rose to 5.4×10^{-12} and then started to decrease. Successive reversals gave the values shown in the lower curve of Fig. 1. At 500 volts, the measured conductance was about twice as high as at 50 volts, and depended on duration of current as shown in the upper curve of Fig. 1. On heating the sample to 75°, the conductance naturally increased: the initial value measured at 50 volts was 100×10^{-12}; reversal raised this somewhat as shown in the lower curve of Fig. 2. On raising the voltage to 500, the conductance went up to 1600×10^{-12} (Fig. 2, top curve), and increased still further on successive reversals. Remeasurement at 50 volts gave a conductance centering around 1000×10^{-12} (Fig. 2, center curve), about ten times the initial 75–50 volt reading. Obviously the data of Figs. 1 and 2 demonstrate the fact that the "d.c. conductance" of plastics as usually measured is not a reliably reproducible property. Similar results for other systems were also observed; the data are omitted in order to conserve space.

Bromidized silver electrodes were then applied to the sample, as described in the preceding section. The first readings at 25° were still somewhat erratic (lower two curves, Fig. 3; note the *difference in scales* between Figs. 3 and 1), but after the first reversal, the change with time was much reduced

(10) D. Edelson, W. N. Maclay and R. M. Fuoss, *J. Chem. Educ.*, **27**, 644 (1950).

(11) R. M. Fuoss, *J. Am. Chem. Soc.*, **60**, 451 (1938).

and the 50 and 500 readings agreed to about 5%. Most significant of all, however, is the magnitude of the conductance: 90×10^{-12} as contrasted to $5\text{–}10 \times 10^{-12}$ with foil–Vaseline contacts. Similarly, at 75°, the conductance was found to be $11{,}500 \times 10^{-12}$ instead of $1\text{–}2{,}000 \times 10^{-12}$. (Only a 10-volt reading was made at 75° because the conductance was so large). On cooling to 25°, a high resistance (50×10^{-12}) was again obtained, but examination showed that this was merely the consequence of oil seepage. On cleaning the sample and electrodes with carbon tetrachloride and reassembling with fresh PS adhesive, the upper curves of Fig. 3 were obtained. It will be noted that the time dependence is practically eliminated. This result was found to be general: (PS, Ag) or (PVC, Ag) measurements were substantially independent of time or voltage (unless the voltage was high enough to heat the sample[12]), while (V, Sn) measurements were essentially unpredictable. Occasionally, initial readings were erratic (*cf.* Fig. 3), suggesting that a little time is required to establish equilibrium in the electrode layers, but subsequent values were always reproducible to better than 10%.

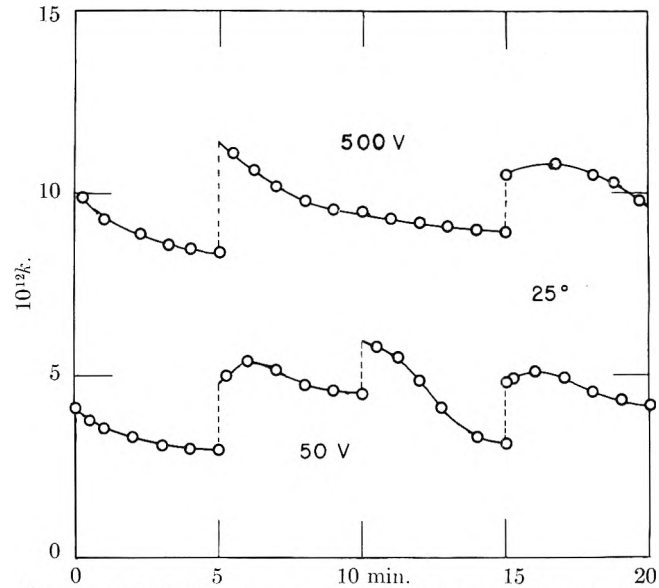

Fig. 1.—Polarization curves: sample 27–0, (V, Sn), at 25°.

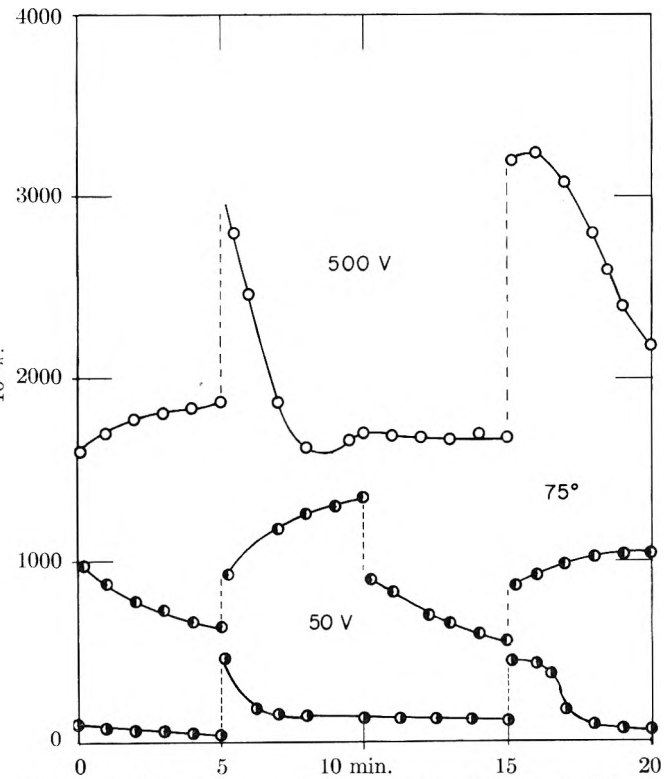

Fig. 2.—Polarization curves: sample 27–0 (V, Sn) at 75°.

The d.c. conductance κ_0 increases rapidly with increasing temperature, as shown in Fig. 4, where logarithm of conductance is plotted against reciprocal absolute temperature. Over the 50° temperature range, the curves approximate linearity. The quantity Q, defined by the equation

$$\log \kappa_0 = A - Q/RT$$

is given in the last column of Table I for the quaternized samples. There appears to be a definite trend of Q toward higher values as the plasticizer content increases, but no systematic dependence on extent of quaternization is evident. It should be noted that different Q-values mean that the κ_0 *vs.* T curves cross, and hence the sequence of conductances of a given series of samples may change with temperature if the intersection appears in the working range of temperatures.

Since the apparent d.c. resistance of the various samples decreases markedly on going from (V, Sn) contacts to (PVC, Ag) contacts, we may assume that the Vaseline layers act as lossy condensers in series with the sample, while the electrolyte gel acts essentially as a series resistor whose impedance is negligibly small compared to that of the sample. We would therefore expect the apparent a.c. properties to depend on the nature of the electrode contact. That this is the case is illustrated by the data for sample 27-0 shown in Fig. 5, where the open circles are for the conventional (V, Sn) contacts and the solid circles are for the (PVC, Ag) contacts. The loss factors plotted in the figure are computed by the equation

$$\epsilon'' = \epsilon''\,(\text{total}) - 180 \times 10^{12}\kappa_0/f$$

where ϵ'' (total) is the a.c. loss factor measured on the a.c. bridge at frequency f and κ_0 is the d.c. conductance. We note first that the dielectric constant with (V, Sn) is too low, as might be expected in a circuit comprising a material of low dielectric constant (Vaseline) in series with one of high (polyelectrolyte). The discrepancy decreases with increasing frequency. That the effect is primarily due to a series capacity is shown by direct calculation: the difference between the (V, Sn) and (PVC, Ag) ϵ'-curves of Fig. 5 leads to a value of 200–400 $\mu\mu$f. for the series capacity over the range 0.030 to 4.0 kc. Assuming a dielectric constant of about 2 for Vaseline, this capacity gives a thickness of 0.007 cm. for the Vaseline film, which seems quite reasonable.

(12) R. M. Fuoss, *J. Am. Chem. Soc.*, **60**, 456 (1938).

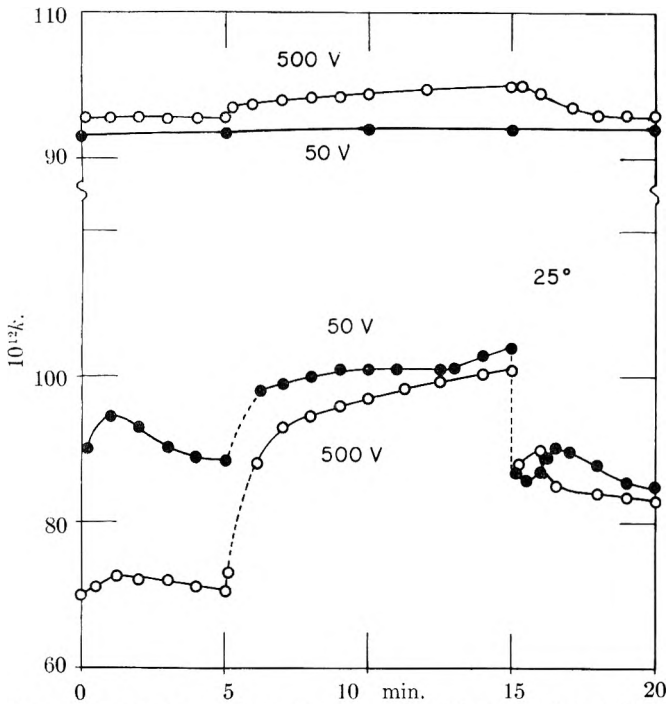

Fig. 3.—Conductance–time curves, sample 27–0 (PS, Ag) at 25°.

At higher temperatures the discrepancy between (V, Sn) and (PVC, Ag) electrodes increases rapidly, and is far greater than can be accounted for solely on the basis of a series film capacity. For example, Disc 27-0 gave at 70° and 60 cycles $\epsilon' = 85.8$ with (V, Sn) contacts, and $\epsilon' = 27.2$ with (PVC, Ag) contacts. At the higher temperature, ionic mobilities are naturally higher and space charges at the boundaries (sample/Vaseline) can readily build up by ionic motion. The corresponding stored charge acts as a series capacitor and leads to a spurious high apparent dielectric constant when ϵ' is calculated from the total capacity. The impedance of the sample is here low compared to the impedance of the surface layers, and hence the apparent dielectric constant is far too high. This result is readily predictable by a generalization of the equations developed in the first paper of this series.[7] With the (PVC, Ag) contacts, a Maxwell-Wagner mechanism could still act, but the resistance of the conducting salt layer is very low compared to that of the sample and effectively shorts itself out of the circuit; hence the bridge sees only the sample impedance.

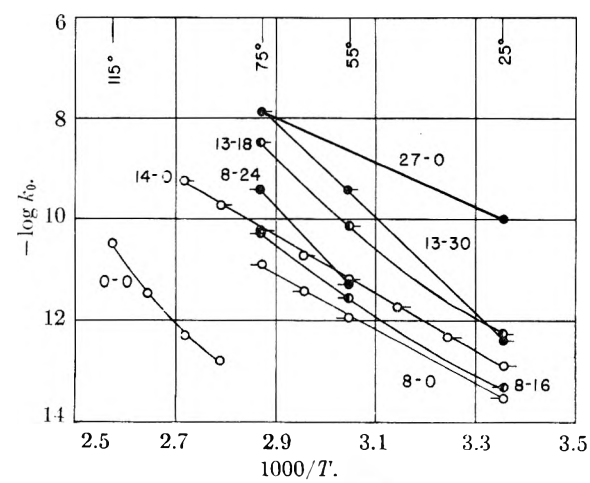

Fig. 4.—Dependence of d.c. conductance on temperature for samples of Table I.

The loss factor curve has an entirely different appearance for the two cases. With (V, Sn), the ϵ''–$f^{-1/2}$ curve is linear, as has been reported[3,4] for several other systems, while with (PVC, Ag) the curve has a maximum. The latter is a much more readily understandable curve, and leads us to conclude that the previously reported linear $\Delta\epsilon''$–$f^{-1/2}$ behavior has its origin in interfacial polarization between electrodes and sample. Both the dielectric constant and loss factor increments thus appear to be the consequence of space charges which arise when ions are moved to boundaries where they cannot discharge.

The observed dependence of the surface effects on temperature clearly shows that they are due to ionic motion. If we define $\Delta\epsilon'$ and $\Delta\epsilon''$ as the difference between the dielectric constant and loss factor (at a given frequency and temperature) of a quaternized sample measured with (V, Sn) contacts and sample 0-0, then $\Delta\epsilon'$ and $\Delta\epsilon''$ are measures of the contributions to electrical properties (both surface and volumes) produced by the ionic content. When the data for *all* frequencies and temperatures for a given disc are plotted on the same $\Delta\epsilon''$–$\Delta\epsilon'$ map, a *single* curve is obtained. In other words, a given point of the $\Delta\epsilon''$–

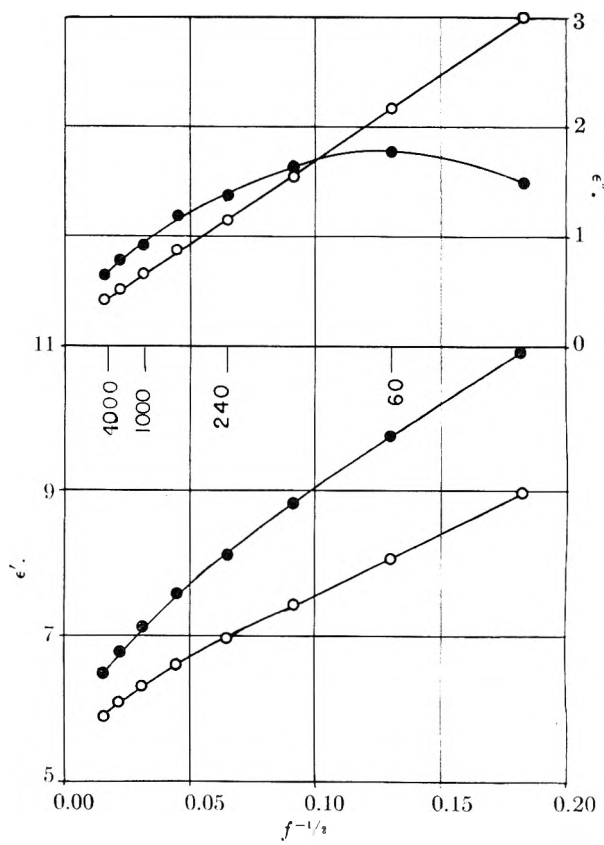

Fig. 5.—Dependence of a.c. properties on nature of electrode contacts; open circles, (V, Sn); solid circles, (PS, Ag); sample 27–0 at 25°

$\Delta\epsilon'$ curve can be obtained by a continuous range of temperatures and frequencies in which a higher frequency can be uniquely paired with a higher temperature (*i.e.*, lower viscosity in the polymer). Obviously therefore a viscosity controlled motion of charges is responsible for the increments $\Delta\epsilon'$ and $\Delta\epsilon''$.

In order to test the (PVC, Ag) electrodes further, measurements were made at several thicknesses of the same material. In order to guarantee the same thermal history for the different samples, a given sample was measured electrically, and then was made thinner by turning stock off of both faces on a lathe. The surfaces of the molded disc are of course glassy-smooth, while the turned surfaces, even with a fine cut, are ridged. The conducting adhesive fills the grooves, while the micrometer measures the thickness across the tops of the ridges. Hence a turned sample is a layered dielectric, with the test material sandwiched between two thin composite dielectrics. Consequently measurements on the molded disc and on the turned discs made from it cannot be compared directly. But by measuring *two* discs, turned successively from the same molded sample, the surface effects can be eliminated by assuming that the series contribution of the turned surfaces is constant (R_s, C_s in parallel) while the contribution due to the sample depends on the thickness of the center stock ($d - 2\delta$), where d is micrometer thickness and δ is the depth of the lathe grooves. The corresponding calculation, while tedious, is perfectly straightforward and will be omitted here. The results can be summarized[13] by saying that the volume properties calculated from two different machined thicknesses (PS, Ag)$''$ and (PS, Ag)$''$ ' agreed within better than 10% (usually within 5%) with the values determined on the original molded disc. Without the precautions described here, apparent electrical properties measured on samples of different thicknesses have been found to vary by factors of two or more. We therefore believe that the bromidized silver electrodes and the bromide-containing adhesive eliminate most of the surface effects for conducting plastics containing bromide ions at least. Plastics whose conductance is due to other ions should also eventually be investigated, of course; it is likely that each system will present special problems.

The a.c. properties of representative compositions are summarized in Figs. 6 and 7, where dielectric constant and loss factor at 75° are plotted against the logarithm of frequency. Measurements were made with either (PVC, Ag) or (PS, Ag) contacts. The presence of electrolytic charges on the pyridine groups attached to the polymer chain permits an external field to exert a torque on segments of the chain, and therefore a frequency-sensitive process of energy absorption is set up. The mechanism is frequency dependent because the polymeric medium retards the hydrodynamic motion of the polymer segments. There probably is also a dipole contribution in the a.c. properties as a consequence of the presence of ion pairs (pyridinium ion plus bromide ion) in the medium. Figures

(13) M. Yamin, Thesis, Yale University, 1952.

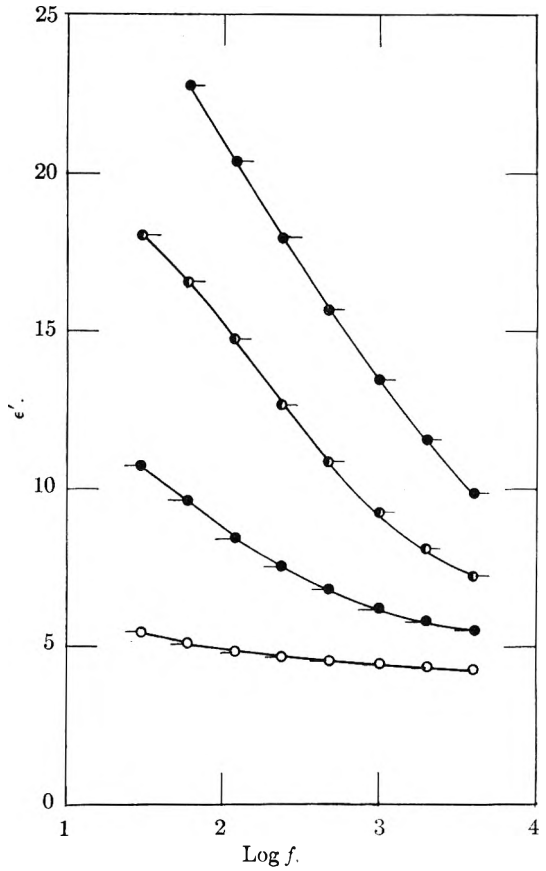

Fig. 6.—Dielectric constant as a function of frequency and composition at 75°: open circles, sample 8–0; solid circles, dash left, 8–24; half-shaded circles, 13–18; solid circles, dash right, 13–30; all at 75°.

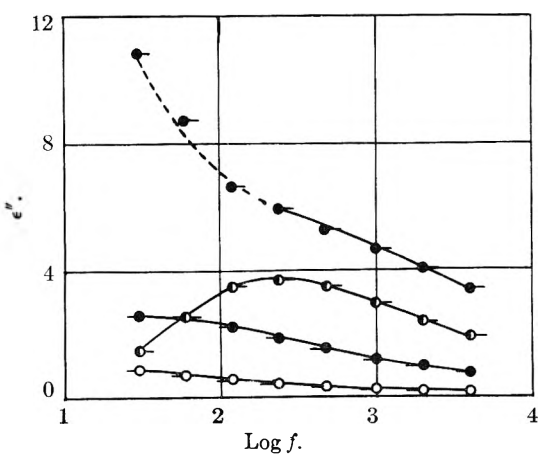

Fig. 7.—Loss factor as a function of frequency and composition at 75°; same code as Fig. 6.

6 and 7 are typical dispersion curves of the familiar pattern; it is, of course, well known that one cannot deduce the mechanism of dispersion from such curves. The magnitude of the polarizability increases (at fixed T, f) with increasing extent of quaternization; increased plasticizer produces the changes which are associated with decreased viscosity. Sample 13-30 shows a peculiar rise in loss factor at low frequencies; since its audio-frequency properties match those of sample 13-18 when allowance is made for viscosity, the dotted portion of the curve for 13-30 in Fig. 7 may well be simply due

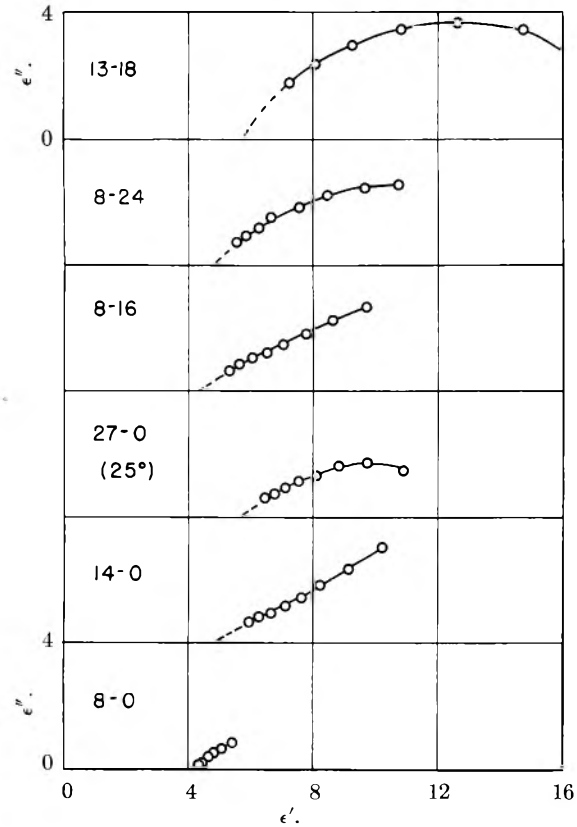

Fig. 8.—Cole plots for conducting plastics.

to experimental uncertainty in ϵ'' at power frequencies. It will be recalled that ϵ'' is obtained from the difference between a.c. and d.c. conductivities, and at 75° for example, the 30-cycle conductance of 13-30 is 16.04×10^{-9} while the d.c. value is 15.86×10^{-9}. These figures are cited in order to emphasize the need for precision in work at low frequencies; obviously an error of only 0.5% in either κ_{30} or κ_0 would change ϵ'' by ±50% in the above example.

Our frequency range was not wide enough to determine the complete a.c. properties of the conducting plastics, but enough information was obtained to show that a distribution of relaxation times[14] is needed to describe the response to a periodic electrical field. In Fig. 8, the a.c. loss factor (calculated from the excess of a.c. conductance over the observed d.c. conductance) is plotted against dielectric constant for several of the samples at 75° (except 27-0, whose curve refers to 25°). Most of the Cole plots can be approximated by circular arcs with centers below the ϵ'-axis, and hence a single relaxation time does not suffice to describe the a.c. response. It will also be noted that quite long time constants are necessary, because even at 30 cycles, the static dielectric constant is still quite far away. Furthermore, another unknown mechanism for energy dissipation must appear at frequencies beyond our upper limit, because the apparent high frequency limits in Fig. 8 are considerably larger than the square of the index of refraction. Similar results also have been obtained in other polymeric systems which did not contain electrolyte.[15]

(14) R. M. Fuoss and J. G. Kirkwood, *J. Am. Chem. Soc.*, **63**, 385 (1941).

(15) D. J. Mead and R. M. Fuoss, *ibid.*, **63**, 2832 (1941).

POLYMERIZATION AND DEPOLYMERIZATION PHENOMENA IN PHOSPHATE–METAPHOSPHATE SYSTEMS AT HIGHER TEMPERATURES. II. THE THERMAL BEHAVIOR OF ALKALI METAL MONOHYDROGEN SULFATE–MONOHYDROGEN PHOSPHATE MIXTURES

BY L. F. AUDRIETH, JOHN R. MILLS[1,2] AND L. E. NETHERTON

W. A. Noyes Laboratory of Chemistry at the University of Illinois, Urbana, Illinois, and the Victor Chemical Works Research Laboratory, Chicago Heights, Illinois

Received January 22, 1954

When equimolar mixtures of sodium monohydrogen sulfate and sodium monohydrogen phosphate are heated an initial exothermic acid–base reaction occurs below 200° resulting in the formation of sodium sulfate and the dihydrogen phosphate. The latter substance then undergoes stepwise dehydration–condensation resulting in the eventual formation at temperatures above 600° of the glassy metaphosphate. No evidence for a sulfatophosphate could be adduced from differential thermal analysis and X-ray diffraction studies, chemical analysis or weight loss experiments. Equimolar mixtures of potassium hydrogen sulfate and potassium dihydrogen phosphate behave in an analogous fashion. The initial highly exothermic proton transfer reaction takes place at about 200° whereupon conversion of the dihydrogen phosphate to the metaphosphate occurs, representing the only further detectable chemical change as the temperature is raised.

Introduction

Recognition of the fact that the fundamental structural unit which characterizes all phosphates, polyphosphates and polymetaphosphates is the PO_4 tetrahedron has made it possible to interpret more precisely the many interesting aggregation reactions which the various hydrogen phosphates undergo at higher temperatures. Conversion of orthophosphate into pyrophosphate, triphosphate, and the high molecular weight polyphosphates involves the linking together of such PO_4 tetrahedra through oxygen atoms. The same structural unit also characterizes the cyclic metaphosphates in which stable structures consisting of three and four

(1) Abstracted in part from the doctoral dissertation presented to the Graduate College of the University of Illinois, 1952.

(2) Victor Chemical Works Research Fellow in Chemistry, University of Illinois, 1951–1952.

PO_4 tetrahedra are built up which may be regarded as six- and eight-member ring ions containing alternate phosphorus and oxygen atoms.

Other neighboring acid forming elements, specifically silicon, chromium, sulfur and arsenic, each in their higher valence states, form similar structural XO_4 units which may be condensed to form polystructures resembling those specified for the poly- and metaphosphates. It is interesting to note that the X–O bond lengths in each of these units differ only slightly, even though the charge on the oxo complex will vary depending upon the formal charge on the central atom. Recognition of the fact that these structural units are approximately of the same size leads to the interesting possibility that simple mixed poly-acids, in which a PO_4 tetrahedron is replaced by any one of the other tetrahedra, may be capable of existence. There is already some evidence in the literature that such acids or their salts have been synthesized. Thus, for instance, the well-known hydrocarbon cracking catalyst material called silicophosphoric acid may conceivably be a polysilicic acid in which the SiO_4 tetrahedra are replaced in part by PO_4 structures. It also has been shown that if sodium dihydrogen phosphate is fused with a relatively small amount of sodium dihydrogen arsenate, a product is obtained in which AsO_4 tetrahedra replace PO_4 groups in the lattice of the resulting insoluble metaphosphate.[3]

Poni and Cernatescu[4] claim to have prepared a compound by fusion of sodium monohydrogen sulfate and sodium monohydrogen phosphate which may be regarded as a sulfatophosphate, *i.e.*, a pyrophosphate in which one of the PO_4 tetrahedra is replaced by an SO_4 structural unit. Such a compound would represent one of the simplest heteropoly acids capable of existence. However, application of Pauling's rules[5] governing the linking of coördination polyhedra indicates that such compound formation is improbable even though the P–O and S–O bond distances in the respective tetrahedra are quite similar (P–O, 1.55 Å. and S–O, 1.51 Å.). The formation of a sulfatophosphate in which both central atoms have a high formal charge and a relatively low coördination number would thus appear improbable on the basis of Pauling's generalizations. A more thorough investigation of the validity of the claims of Poni and Cernatescu was therefore considered advisable.

The investigation of the reaction between sodium hydrogen sulfate and sodium monohydrogen phosphate has revealed that no compound formation occurs. Instead a preliminary exothermic, acid–base type reaction takes place involving transfer of the proton from the hydrogen sulfate to the monohydrogen phosphate ion to yield sodium sulfate and sodium dihydrogen phosphate. The resulting sodium dihydrogen phosphate undergoes further dehydration and condensation upon heating to form disodium dihydrogen pyrophosphate, then the metaphosphates and finally the metaphosphate glass as the temperature is raised.

Considerable evidence has, however, been presented by various investigators to demonstrate that the size of the cation has an appreciable influence on the stability of oxygen bridges in polyanionic aggregates consisting of linked coördination tetrahedra such as the PO_4 and SO_4 groups. In general, the larger the cation the more stable thermally is the condensed anion. The reaction of potassium monohydrogen sulfate with potassium monohydrogen orthophosphate was therefore studied in the hope that the larger potassium ion might possibly favor the formation of such a sulfatophosphate. Again, a strongly exothermic process occurs first, and is followed by a series of changes which are characteristic for mixtures of potassium sulfate and potassium dihydrogen phosphate as the temperature is raised.

Experimental Procedures.—The method of differential thermal analysis was used to gain some preliminary insight concerning the nature of the reactions which occur when composite samples of the reactants were heated at a controlled rate of approximately eight to ten degrees per minute. Weights of samples subjected to differential thermal analysis were standardized at ten grams. Check runs were also carried out subsequently using the newer Brown Electronik differential thermal analysis equipment now available for the study of reactions at higher temperatures and in the solid state. The identity of the intermediate and the final products was verified by chemical methods and X-ray diffraction studies. In general, procedures were similar to those which have been described previously by Osterheld and Audrieth.[6]

Thermal Changes in the System $NaHSO_4$–Na_2HPO_4

The differential thermal analysis curves for the system $NaHSO_4$–Na_2HPO_4 and related mixtures and for various pure components are depicted schematically in Fig. 1. Reference to A (Fig. 1) shows that a strong exothermic reaction, commencing at approximately 150° and reaching its peak at 180°, is the first process which is evident when equi-molecular quantities of the two materials are heated after having been ground together to form an intimate mixture. The thermal changes which characterize this mixture most certainly do not correspond to those which are observed when either of the pure components (B and C) is heated. On the other hand, except for the initial exothermic reaction, the thermal behavior of the system under investigation is completely analogous to that which characterizes a mixture consisting of equimolar quantities of sodium sulfate and monosodium dihydrogen phosphate (D). The thermal changes which occur when pure samples of sodium sulfate and of the monosodium dihydrogen phosphate are heated are depicted by E and F in Fig. 1.

These findings lead to the conclusion that an exothermic acid–base reaction occurs initially involving proton transfer from the HSO_4^- to the $HPO_4^=$ ion in accordance with the equation

$$NaHSO_4 + Na_2HPO_4 \rightarrow Na_2SO_4 + NaH_2PO_4$$

after which each of the resulting components undergoes those high temperature changes characteristic of each. It is interesting to point out (a) that the

(3) E. Thilo and G. Schulz, *Z. anorg. allgem. Chem.*, **266**, 34 (1951).

(4) M. Poni and R. Cernatescu, *Ann. Sci. Univ. Jassy*, **28**, Sec. I, 3 (1942).

(5) L. Pauling, *J. Am. Chem. Soc.*, **51**, 1010 (1929).

(6) R. K. Osterheld and L. F. Audrieth, THIS JOURNAL, **56**, 38 (1952).

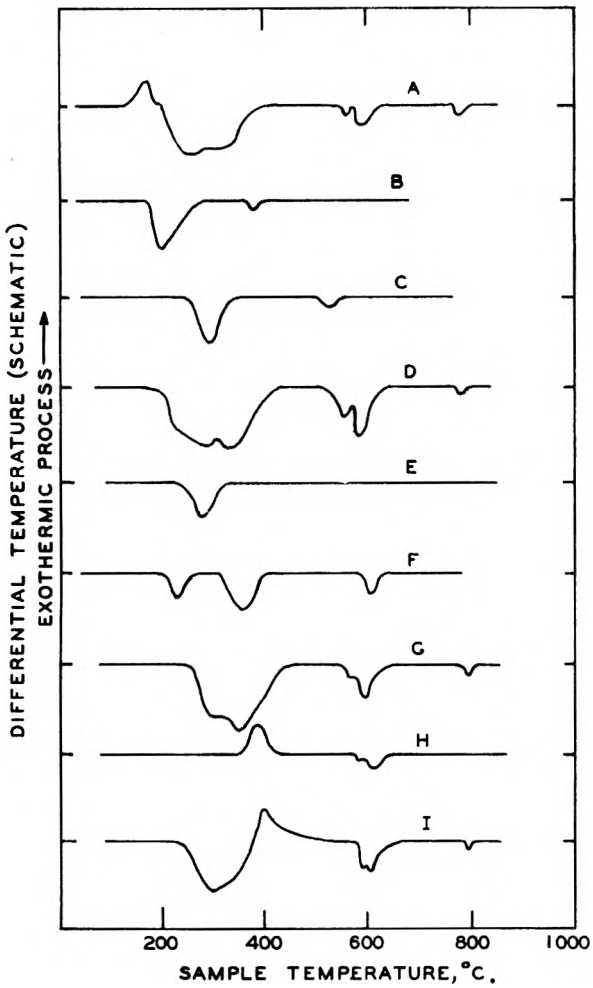

Fig. 1.—Schematic presentation of thermal changes which occur for components and products in the system $NaHSO_4$–$NaHPO_4$: A, $NaHSO_4$ and Na_2HPO_4 in equimolar quantities; B, $NaHSO_4$; C, Na_2HPO_4; D, Na_2SO_4–NaH_2PO_4 in equimolar quantities; E, Na_2SO_4; F, NaH_2PO_4; G, Na_2SO_4 and $Na_2H_2P_2O_7$ (in 2:1 mole ratio); H, $(NaPO_3)_x$; I, fusion product from equimolar quantities of $NaHSO_4$ and Na_2HPO_4.

initial exothermic heat effect is of sufficient magnitude to cancel out the considerable endothermic effect which accompanies the melting and concomitant decomposition of the sodium hydrogen sulfate, and (b) that the proton transfer reaction occurs in that temperature range over which the phase change, *i.e.*, melting of sodium hydrogen sulfate, takes place (m.p. of $NaHSO_4$ is listed at 186° in the literature). The system thus becomes more labile and more susceptible to chemical change.

A continuing series of endothermic changes then takes place beginning at approximately 200°. These changes may be looked upon as involving first the conversion of the dihydrogen phosphate into the dihydrogen pyrophosphate which has been shown to take place rapidly at 220° (see Fig. 1(D)) followed by the endothermic solid phase transition of sodium sulfate from the low temperature orthorhombic form to the high temperature hexagonal lattice (transition temp. 234°) and then by the further dehydration–condensation of the dihydrogen pyrophosphate into the insoluble sodium metaphosphate which normally takes place between 310 to 375°.[7] That the above interpretation of the process is correct is verified by thermal analysis of a mixture consisting of a 2:1 mole ratio of sodium sulfate–disodium dihydrogen pyrophosphate (see Fig. 1 (G)).

That the second process beginning at 200° results in formation of the dihydrogen pyrophosphate has been verified by carrying out weight loss experiments to determine quantitatively the amount of water eliminated when equimolar mixtures of $NaHSO_4$ and Na_2HPO_4 are heated at this temperature for an extended period of time. The data are depicted graphically in Fig. 2, and show that approximately one-half mole of water is lost per mole of mixture.

$$2Na_2SO_4 + 2NaH_2PO_4 \longrightarrow 2Na_2SO_4 + Na_2H_2P_2O_7 + H_2O$$

The product obtained by heating this mixture for 17 hours at 200° was found to give an X-ray pattern showing excellent agreement with that corresponding to a mixture of sodium sulfate and disodium dihydrogen pyrophosphate. Chemical analysis of the product was found to give values of 25.1 and 24.9% P_2O_5 as pyrophosphate; these results agree fairly well with the theoretical value of 28.1% demanded by the above equation.

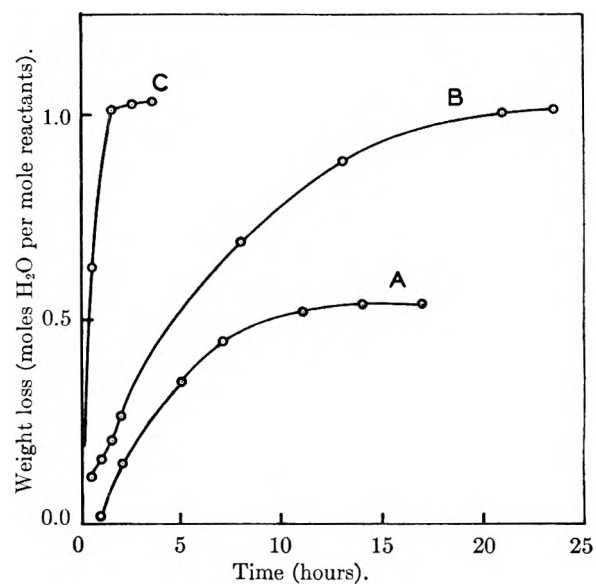

Fig. 2.—Weight loss curves for equimolar mixtures of: A, $NaHSO_4$–Na_2HPO_4 at 200°; B, $KHSO_4$–K_2HPO_4 at 210°; C, $KHSO_4$–K_2HPO_4 at 350°.

Although specific conditions are not disclosed by Poni and Cernatescu, it was their claim that an alleged phosphatosulfate is obtained when sodium monohydrogen phosphate dihydrate and sodium hydrogen sulfate are fused. It was still conceivable, although considered unlikely, that such compound formation might occur at temperatures above 600°. A sample of these components in

(7) Exact reproducibility with respect to temperatures at which these changes occur is not possible due to the rapid heating rate which is employed in studying the thermal changes by the method of differential thermal analysis. Sufficient time is not available to effect completion of a reaction at the temperature at which the reaction begins to take place.

equimolar amounts and intimately mixed, was therefore heated gradually to 800° over a period of one hour and maintained at this temperature for ten minutes. The sample was found to have undergone a weight loss corresponding to three moles of water per mole of reactants. An X-ray diffraction pattern of the product formed by rapid cooling of the melt was found to reveal only the pattern of the high temperature form of sodium sulfate, leading to the assumption that the glassy metaphosphate had been formed as the other product.

The presence of the glassy metaphosphate was verified by subjecting the fusion product to differential thermal analysis. A strong exothermic reaction occurs when an authentic sample of the glassy metaphosphate is heated to approximately 320–400° (curve H in Fig. 1). This reaction is due to devitrification and conversion of the glassy polymer into the stable crystalline trimetaphosphate.[8]

The thermal analysis curve for the fusion product (curve I, Fig. 1) discloses an identical exothermic break with a maximum at about 400°—leading to the conclusion that the product formed by melting together $NaHSO_4$ and Na_2HPO_4 is not a sulfatophosphate, but a mixture of sodium sulfate and glassy sodium metaphosphate.[9]

The System $KHSO_4$–K_2HPO_4

The thermal changes which occur when equimolar mixtures of $KHSO_4$ and K_2HPO_4 are heated are represented schematically by (A) in Fig. 3. For comparison the curves for potassium hydrogen sulfate (B), potassium monohydrogen phosphate (C), potassium dihydrogen phosphate (D) and potassium sulfate (E) are also given.

The marked endothermic change which begins at about 200° when potassium hydrogen sulfate is heated corresponds to melting (reported variously in the literature as 200 to 210°) followed by dehydration and decomposition to form the pyrosulfate, thus accounting for continuation of the endothermic break beyond the melting point. The further endothermic break at approximately 420° corresponds to the melting point of the pyrosulfate.

The thermal changes which occur when potassium monohydrogen orthophosphate and potassium dihydrogen orthophosphate are heated have been studied in detail by Osterheld and Audrieth.[6] Dipotassium hydrogen phosphate is converted to potassium pyrophosphate whereas monopotassium dihydrogen phosphate changes at a temperature somewhat over 200° into the insoluble potassium metaphosphate. The final break at about 800° corresponds to the melting point of the water-insoluble potassium metaphosphate. Reference is also made to the fact that potassium sulfate undergoes an endothermic change just below 600° corresponding to a solid phase transition from the rhombic to hexagonal lattice. The reported value in the literature for this transition is 588°.

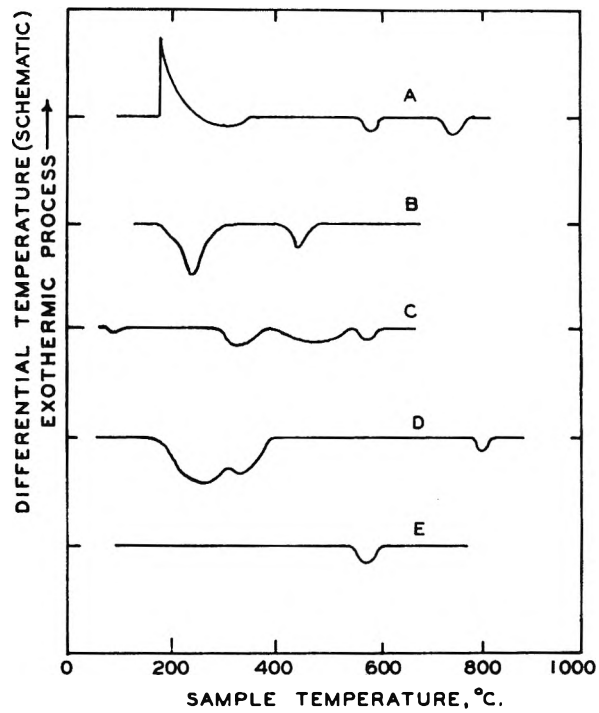

Fig. 3.—Schematic presentation of thermal changes which occur for components and products in the system $KHSO_4$–K_2HPO_4: A, $KHSO_4$ and K_2HPO_4 in equimolar quantities; B, $KHSO_4$; C, K_2HPO_4; D, KH_2PO_4; E, K_2SO_4.

If the heating curves for the various pure substances are compared with the differential curve characteristic of equimolar mixtures of potassium hydrogen sulfate and dipotassium hydrogen phosphate, it becomes immediately apparent that the initial strong exothermic reaction may be accounted for by assuming that an acid–base type of reaction takes place which leads to formation of potassium sulfate and potassium dihydrogen phosphate. This exothermic reaction is indeed much more marked in the potassium system than observed in the corresponding sodium system. It occurs at a somewhat higher temperature but again just a few degrees below the temperature at which the acid hydrogen sulfate begins to melt and undergo further dehydration.

The dihydrogen orthophosphate then undergoes dehydration to the insoluble metaphosphate whereas potassium sulfate undergoes no further change until a temperature just below 600° is

(8) Reference should also be made to the fact that two small endothermic breaks occur above 600°, the second corresponding to the melting of the trimetaphosphate which takes place at approximately 625°. The cause for the first of these endothermic breaks has not been definitely established. Both of these endothermic breaks occur at somewhat lower temperatures when NaH_2PO_4 and the 1:1 mixture of $NaHSO_4$ and Na_2HPO_4 are heated. These breaks are also evident in the thermal analysis curve for the fusion product.

(9) Further proof for this conclusion was sought by undertaking a study of phase relationships for the system Na_2SO_4–$(NaPO_3)_x$ varying from 0 to 60 mole per cent. metaphosphate. The method of differential analysis is not well adapted for this purpose even when samples were originally heated to fusion, cooled to 300°, and then reheated at a controlled rate to determine thermal changes occurring at higher temperatures. Endothermic breaks corresponding to initial melting and complete melting were interpreted as corresponding, (a) to the eutectic temperature (approximately 595°) and the melting points of the various mixtures which decreased continuously from 885° to 725° for a mixture containing 60 mole per cent. metaphosphate. No compound formation appears to be indicated for mixtures containing 50 mole per cent. of each constituent. Consistent results could not be obtained for mixtures containing high percentages of the glassy metaphosphate and weight losses varying from 1 to 4% were also observed. These may be ascribed to a high temperature acid–base reaction between poly-metaphosphate and sulfate resulting in elimination of sulfur trioxide.

reached where an endothermic reaction occurs corresponding to a change from the orthorhombic to the hexagonal form. The final break at 800° is due to the melting of potassium metaphosphate.

Weight loss experiments for equimolar samples heated at 210 and at 350° are presented in Fig. 2 and demonstrate that the reaction occurring slowly at the lower temperature and more rapidly at the higher one can be represented by the equation

$$KHSO_4 + K_2HPO_4 \longrightarrow K_2SO_4 + KPO_3 + H_2O$$

Chemical and X-ray diffraction analyses were performed on products obtained upon cooling melts produced by heating equimolar mixtures. The X-ray diffraction patterns were found to correspond with those consisting of intimately ground equimolar mixtures of potassium metaphosphate and potassium sulfate and composite patterns of each of the pure components. The insoluble potassium metaphosphate was determined by leaching thoroughly with water and weighing the insoluble residues. The soluble metaphosphate in the filtrate also was determined. Typical samples were found to contain 36.2 and 36.1% insoluble KPO_3, 5.09% soluble KPO_3 giving a total of 41.3% metaphosphate (required by theory, 40.4%).

It is again apparent that no sulfatophosphate is formed when potassium hydrogen sulfate and dipotassium hydrogen phosphate are heated even up to the fusion point, but that instead an initial acid–base reaction occurs resulting in the formation of potassium sulfate and potassium dihydrogen phosphate, both of which subsequently undergo those thermal changes which characterize each of them as pure components.

NOTE ON PROPERTIES OF AQUEOUS SUSPENSIONS OF TiC AND TiN

By T. Vasilos and W. D. Kingery

Ceramics Division,[1] Department of Metallurgy, Massachusetts Institute of Technology, Cambridge, Massachusetts

Received February 9, 1954

An investigation of cataphoresis, *p*H and conductimetric titrations, and viscosity indicates that TiC, TiN and ZrN form stable electrocratic suspensions in an acid medium. Hydrogen ions adsorbed on the particle surfaces, together with a diffuse layer of anions, lead to positively-charged particles.

Introduction

There have been no previous investigations reported on the properties of nitride–water or carbide–water systems. The properties of suspensions of these materials are of general interest in the preparation of stable suspensions, and in particular for the fabrication of various test suspensions and crucibles by casting in plaster molds. In the present study, experiments have been mainly concerned with TiN and TiC. A few experiments with ZrN were undertaken, but in a finely-ground form its reaction with water is fairly rapid.

There have been quite extensive investigations of the properties of various clay–water suspensions.[2] In these systems, the clay particles are negatively charged, the charge and suspension stability being largely determined by the nature of a diffuse layer of exchangeable cations. Investigations of oxide–water systems have shown that stable suspensions of finely-ground materials like aluminum oxide can be formed.[3,4] In an acidic suspension, hydrogen ions are preferentially adsorbed, while in alkaline suspensions hydroxyl ions are preferentially adsorbed.

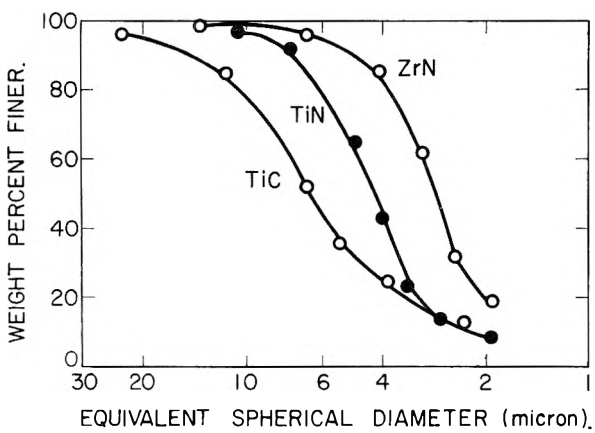

Fig. 1.—Particle size distribution of TiC, TiN and ZrN.

Experimental

Samples of TiN and ZrN (Metal Hydrides Company, 300 mesh) and TiC (Kennametal Company, 200 mesh) were ground for 24 hours in steel ball mills using ethanol as a grinding medium. After grinding, tramp iron was removed with a magnetic separator and repeated leaching with hydrochloric acid. The particle size distribution was determined by a hydrometer-sedimentation method,[5] and is given in Fig. 1.

Cataphoresis measurements were made with a U-tube having platinum electrodes in each arm connected through a series rheostat (to prevent overheating) to 110 volts d.c. The concentration of solids was 20 g./l.

A quantitative measure of hydrogen ion adsorption was determined by *p*H and conductivity titrations with dilute hydrochloric acid. Prior to testing, the solids were repeatedly washed with distilled water.

Measurements of viscosity at various supensions specific gravities and *p*H values were made with a modified MacMichael viscosimeter.

Results

Cataphoresis experiments in acid medium gave deposits of TiC, TiN and ZrN at the negative electrode only, indicating that the particles in all cases

(1) With funds from the United States Atomic Energy Commission.

(2) F. H. Norton and A. L. Johnson, *J. Am. Ceram. Soc.*, **24**, 189 (1941).

(3) W. E. Hauth, Jr., This Journal, **54**, 150 (1950).

(4) W. E. Hauth, Jr., *J. Am. Ceram. Soc.*, **32**, 394 (1949).

(5) F. H. Norton and S. Spiel, *ibid.*, **21**, 89 (1938).

were positively charged. In neutral and alkaline media, settling was much more rapid and in all cases, light deposits were found on both electrodes.

Results of *p*H and conductivity titrations of TiC are shown in Fig. 2. The end-point in each case

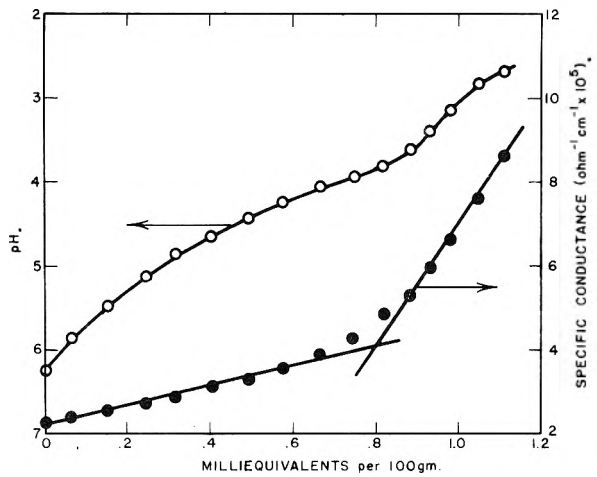

Fig. 2.—Titration of TiC suspension with HCl.

occurs in the range 0.80–0.83 milliequivalent of HCl per 100 grams of TiC. These data, together with the cataphoresis experiments, indicate that hydrogen ions are adsorbed on the TiC surface giving a positively-charged particle, *i.e.*

$$TiC + H^+Cl^- = TiC - H^+ \vdots Cl^- \qquad (1)$$

Chloride ions act as counter ions forming a diffuse secondary layer around the particles. Presumably, the adsorbed ions are hydrated, and an adsorbed water shell may be present in a neutral suspension as well.

With titanium nitride the process is complicated by slow hydrolysis, forming ammonium hydroxide

$$2TiN + 5H_2O = 2NH_4OH + Ti_2O_3 \qquad (2)$$

The titration curves for TiN (used as received, 300 mesh, to decrease the hydrolysis rate) are shown in Fig. 3. An end-point in the titration at a *p*H of 5.1 is due to neutralization of ammonium hydroxide.[6] Another end-point at a *p*H of 4.3 is due to adsorption of hydrogen ions on the surface, which is probably largely converted to oxide. The straight initial portion of the *p*H curve indicates that both reactions must take place coincidentally during the initial part of the titration. After neutralization of the ammonium hydroxide is completed (equation 3), further adsorption takes place (equation 4)

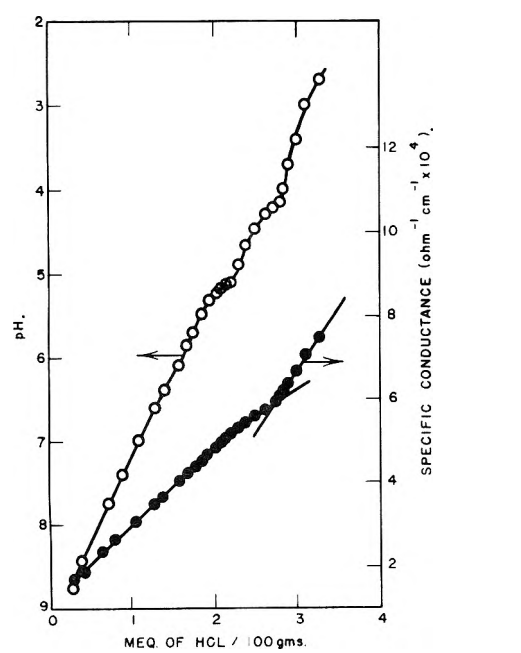

Fig. 3.—Titration of TiN suspension with HCl.

$$NH_4OH + H^+Cl^- = NH_4^+ + Cl^- + H_2O \qquad (3)$$

$$TiN + H^+Cl^- = TiN - H^+ \vdots Cl^- \qquad (4a)$$

$$Ti_2O_3 + H^+Cl^- = Ti_2O_3 - H^+ \vdots Cl^- \qquad (4b)$$

In order to ascertain that ammonium hydroxide was being formed, a sample of the TiN suspension

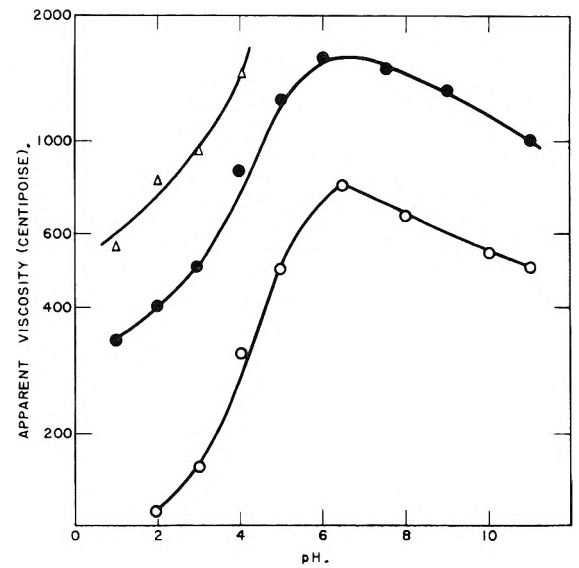

Fig. 4.—Viscosity of suspensions of TiC at suspension specific gravities of 3.0 (upper curve), 2.5 and 2.0 g./cc.

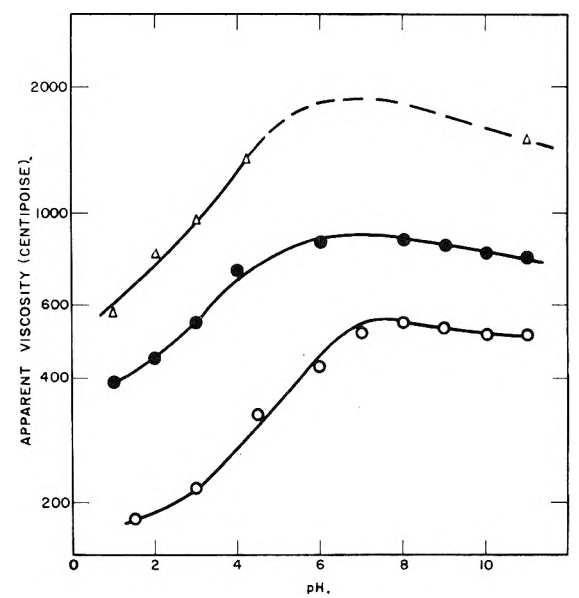

Fig. 5.—Viscosity of suspension of TiN at suspension specific gravities of 2.8 (upper curve), 2.4 and 1.9 g./cc.

(6) I. M. Kolthoff and E. B. Sandell, "Textbook of Quantitative Inorganic Analysis, The Macmillan Co., New York, N. Y., 1948.

was centrifuged and an aliquot of the clear liquid was titrated with HCl. An end-point at a *p*H of 5.2 indicated the formation of 2 milliequivalents of NH_4OH per 100 grams of TiN. Zirconium nitride hydrolyzes sufficiently rapidly, giving soluble products,[7,8] that acid titrations were not attempted. Colorimetric tests[9] of acidified TiN and TiC filtrates with H_2O_2 for titanium were negative.

Results of viscosity measurements for TiC and TiN suspensions are shown in Figs. 4 and 5. Similar results were found for ZrN suspensions. In all cases, there is a marked lowering of viscosity in an acid medium. This is accompanied by a marked increase in the stability of the suspension and is due to repulsive forces between particles. In contrast to Al_2O_3 and ZrO_2 suspensions,[3,4] there is no marked decrease in viscosity in alkaline suspensions.

Discussion

Results of cataphoresis, *p*H and conductivity titrations, and viscosity measurements indicate that stable suspensions can only be formed in an acid medium. The stability of these suspensions is due to adsorption of hydrogen ions, with anions forming a diffuse double layer. This leads to a stable electrocratic suspension due to repulsive forces between particles. This stability is very similar to that found for oxide–water suspensions, except that a lower *p*H is required, less hydrogen adsorption occurs, and the suspensions are less stable as indicated by a smaller lowering of viscosity.

Even the most stable nitride, TiN, hydrolyzes slowly when in the form of fine powder in a water suspension. The resulting formation of NH_4OH requires the addition of considerably more acid than is required for TiC. A titanium oxide is probably formed on the particle surfaces. In the case of ZrN, the oxidation products are in an acid medium and hydrolysis proceeds much more rapidly.

In an acid medium, suspensions are sufficiently stable that samples and crucibles can be formed by casting the suspension in plaster molds. After thorough drying and firing at about 2000°, strong dense samples of TiC, TiN and ZrN are obtained.

(7) L. S. Foster, *et al.*, Atomic Energy Commission, Report No. 2942 (1945).

(8) P. Schwarzkopf and R. Kieffer, "Refractory Hard Metals," The Macmillan Co., New York, N. Y., 1953.

(9) F. D. Snell and C. T. Snell, "Colorimetric Methods of Analysis," Vol. 1, D. Van Nostrand Co., Inc., New York, N. Y.

THE DENSITY, SURFACE TENSION AND VISCOSITY OF DEUTERIUM OXIDE AT ELEVATED TEMPERATURES[1]

BY J. R. HEIKS, M. K. BARNETT, L. V. JONES AND E. ORBAN

Mound Laboratory, Monsanto Chemical Company, Miamisburg, Ohio[2]

Received February 11, 1954

The density and viscosity of 99.20% deuterium oxide have been determined from 30 to 250° while surface tension measurements were made from 100 to 216°. A bob suspended from a 200-micron fused quartz fiber spiral inside of a pressure vessel was used to determine the densities to the nearest 0.0003 g./cc. The ratio of the densities of deuterium oxide to ordinary water increases with temperature up to about 80°, but decreases with still further increases in temperature. A Lawaczeck falling body viscometer, in which the time of fall of a radioactive plummet was measured with the use of coincident counting tubes, showed the viscosity of deuterium oxide to be 21% higher than ordinary water at 30° while at 250° this difference decreased to 9.7%. The height of rise of liquid in a capillary tube showed that the surface tension of deuterium oxide and ordinary water are about the same at 100°, but with increasing temperature the surface tension for deuterium oxide becomes steadily less until at 220° it is about 3% less than the value for ordinary water.

The density of deuterium oxide at room temperature has been measured by numerous investigators[3–6] but little work has been reported at elevated temperatures. Density values to 100° have been reported by Chang and Chien,[7] Chang and Tung[8] and more recently by Schrader and Wirtz.[9] Hardy and Cottington[10] measured the density of deuterium oxide at various temperatures between 90 and 125°. The values reported by the latter are slightly lower than those reported by Schrader and Wirtz. The densities of deuterium oxide and ordinary water at their respective critical points were reported by Riesenfeld and Chang.[11] However, information on the density of deuterium oxide between 125° and its critical temperature is not available.

Although a number of workers have reported that the surface tension of deuterium oxide at room temperature differs markedly from that of ordinary water[12–14] others have indicated that there is essentially no difference between these values.[15–18] The latter conclusion now presumably has the

(1) Delivered at Kansas City Meeting of Division of Physical and Inorganic Chemistry, American Chemical Society, March, 1954.

(2) Mound Laboratory is operated by Monsanto Chemical Co., under A.E.C. Contract AT-33-1-GEN-53.

(3) L. Tronstad and J. Brun, *Trans. Faraday Soc.*, **34**, 766 (1938).

(4) K. Stokland, E. Ronaess and L. Tronstad, *ibid.*, **35**, 312 (1939).

(5) H. L. Johnston, *J. Am. Chem. Soc.*, **61**, 878 (1939).

(6) K. Wirtz, *Naturwissenschaften*, **30**, 330 (1942).

(7) T. L. Chang and J. Y. Chien, *J. Am. Chem. Soc.*, **63**, 1709 (1941).

(8) T. L. Chang and L. H. Tung, *Chin. J. Physics*, **7**, 230 (1949).

(9) Jon R. Schrader and K. Wirtz, *Z. Naturforschung*, **62**, 220 (1951).

(10) R. C. Hardy and R. L. Cottington, *J. Research Natl. Bur. Standards*, **42**, 573 (1949).

(11) E. H. Riesenfeld and T. L. Chang, *Z. physik. Chem.*, **B30**, 61 (1935); **B28**, 408 (1935).

(12) P. W. Selwood and A. Frost, *J. Am. Chem. Soc.*, **55**, 4335 (1933).

(13) R. Indovina, *Ann. Chim. Applicata*, **30**, 51 (1940).

(14) M. K. Phibbs and P. A. Giguere, *Can. J. Chem.*, **29**, 173 (1951).

(15) H. Lachs and I. Minkow, *Roczniki Chem.*, **17**, 363 (1937).

(16) G. Jones and W. A. Ray, *J. Chem. Phys.*, **5**, 505 (1937).

(17) H. Lachs and I. Minkow, *Nature*, **134**, 186 (1935).

(18) H. Flord and L. Tronstad, *Z. physik. Chem.*, **A175**, 347 (1936).

weight of authority.[19] Measurement of the surface tension of deuterium oxide at elevated temperatures has been undertaken infrequently. Sugita and Inai[20] measured the surface tension to 100° and found the surface energy to be a decreasing linear function of the temperature. Cockett and Ferguson[21] made measurements to 75° and reported that the temperature coefficient of surface tension became more negative with increasing temperature.

Most of the early work on the viscosity of deuterium oxide was carried out near room temperature on a microscale using capillary type viscometers. Generally, determinations were made on deuterium oxide–ordinary water mixtures rich in deuterium oxide. Values reported for 100% deuterium oxide were obtained by extrapolation. Selwood and Frost[12] were among the first to report a viscosity value for 100% deuterium oxide. Their value of 1.42 centipoises at 20° was later corrected to 1.260 centipoises in a communication to the editor by Taylor and Selwood.[22] Lewis and MacDonald[23] reported values for the viscosity of 100% deuterium oxide at 5° intervals from 5 to 35°, their value at 20° was also 1.260 centipoises. Baker and LaMer[24] measured the viscosity of ordinary water–deuterium oxide mixtures ranging from pure ordinary water to pure deuterium oxide at 25°. After an investigation of similar solutions Jones and Fornwalt[25] proposed an equation relating the viscosities of mixtures of ordinary water and deuterium oxide to those of pure ordinary water at 25°. Lemonde[26] determined the viscosity of a deuterium oxide–ordinary water mixture containing 99.45% deuterium oxide at several temperatures between 4 and 20°, his value at 20° was 1.22 centipoises. The recent work of Hardy and Cottington[10] extended the investigation of the viscosity of deuterium oxide to 125°. Their value for 100% deuterium oxide at 20° was reported as 1.2514 centipoises.

The deuterium oxide for all of our measurements was obtained from the Atomic Energy Commission, Oak Ridge National Laboratory, Radioisotopes Division, Oak Ridge, Tennessee. It had the following specifications: conductivity, 1.7×10^{-5} mho; *p*H, 7.52; purity, 99.20% deuterium oxide.

Density

Apparatus and Procedure.—The density measurements reported in this paper were made with a Jolly balance which consisted essentially of a 60-turn 3/8-inch diameter spiral made from 200-micron fused quartz fiber, and a fused quartz sinker having a mass of 983 mg. and a volume of 0.439 cc. The spiral had a sensitivity of approximately 10 mg. per mm. extension. The Jolly balance assembly was housed in a high pressure vessel fitted with a suitable window and mounted in a constant-temperature oven having an observation window. Four thermocouple junctions in the walls of the vessel were connected to a standard potentiometer which measured temperature to ±0.1°. Under equilibrium conditions, the temperature of the liquid could be taken as identical to that of the wall of the vessel.

The fused quartz spiral was calibrated prior to its use for these measurements, *i.e.*, its sensitivity was determined under various loads to 1 g. at various temperatures to 250°. The volume of the sinker was also determined at temperatures to 250° using multiple distilled water in the apparatus. The extension of the quartz spiral at each temperature was observed with a precision cathetometer, readable to ±0.02 mm. At least ten cathetometer readings were taken at each temperature.

Conventional calculations were used for obtaining the density of deuterium oxide at each temperature, *i.e.*, the loss in weight of the sinker divided by its volume is equal to the density of the medium. A description of the apparatus and operating procedure is reported elsewhere.[27]

Results.—The density values obtained in this investigation are listed in Table I and are plotted in Fig. 1. The density values of 100% deuterium oxide listed in Table I were calculated on the assumption that mixtures of deuterium oxide and

TABLE I

DENSITY OF DEUTERIUM OXIDE AND ORDINARY WATER

Temp., °C.	Density, 99.20% D_2O Smoothed, g./cc.	Obsd., g./cc.	Density, H_2O,[a] g./cc.	Density, 100% D_2O (calcd.), g./cc.	$\rho_{D_2O}^T / \rho_{H_2O}^T$
30	1.1023		0.99564	1.1032	1.1080
34.3	1.1009	1.1009			
40	1.0990		.99221	1.0999	1.1085
50	1.0948		.98804	1.0957	1.1090
51.1	1.0940	1.0939			
60	1.0897		.98321	1.0906	1.1092
70	1.0838		.97778	1.0847	1.1093
74.9	1.0806	1.0806			
80	1.0773		.97180	1.0782	1.1095
90	1.0700		.96531	1.0708	1.1093
100	1.0622		.95835	1.0630	1.1092
101.4	1.0611	1.0612			
109.2	1.0549	1.0549			
110	1.0539		.9510	1.0547	1.1090
120	1.0451		.9434	1.0459	1.1086
130	1.0358		.9352	1.0366	1.1084
131.5	1.0344	1.0340			
140	1.0260		.9264	1.0268	1.1084
150	1.0159		.9173	1.0167	1.1084
151.0	1.0145	1.0143			
160	1.0050		.9076	1.0058	1.1082
170	0.9942		.8980	0.9950	1.1080
173.3	.9899	0.9903			
177.7	.9840	.9831			
180	.9818		.8874	.9826	1.1073
183.5	.977	.978			
190	.969		.8761	.970	1.107
200	.956		.8649	.957	1.106
207.2	.946	.947			
210	.942		.8528	.943	1.106
220	.927		.8403	.928	1.104
226.1	.919	.920			
230	.912		.8273	.913	1.104
240	.896		.8138	.897	1.102
246.1	.886	.885			
250	.880		.7991	.881	1.102

[a] F. G. Keyes and L. B. Smith, *Mech. Eng.*, **53**, 132 (1931).

(19) I. Kirschenbaum, G. M. Murphy and H. C. Urey, "Physical Properties, Methods of Analysis, and Natural Abundance of Heavy Water," Harold Urey and George M. Murphy, ed., NNES III-4a, McGraw-Hill Book Co., Inc., New York, N. Y., 1951, p. 33.

(20) T. Sugita and T. Inai, *Proc. Phys. and Math. Soc., Japan*, **19**, 552 (1937).

(21) A. H. Cockett and A. Ferguson, *Phil. Mag.*, **28**, 685 (1939).

(22) H. S. Taylor and P. W. Selwood, *J. Am. Chem. Soc.*, **56**, 998 (1934).

(23) G. N. Lewis and R. T. MacDonald, *ibid.*, **55**, 4730 (1933).

(24) W. N. Baker and V. K. LaMer, *J. Chem. Phys.*, **3**, 406 (1935).

(25) G. Jones and H. J. Fornwalt, *ibid.*, **4**, 30 (1936).

(26) H. Lemonde, *Compt. rend.*, **212**, No. 2, 81 (1941).

(27) J. R. Heiks, M. K. Barnett, L. V. Jones, W. C. McCluggage, Mound Laboratory Report MLM-799 Rev., January 14, 1953.

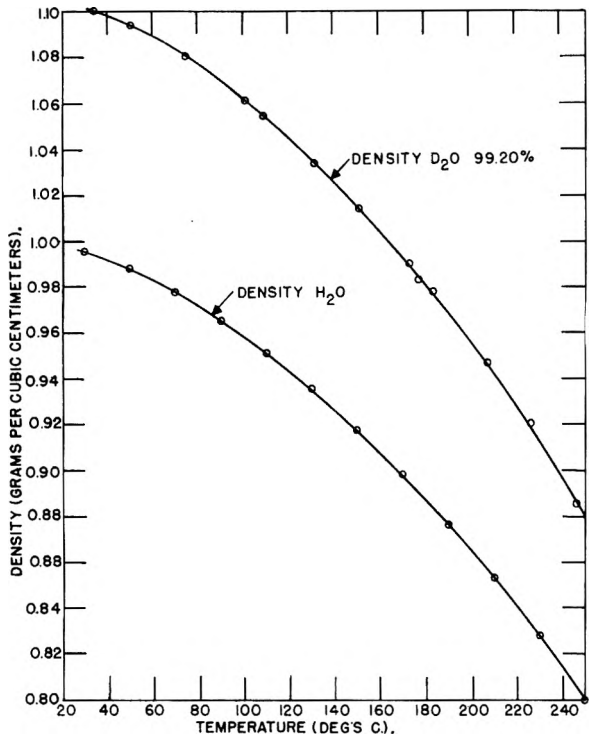

Fig. 1.—Effect of temperature on the density of 99.20% D_2O and of ordinary water.

ordinary water form ideal solutions, thus permitting extrapolation. The density of ordinary water[28] at various temperatures is tabulated in Fig. 1 for comparison. The ratio of the densities of deuterium oxide to ordinary water increases with temperatures to about 80° but decreases with further increases in temperature. This is consistent with the data of Riesenfeld and Chang[11] which indicate that deuterium oxide and ordinary water have equal densities at 370°.

The relative standard deviation of the density determination at room temperature was calculated to be 0.23%. Because of the tendency of droplets to condense on the spiral under equilibrium conditions, fewer measurements of the extension were made at the higher temperatures with a reduction in precision. The relative standard deviation at the higher temperatures was estimated to be 0.6%.

Surface Tension

Apparatus and Procedure.—For the measurements reported in this paper, the capillary rise method was adapted to conditions prevailing at elevated temperatures and pressures. The apparatus previously has been described in detail.[27]

A single precision capillary tube was used throughout the measurements. The tube was mounted in the head of a stainless steel pressure vessel equipped with windows for observing the menisci. Introduction of liquid into the vessel was preceded by evacuation and drying of the vessel. Observation of the menisci, by means of a cathetometer, was always preceded by flushing of the capillary tube with fresh portions of the liquid. This flushing action was accomplished by instantaneous venting, into a second pressure vessel, through a steel tube connected to the top of the capillary tube. The violence of the flushing action was controlled by varying the pressure in the second vessel. Both vessels were mounted on a stand in a constant-temperature oven. Temperatures were measured to the closest tenth of a degree by means of a thermocouple housed in a thermowell immersed in the main body of the liquid.

(28) F. G. Keyes and L. B. Smith, *Mech. Eng.*, **53**, 132 (1931).

The surface tension was calculated by means of the standard formula

$$\gamma = \frac{1}{2}\left(h + \frac{r}{3}\right)(d - d^\circ)gr$$

where h is the capillary rise, r the radius of the tube, d the density of the liquid, d° the density of the vapor, and g the acceleration due to gravity. The average radius of the tube, determined by measuring the length of a weighed mercury thread at different positions in the tube, was 0.2084 mm. The density of the liquid was determined as described above. The density of the vapor was estimated from the density of saturated water vapor and the molar ratio

$$M_{D_2O}/M_{H_2O} = 1.1117$$

The over-all precision of these measurements did not justify a correction for the difference between the vapor pressures of deuterium oxide and that of ordinary water.

Results.—Nine values of the surface tension in the range 99 to 216° were determined and are tabulated in Table II. The values of the molecular

TABLE II

SURFACE TENSION AND SURFACE ENERGY OF DEUTERIUM OXIDE

Temp., °C.	Surface tension, dynes/cm.	Molecular free surface energy, ergs	Temp., °C.	Surface tension, dynes/cm.	Molecular free surface energy, ergs
99.0	58.5	414	174.6	42.4	315
110.8	56.0	399	184.8	39.9	299
124.0	53.8	386	193.8	38.0	287
145.6	48.7	355	216.0	32.8	253
160.8	45.3	333			

free surface energy reported in the last column of the table were calculated as $\gamma(M\eta)^{2/3}$ where γ is the surface tension, η is the specific volume and M is the molecular weight. Each value of the surface tension is based on the average of four to six determinations of the capillary rise. In Fig. 2 the surface tension is plotted against temperature. The surface tension curve indicates that the magnitude of

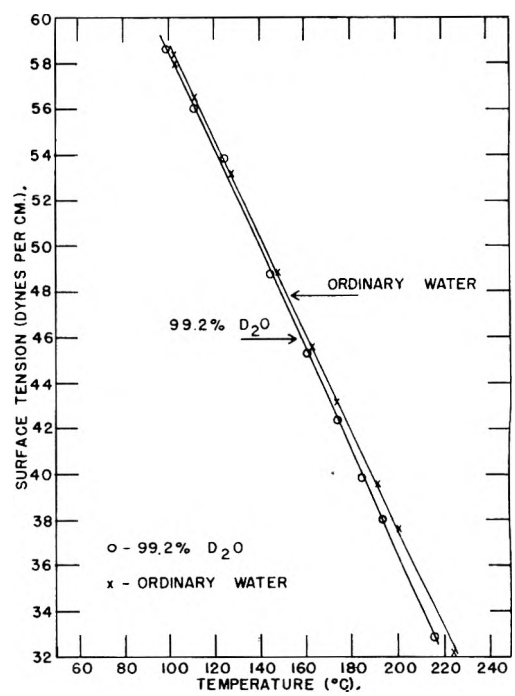

Fig. 2.—Effect of temperature on the surface tension of 99.20% D_2O and of ordinary water.

the temperature coefficient increases slightly with temperature. The magnitude of the temperature coefficient of the free surface energy also increases with temperature, indicating that deuterium oxide is associated.

Values of the surface tension of ordinary water in the presence of its own vapor are listed in Table III. These measurements were made in the same apparatus as that used for deuterium oxide. From an examination of Fig. 2 one concludes that the surface tension of deuterium oxide differs little from that of ordinary water at 100° but that, with increasing temperature, the value for deuterium oxide becomes progressively less than that for ordinary water.

TABLE III

SURFACE TENSION OF ORDINARY WATER

Temp., °C.	Surface tension, dynes/cm.	Temp., °C.	Surface tension, dynes/cm.
101.8	58.4	163.8	45.6
103.0	57.9	174.4	43.1
110.8	56.4	191.2	39.5
128.2	53.1	201.0	37.5
148.8	48.9	224.4	32.0

Thus in the neighborhood of 220° the surface tension of deuterium oxide appears to be about 1 dyne/cm., or 3%, less than the value for ordinary water.

The precision of the surface tension measurements was calculated from the uncertainty in the capillary rise, density and radius of the tube. The relative standard deviation of the surface tension was estimated to be 0.3% at the lower temperatures and 0.7% at the higher temperatures.

Viscosity

Apparatus and Procedure.—The viscosity values reported in this paper were obtained with a falling body viscometer, consisting essentially of a fall-tube closed at its lower end and having a diameter only slightly greater than that of a cylindrical plummet contained therein. The fall-tube is placed concentrically within a stainless steel pressure vessel designed to safely hold the maximum pressure used. Elevated temperatures, measured to the nearest 0.2° with a single-junction copper–constantan thermocouple, were obtained by an electric heating mantle surrounding the pressure vessel.

Relative viscosities were determined by measuring the time required for the plummet to fall a distance of 20 inches, under the influence of gravity, first in distilled water and then in deuterium oxide at various temperatures between 30 and 250°. A γ-ray activated timer was used for timing the fall of the plummet in the fall tube.

The following relationship was used for the calculation of the relative viscosity

$$\frac{\eta}{\eta_0} = \frac{(\sigma - \rho)t}{(\sigma_0 - \rho_0)t_0}$$

Here η and η_0 are the absolute viscosities of deuterium oxide and water, σ and σ_0 are the densities of the plummet filled with deuterium oxide and water, ρ and ρ_0 are the densities of deuterium oxide and water, and t and t_0 are the fall times of the plummet in deuterium oxide and in water, respectively. The densities of deuterium oxide, used in these calculations, were determined independently as described above. The viscosity values of ordinary water for converting the relative viscosity of deuterium oxide into absolute units are those reported by Jaumotte.[29]

A complete description of the apparatus and procedure used in this work can be found in another report.[27]

(29) A. Jaumotte, *Rev. Universelle Mine*, **17**, 213 (1951).

Results.—The viscosity of 99.20% deuterium oxide as determined at twelve temperatures from 30 to 250° is given in Table IV. Four viscosity values of 100% deuterium oxide reported by Hardy and Cottington[10] are included for comparison.

TABLE IV

VISCOSITY OF DEUTERIUM OXIDE

Temp., °C.	η_{D_2O}/η_{H_2O} 99.20% D_2O	η_{H_2O},[a] cp.	η_{D_2O}[b] 100% D_2O, cp.	η_{D_2O} 99.20% D_2O, cp.
30	1.21	0.8007		0.969
45	1.19	.5988		.713
60	1.18	.4688	0.5513	.552
75	1.17	.3799		.445
90	1.15	.3185	.3658	.365
100	1.14	.2833	.3265	.323
125	1.13	.2227	.2551	.252
150	1.12	.1863		.208
175	1.11	.1578		.175
200	1.11	.1362		.151
225	1.10	.1225		.135
250	1.10	.1127		.124

[a] A. Jaumotte, *Rev. Universelle Mine*, **17**, 213 (1951). [b] R. C. Hardy and R. L. Cottington, *J. Research Natl. Bur. Standards*, **42**, 573 (1949).

A comparison of the viscosity values of deuterium oxide and ordinary water as listed in Table IV shows that deuterium oxide is approximately 21% more viscous than ordinary water at 30° while at 250° this difference decreases to 9.7%.

In Fig. 3 the logarithm of the viscosity of deuterium oxide and that of ordinary water are plotted against the temperature. The effect of temperature on the viscosity of these two liquids appears to be similar, which would indicate that they have a similar degree of association.

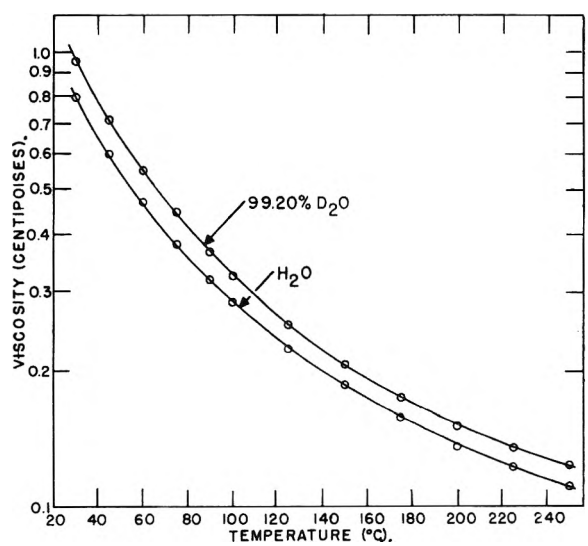

Fig. 3.—Effect of temperature on the viscosity of 99.20% D_2O and of ordinary water.

Using the same apparatus and procedure as in this work, the standard deviation of a single determination, based on duplicate runs on an aqueous salt solution at ten different temperatures, was calculated to be 0.00213 centipoise. The viscosity range of this solution varied from 1.04 to 0.156 centipoises between 30 and 200°, respectively.

CHARCOAL SORPTION STUDIES. II. THE SORPTION OF WATER BY HYDROGEN-TREATED CHARCOALS[1]

BY H. L. McDERMOT AND J. C. ARNELL

Contribution from the Defence Research Chemical Laboratories, Canada

Received February 12, 1954

Oxygen has been removed from three types of charcoal by treating them with hydrogen at 1000°. It has been shown that this results in a lowered water sorption at humidities of less than 80% for all three charcoals. The amount of oxygen so removed has been measured for one of these charcoals (coconut shell). Surface areas are substantially unchanged by the removal of oxygen. Oxidation of the surface is shown to increase the sorption of water by charcoal. It is suggested that the data are in accord with the cluster theory of Pierce and Smith.[2]

Introduction

The effect of the addition of oxygen to the surface of charcoal on the sorption of water by the charcoal has been demonstrated by King and Lawson,[3] by Emmett[4] and by Dubinin and Zaverina.[5] In every case the sorption of water has been increased by oxidation of surface. Recently Pierce, Smith, Wiley and Cordes[6] have increased the amount of water sorbed by Graphon (a graphitized carbon black) by oxidizing its surface. Their oxidations were carried out by exposing samples of Graphon to water vapor at temperatures varying from 25 to 150°. Analysis of the vapor after exposure showed by the presence of carbon dioxide and hydrogen that reaction had occurred. It also was observed that while the isotherm of the untreated sample of Graphon was reversible, that of the oxidized sample displayed limited hysteresis. Pierce and Smith[2] have explained the hysteresis loop observed in the sorption of water by oxidized Graphon as well as those loops found in the water–charcoal system by postulating that sorption occurs initially on active centers in the form of clumps of adsorbate which later merge to form a continuous film. Multilayer adsorption or capillary condensation follow later. Desorption occurs at lower pressures than adsorption because the forces which were previously confined to isolated clumps then extend continuously throughout the film or capillary condensed liquid. Juhola and Wiig[7] have studied the sorption of water by charcoal and maintain that hysteresis in these systems is caused by the presence of constricted pores in the charcoal. In their view capillary condensation occurs on both branches of the hysteresis loop and chemisorbed oxygen plays no significant part in the sorption of water by activated charcoal. The present work supports the concept due to Pierce as it is shown that the magnitude of the hysteresis loop depends on the quantity of oxygen chemisorbed by the charcoal. Further it is demonstrated that removal of oxygen from the surface diminishes the amount of water sorbed during the first stages of sorption without substantially changing the surface area of the charcoal. Evidence is adduced to show that oxygen is present on the surface in the form of isolated centers and since removal of these decreases the weight of water initially sorbed then sorption must have occurred by selective sorption on these centers. Finally the reverse effect is demonstrated. A hydrogen treated charcoal is oxidized with water vapor and found to sorb more water than it did before oxidation.

(1) Issued as D.R.C.L. Report No. 78.

(2) C. Pierce and R. N. Smith, THIS JOURNAL, **54**, 784 (1950).

(3) A. King and C. G. Lawson, *Trans. Faraday Soc.*, **30**, 1094 (1934).

(4) P. H. Emmett, *Chem. Revs.*, **43**, 69 (1948).

(5) M. M. Dubinin and E. D. Zaverina, *J. Phys. Chem. (U.S.S.R.)*, **21**, 1373 (1947).

(6) C. Pierce, R. N. Smith, J. W. Wiley and H. Cordes, *J. Am. Chem. Soc.*, **73**, 4551 (1951).

(7) A. J. Juhola and E. O. Wiig, *ibid.*, **71**, 2069 (1949).

Experimental and Results

Measurement of Water Isotherms.—The water isotherms were measured by the method reported previously.[8] All isotherms were measured at 27°.

Deoxygenation of the Charcoals.—Oxygen was removed from the charcoals by exposing them to a stream of hydrogen at 1000°. Zinc chloride activated wood charcoal was so reduced by tumbling it in a stainless stee. cylinder, which rotated inside an electric furnace. Small vanes along the inside of the cylinder ensured a positive tumbling action. Universal couplings made it possible to pass a stream of hydrogen through the rotating cylinder. The charcoals were in general exposed to air after cooling while being transferred from the furnace to the sorption apparatus. In order to test for any effect due to exposure to air after the reducing treatment, one sample of zinc chloride activated charcoal was transferred to the sorption cell in an atmosphere of nitrogen. The charcoal samples were all evacuated for at least 12 hours at 200° prior to a sorption run. The only exception was the sample transferred to the sorption cell without exposure to air. In this case the water isotherm was measured after a simple evacuation.

The method of treatment was modified for some samples as it was felt that accurate density measurements of the charcoal were necessary and the method outlined above did not provide enough charcoal. Accordingly batches of about 5 kg. of a steam activated coconut shell charcoal and of a coal charcoal were treated with hydrogen in a large vertical furnace. The furnace was cylindrical and the charcoal was supported by a stainless steel mesh in the center of the heating zone. The supply of zinc chloride activated charcoal was limited so that it was not possible to treat a large batch in this manner. However the results though incomplete are reported because it was of interest to include in the study one charcoal which exhibited the S-shaped isotherm characteristic of zinc chloride activated charcoals.

Oxidation of a Coconut Shell Charcoal.—A sample of reduced charcoal was partly reoxidized by exposure to water for three months at 60°. The charcoal was sealed in a glass capsule under vacuum along with some degassed water and placed in a thermostat held at 60°. At the end of three months the charcoal was removed from the capsule and outgassed at 200°. This method was based on the findings of Pierce, Smith, Wiley and Cordes[6] that carbon is oxidized slowly by water even at room temperature. The water isotherm was then determined. At the same time an isotherm was measured for a sample of the same charcoal that had simply been stored during this period in a stoppered bottle.

Analysis of Gases Evolved from Charcoal during Deoxygenation.—In order to confirm that oxygen was present on

(8) H. L. McDermot and J. C. Arnell, *Can. J. Chem.*, **30**, 177 (1952).

TABLE I

COMPOSITION OF GASES EVOLVED FROM CHARCOAL DURING DEOXYGENATION AT 1000°

Run no.	Duration, hr.	Hydrogen flow, cc./min.	Initial wt., g.	Wt. loss g./g. char.	Wt. of gas recovered H_2O	CO_2	CO	Total[b]
					g./g. char.			
				First Series				
2	1	900	5.5342	0.0828	0.0319	[a]		
3	4	900	4.8359	.1418	.0263	[a]		
4	4	900	6.0524	.1131	.0325	[a]		
5	4	350	5.6952	.1181	.0308	[a]		
6	4	350	5.6803	.1563	.0361	[a]		
7	1	350	6.6938	.0850	.0372	[a]		
8	1	350	6.4315	.0855	.0368	0.0257	0.0159	0.0744
10	1	350	7.0917	.0808	.0346	.0152	.0100	.0560
11	1	350	7.2696	.0692	.0328	.0266	.0066	.0624
12	1	350	5.6268	.0929	.0351	.0255	.0123	.0729
				Second Series				
2A	1	60	5.8475	0.0683	0.0274	0.0298	0.0263	0.0805
3A	1	90	6.4258	.0668	.0302	.0266	.0277	.0811
4A	1	75	6.0769	.0610	.0240	.0333	.0273	.0819
5A	1	95	6.3319	.0677	.0302	.0298	.0340	.0906
6A	1	320	5.9068	.0751	.0324			
7A	4	900	5.1254	.0975	.0323			

[a] The "Ascarite" used in runs 2–7 incl. was oven-dried in air and did not function. [b] The figures for water have been reduced to oxygen before totalling, as the hydrogen is considered to have been added.

the charcoal surfaces and that it was removed by the hydrogen treatment, two series of experiments were performed at 1000° using the apparatus described for the treatment of the zinc chloride activated charcoal, but with the addition of an absorption train for the estimation of water and carbon oxides in the effluent gases. The presence of a large excess of hydrogen greatly complicated the problem of analyzing for carbon monoxide.

In the first series of ten experiments the effluent gases from the furnace were passed through an absorption train of standard U-tubes fitted with stopcocks that could be closed for weighing. In the first six runs the absorption train consisted of a U-tube filled with glass wool to serve as a dust trap, two U-tubes filled with "Drierite" to absorb water vapor and finally a U-tube filled with "Ascarite" to absorb carbon dioxide. In the last four runs another U-tube filled with "Drierite" was placed after the "Ascarite" trap to absorb some of the water produced in the carbon dioxide–sodium hydroxide reaction. It had been found that a small amount of the water produced in this reaction was not retained by the Ascarite. On leaving the train the effluent gas was passed through a charcoal trap cooled in liquid air. On completion of each of these latter runs the charcoal trap was gradually warmed to room temperature and the desorbed gas carried by a stream of nitrogen was passed through a bed of silver permanganate–zinc oxide reagent[9] which converted any carbon monoxide to carbon dioxide. The carbon dioxide was absorbed by a train of U-tubes containing "Ascarite" and "Drierite."

This method of determining carbon monoxide in the presence of a large amount of hydrogen was checked using a stream of hydrogen to which a known quantity of carbon monoxide had been added, at the same flow rate as that used in the above experiment. In duplicate runs, it was found that only 57 to 59% of the carbon monoxide was recovered, with the result that the carbon monoxide figures have been multiplied by 5/3 to correct for this low efficiency.

In the second series of six experiments, four were carried out to provide a check on the carbon monoxide content of the effluent gas. Instead of depending on an oxidizing catalyst, it was decided to use the same five U-tubes as before to determine the water and carbon dioxide formed during the hydrogen treatment and then to introduce oxygen into the hydrogen stream in a sufficient quantity to ensure the complete oxidation of the hydrogen and any carbon monoxide present to water and carbon dioxide. The hydrogen was ignited before the furnace was brought up to temperature. Following combustion the gases were passed through several large drying towers and four U-tubes containing "Drierite," two "Ascarite" and "Drierite," respectively It was necessary to reduce substantially the hydrogen flow rate for these experiments in order to prevent the formation of excessive quantities of water.

The results of all the experiments in both series have been reduced to the same units and are given in Table I.

Although the above results show wide variations, some definite conclusions may be drawn. At low flow rates of hydrogen, carbon dioxide appears to be formed preferentially to water and the quantity of water produced increases to a constant value which averages 0.033 g./g. charcoal at flow rates greater than 300 cc./min. Increasing the duration of a run has no effect on the amount of water formed, which is taken to mean that all the oxygen that can be stripped off the charcoal surface is removed during the first hour of hydrogenation. However, the observed loss of weight of the sample appears to increase with longer periods of deoxygenation and this is considered to be due to formation of hydrocarbon gas from the reaction of hydrogen with the carbon surface at 1000°. Using the results of the first series, where the average weight losses are 0.083 g./g. charcoal for a one-hour run and 0.132 g./g. charcoal for a four-hour run, the weight of carbon converted to hydrocarbon averages 0.016 g./g. charcoal/hour. The weight of combined carbon oxides formed was computed to be 0.037 g./g. charcoal.

In the second series the carbon monoxide values are too high because the combustion of the effluent gas converts any hydrocarbon present to carbon dioxide. At the time the experiments were performed it was not anticipated that this complicating factor would be present and it was not until the total weights of the recovered gases were found to exceed the weight loss of the charcoal in all four pertinent runs, that this factor was recognized. If it is assumed that the carbon monoxide values reported in column 8 are entirely due to the combus-

(9) M. Katz and S. Halpern, *Ind. Eng. Chem.*, **42**, 345 (1950).

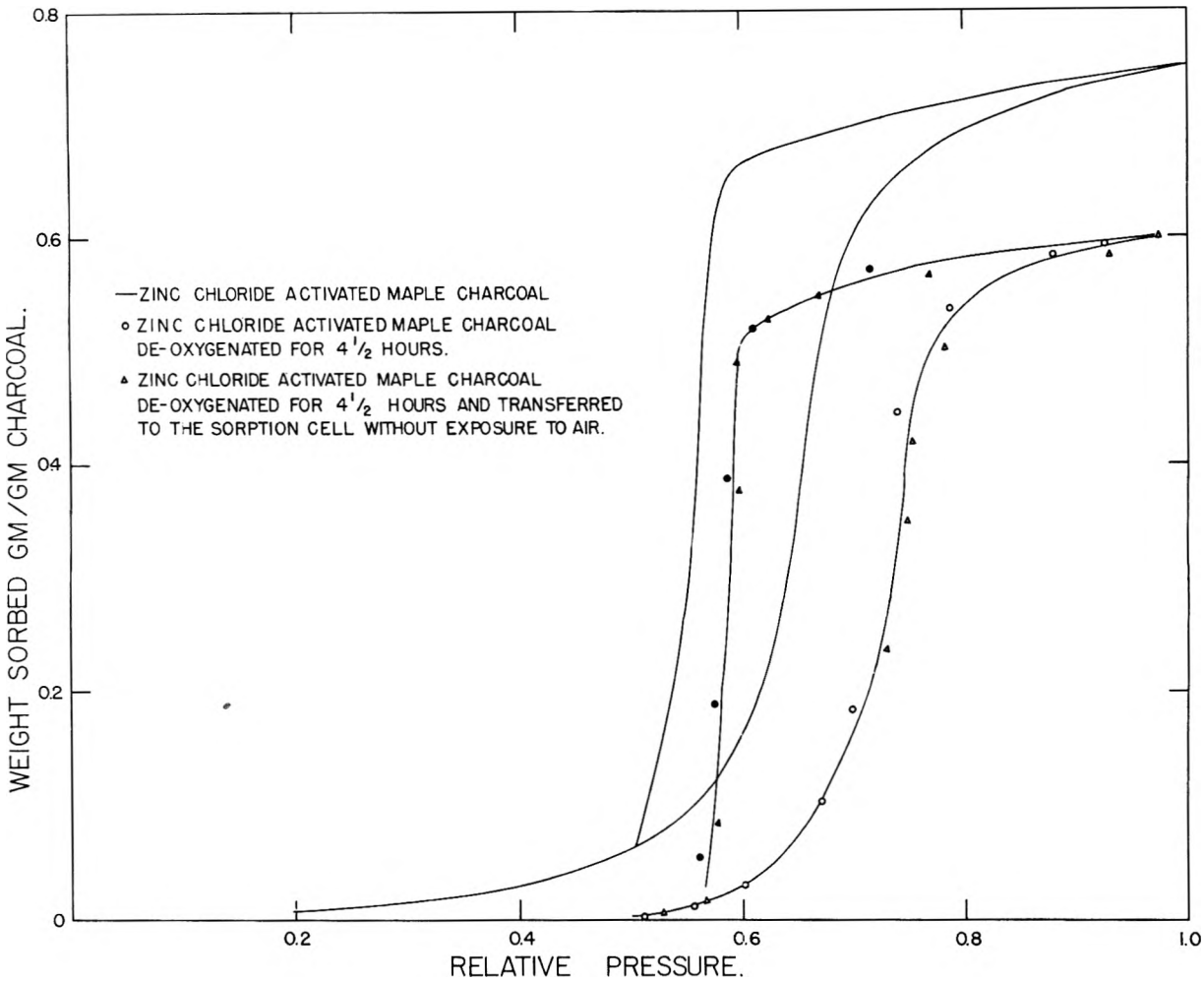

Fig. 1.—Sorption isotherms for the zinc chloride activated charcoals: open symbols denote adsorption; solid symbols denote desorption.

tion of hydrocarbons then these figures may be used to calculate the amount of carbon removed as hydrocarbons. This has been done and the weights of carbon removed have been added to the weights of oxygen removed to give the total weight losses suffered by the charcoals. The calculated weight losses are compared with the actual weight losses in Table II.

Table II

Mass Balance of Results of Deoxygenation

Run no.	Wt. oxygen removed as $CO_2 + H_2O$, g./g. char.	Wt. of carbon removed, g./g. char.	Calcd. loss in wt., g./g. char.	Actual loss in wt., g./g. char.
2A	0.0458	0.0150	0.0608	0.0683
3A	.0462	.0158	.0620	.0668
4A	.0456	0156	.0612	.0610
5A	.0484	.0194	.0678	.0677

The carbon loss figures in column 3 of Table II average 0.016 g./g. char./hour, which is in exact agreement with the figure from the first series. The agreement of the carbon loss figures for the two series of runs and the concordance of the values in the last two columns of Table II, justify the assumption that no carbon monoxide is formed at the low hydrogen flow rates.

It is concluded therefore that at low hydrogen flow rates surface oxygen is removed as water and carbon dioxide and no carbon monoxide appears until the greater reducing power of more hydrogen converts some of the carbon dioxide to carbon monoxide and water. Accordingly it is now possible to calculate the amount of oxygen removed from the surface of the charcoal using the data from both series of runs. The results are presented in Table III.

Table III

Quantity of Oxygen Removed from Charcoal

Run no.	Oxygen removed as H_2O	Oxygen removed as CO_2 g./g. char.	Oxygen removed as CO	Total O_2, g./g. char.
8	0.0327	0.0187	0.0091	0.0605
10	.0307	.0111	.0057	.0475
11	.0291	0193	.0038	.0522
12	.0312	.0185	.0070	0567
2A	.0242	.0216	0	.0458
3A	.0262	.0194	0	.0462
4A	.0214	.0242	0	.0456
5A	.0268	.0216	0	.0484
			Av.	0.0504

It is concluded from these results that all the treated charcoals are free of the oxygen, which can be removed by reduction with hydrogen. In the following they will be referred to as "deoxygenated" or "oxygen-free charcoals."

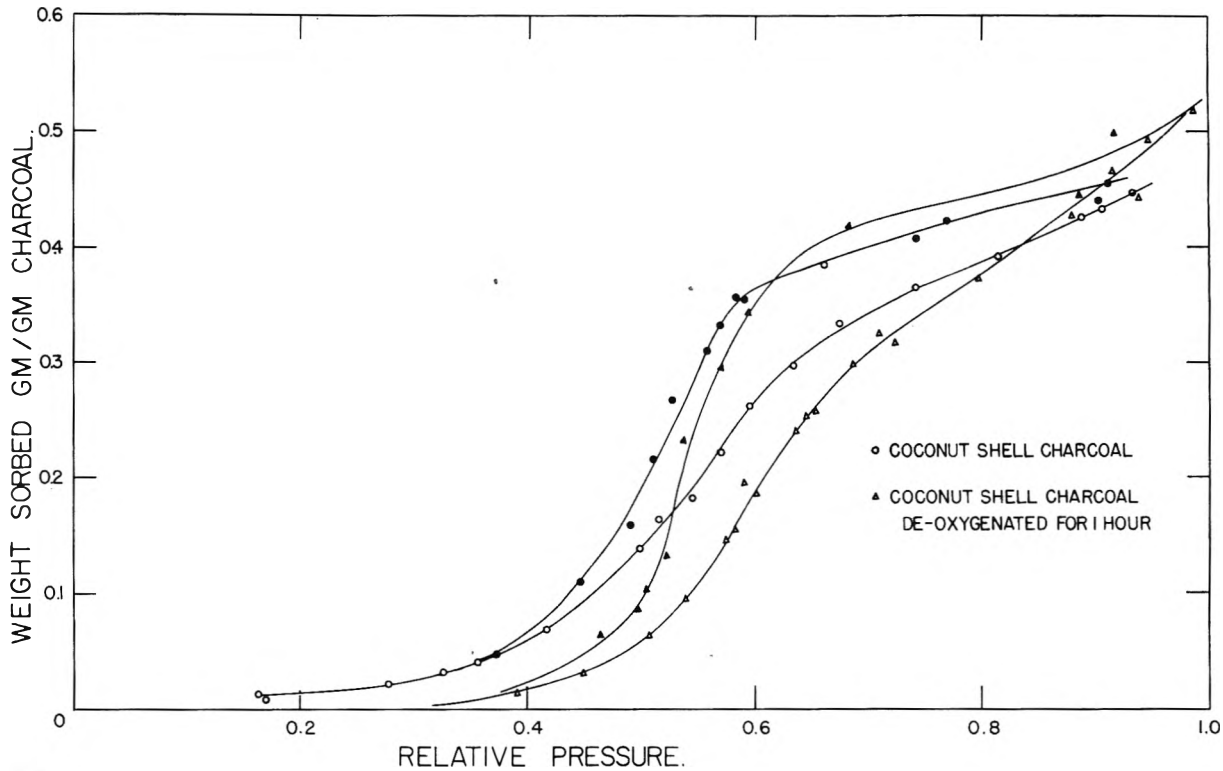

Fig. 2.—Sorption isotherms for the coconut shell charcoals: open symbols denote adsorption; solid symbols denote desorption.

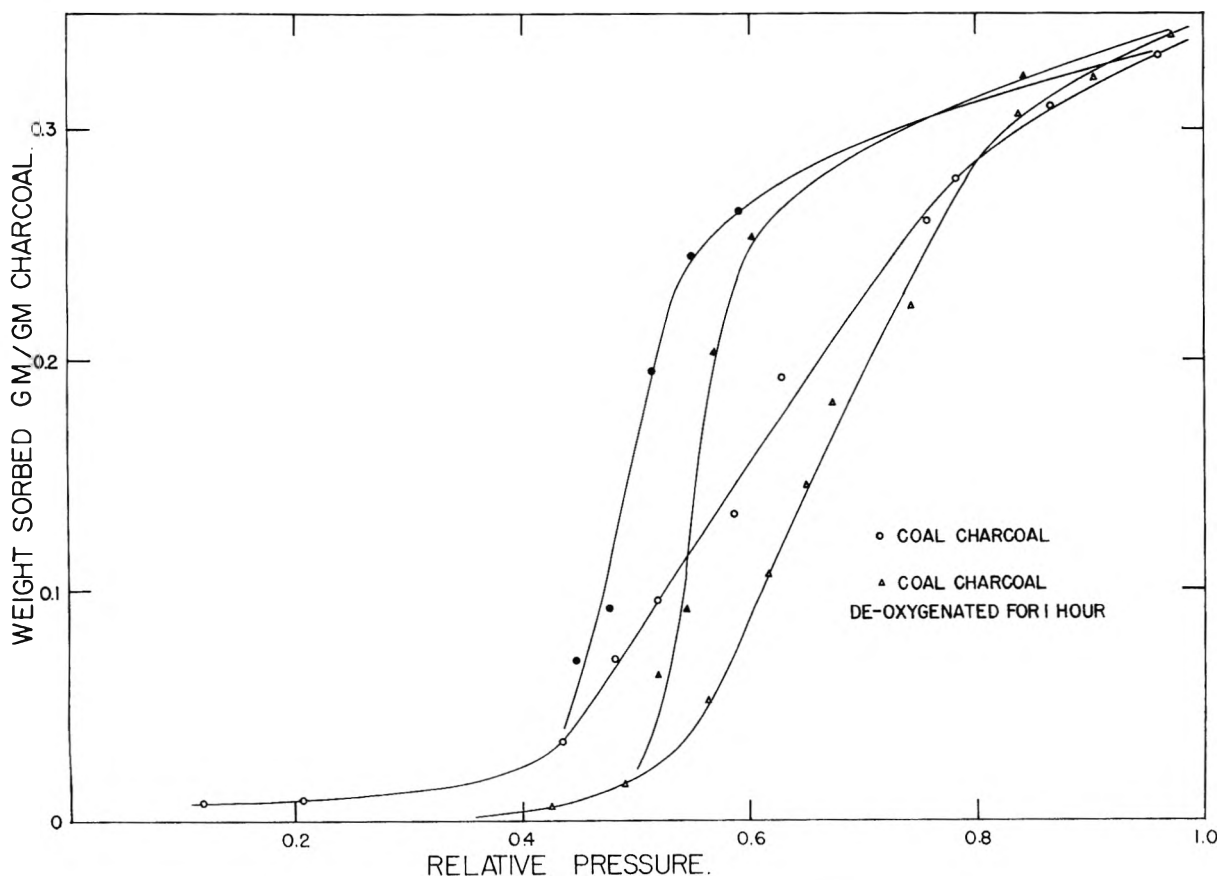

Fig. 3.—Sorption isotherms for the coal charcoals: open symbols denote adsorption; solid symbols denote desorption.

Water Isotherms of Hydrogen Treated Charcoals.—The water isotherms for the charcoals before and after treatment are depicted in Figs. 1 to 3. Figure 1 shows a comparison of the iso-

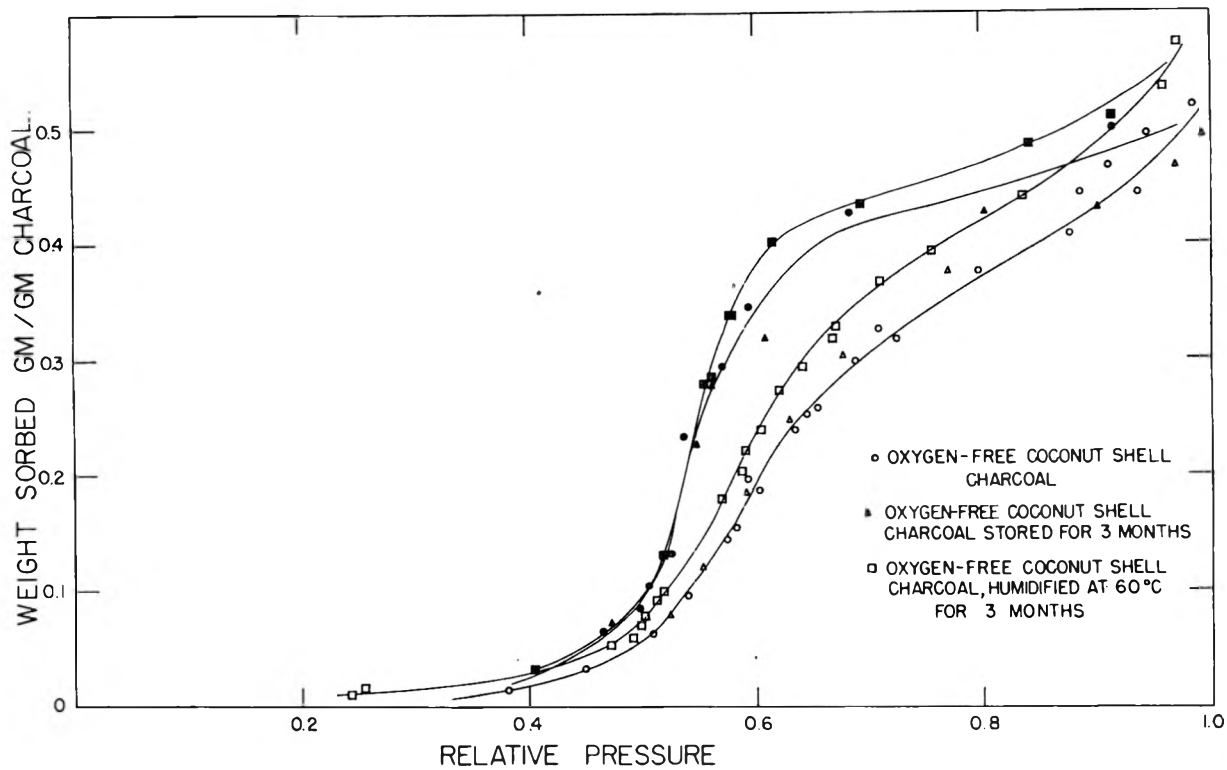

Fig. 4.—Sorption isotherms for the oxygen-free and reoxidized coconut shell charcoals: open symbols denote adsorption, solid symbols denote desorption.

therm for the untreated charcoal with the isotherm of a zinc chloride activated charcoal treated with hydrogen for 4.5 hours at 1000°. Also shown are the points (triangles) for the charcoal treated for 4.5 hours at 1000° and transferred to the sorption cell without exposure to air. The points (circles and triangles) for the two 4.5-hour samples are very close together and it has been concluded that exposure to air after cooling does not affect the water isotherm of a deoxygenated charcoal. Figure 2 shows a similar comparison of the isotherms of a coconut shell charcoal before and after treatment with hydrogen for one hour at 1000°. This coconut shell charcoal was similar to the one used in the analytical work on evolved gases described in the preceding section, but was of smaller granule size. The isotherms for a typical coal charcoal before and after treatment with hydrogen for one hour at 1000° are shown in Fig. 3.

Density and Surface Area of Deoxygenated Charcoal.—The values of the density measurements using mercury and benzene as displacement media are given in Table IV. Also listed are the surface areas of the charcoals calculated from the desorption branch of the water isotherm using the equation[10]

$$A = \int_{V_i}^{V_s} \frac{1}{r}(V)\,dV$$

where A is the surface area, r the pore radius calculated from the Kelvin equation (with $\cos\theta = 0.65$, and V the volume of the unfilled pores. V_s is the volume of water held at saturation and V_i the volume sorbed at the inception of the hysteresis loop. In a few instances the nitrogen surface areas were measured and these also are listed.

(10) S. S. Kistler E. A. Fischer and I. R. Freeman, *J. Am. Chem. Soc.*, **65**, 1909 (1943).

Table IV

Physical Constants of Charcoals

Charcoal	Mercury density, g./cc.	Benzene density, g./cc.	Pore vol., cc./g.	Water surface, m.²/g.	Nitrogen surface, m.²/g.
Coconut shell	0.87	2.079	0.67	630	1190
Treated coconut shell	82	2.082	0.74	670	
$ZnCl_2$ activated wood	63			1120	1580
Treated $ZnCl_2$ activated wood				890	1580
Coal charcoal	.98	2.200	0.57	450	
Treated coal charcoal	.94	2.193	0.61	450	

Oxidation of a Coconut Shell Charcoal.—The water isotherm following the mild oxidation of a deoxygenated coconut shell charcoal is shown in Fig. 4. This oxidized sample sorbs more water over the whole range of humidities than the deoxygenated sample.

Discussion

The isotherms plotted in Figs. 1 to 3 show that the deoxygenation treatment has reduced the sorption of water by all the charcoals at relative pressures of less than 0.8. As the Kelvin equation indicates, at high humidities the pore spaces fill up and in this region the oxygen content has little or no effect on the water sorption. However the data of Table IV illustrate that with exception of the zinc chloride activated wood charcoal, which shows a small reduction in surface area, pore volumes and surface

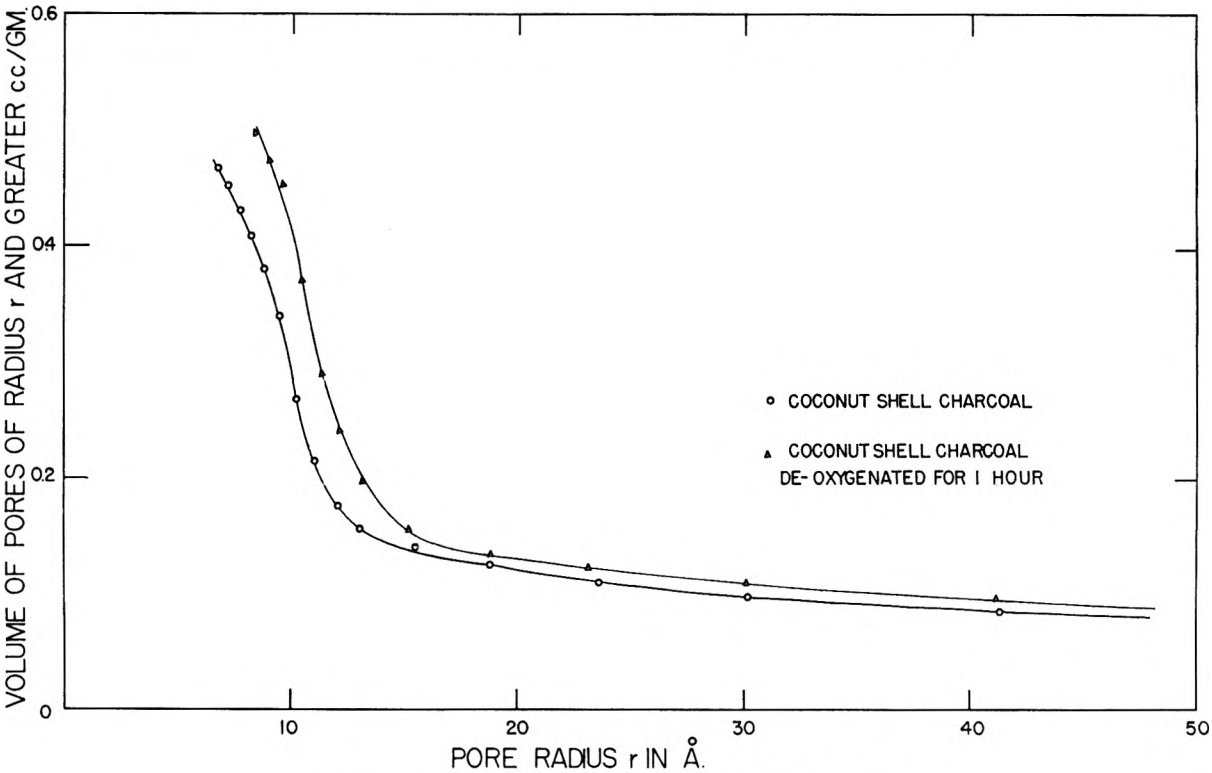

Fig. 5.—Pore distributions for the coconut shell charcoals.

areas have remained unchanged or increased as a result of the removal of oxygen. Therefore it may be concluded that the initial sorption of water depends on the oxygen content of the charcoal and not on the pore volume or surface area of the charcoal. This is not what would be expected if adsorption occurred by capillary condensation as postulated by Juhola and Wiig.[7] Moreover Juhola and Wiig have suggested that the hysteresis loop observed in water isotherms is caused by constrictions in the pores. It has been shown in the analytical work that the treatment with hydrogen removes some carbon along with the oxygen. If constrictions were present, these would be expected to be attacked first by the hydrogen since they are composed of more exposed and thus more active carbon atoms and hence the hysteresis loop should be smaller than that of the original untreated charcoal. The opposite result was actually obtained, as it was found that the hysteresis loop was enlarged by the deoxygenation treatment. It is believed therefore that the concepts of Pierce and Smith[2] which are upheld in our previous paper[8] offer a more plausible explanation of the facts. Sorption initially proceeds on specific sites which are believed to be oxygen molecules or atoms since their removal diminishes the amount of water sorbed. Clusters of water molecules grow on these sites by a mechanism of hydrogen bonding with increasing relative pressure until they reach a size where finally they coalesce to fill the smaller pores. Capillary condensation can occur only subsequently and in the larger pores at relative pressures above the hysteresis region, as it is felt that the hysteresis loop is an indication of cluster formation on adsorption and evaporation from menisci on desorption.

It was found that the coconut shell charcoal contains 0.05 g. oxygen per g. of carbon and sorbs 0.045 g. of water per g. of charcoal at the inception of the hysteresis loop. These weights correspond to a sorption of one molecule of water per atom of oxygen at the inception of the hysteresis loop. If one oxygen atom comprises one possible site for cluster formation then a monolayer is sorbed on the oxygen atoms at the inception of the hysteresis loop. It is reasonable to assume that similar considerations apply to all the charcoals and that the amount of water held at the inception of the hysteresis loop provides an approximate measure of the oxygen held by charcoal. The weights of water held at the lower end of the hysteresis loop before and after deoxygenation are given in Table V.

TABLE V

WEIGHT OF WATER SORBED AT INCEPTION OF HYSTERESIS LOOP

	Before treatment, g./g. char.	After treatment, g./g. char.
Coconut shell charcoal	0.045	0.015
Coal charcoal	.035	.015
Zinc chloride activated wood charcoal	.060	.010

The Density of Hydrogen Treated Charcoal in Benzene.—The density values listed in Table IV show that the densities of coconut shell and coal charcoals were unchanged by the deoxygenation treatment. This is taken to mean that the oxygen on the surface of the charcoal had approximately the same density as the charcoal itself. Moreover the oxygen must have been distributed in the form of isolated atoms or molecules to give rise to such a high density. For example if it were packed

as in the solid state, then its density would be about unity and the density of the coconut shell charcoal would have been 2.05 g./cc. instead of 2.08 g./cc. This supports the original contention that the oxygen was in the form of isolated centers which formed nuclei for cluster formation.

Increase in Pore Volume as a Result of Oxygen Removal.—The enlargement of the pores as a result of the treatment with hydrogen is demonstrated by the pore volumes given in Table IV and by the pore distributions graphed in Fig. 5. The radii of the pores were calculated from the Kelvin equation using a value of 0.65 for cos θ and the "volume of pores of radius r and greater" was obtained by subtracting the volume of water sorbed at a relative pressure corresponding to r from the volume of water sorbed at saturation. These pore distributions are for coconut shell charcoal, and are typical of those found for all the charcoals before and after deoxygenation. In Table VI are listed the measured increases in pore volume calculated from the mercury densities for two of the charcoals.

Two sets of calculated values for the increase in pore volume also have been given. The first of these was computed from the measured increase in pore radius obtained from the relative pore distributions (*cf.* Fig. 5) and the surface area of the charcoal assuming the pore walls to be in the form of parallel plates. The second of these are values calculated from the weight loss suffered by the carbon and the measured densities in benzene. The values calculated by the first method are of the correct order of magnitude, which is all that could be expected. Those calculated from the weight of material removed are much smaller than the measured values and this is taken to mean that most of the increase in the pore volume is caused by swelling of the charcoal during heating.

TABLE VI

Charcoal	Measured increase in pore vol.	Increase in pore vol. calcd. from pore radii, cc./g. of charcoa	Increase in pore vol. calcd. from analytical work
Coconut shell	0.07	0.12	0.03
Coal charcoal	0.04	0.08	0.02

Acknowledgment.—The authors wish to acknowledge the assistance of Mr. N. J. McLeod who performed the chemical analyses.

VINYLTOLUENE–STYRENE COPOLYMER SULFONIC ACIDS. II. IONIC DISSOCIATION IN METHANOL–WATER AND HCl–WATER SOLUTIONS

BY RICHARD A. MOCK, CHARLES A. MARSHALL AND THOMAS E. SLYKHOUSE

Plastics Basic Res. Lab., Dow Chemical Co., Midland, Mich.

Received February 15, 1954

Vinyltoluene–styrene copolymer sulfonic acids in dilute solution exhibit conductance behavior which differs appreciably from that of strong 1:1 electrolytes and other chain polyelectrolytes. The equivalent conductance of the polysulfonic acid shows no observable dependence on either polymer concentration or total solution ionic strength at moderate to very high dilutions. However, sodium poly-*p*-styrenesulfonate shows a variation of equivalent conductance with concentration which is functionally identical to behavior observed by other workers for sodium polymethacrylate and poly-4-vinyl-N-*n*-butylpyridinium bromide. Proton counterions are apparently the major contributors to polysulfonic acid solution conductance, which does not vary greatly with polymer molecular weight. Values of ionic dissociation in methanol–water systems were calculated under the assumption of negligible polysulfonate ion mobility. In the regions 0–60% and 90–100% methanol the dissociation is apparently proportional to the solvent dielectric constant. Elsewhere, the dissociation of the polyacid is not significantly influenced by the methanol content of the solvent.

As a continuation of our experimental studies to obtain a fundamental understanding of the properties of vinyltoluene–styrene copolymer sulfonic acids, an investigation of the dilute solution conductance and dissociation of these polyacids in several media has been undertaken. The first paper[1] in this series was concerned with the viscosity and *p*H of dilute aqueous solutions of the polysulfonic acids, and the influence of solution ionic strength on these properties.

Sulfonated vinyltoluene–styrene copolymers exhibit conductance behavior in dilute solutions which is markedly different from that of strong 1:1 electrolytes. The equivalent conductance of the latter in polar solvents is dependent upon both the individual solute concentration and the total ionic strength of the system. Such dependence is not observed in water and water–methanol solutions of the sulfonated copolymers over the concentration range investigated.

This observation also presents an interesting contrast to previous experience with other polyelectrolytes.[2–4] However, when the polysulfonic acid is neutralized with strong NaOH, the resulting sodium salt appears to conform to the experimental pattern observed for other comparable systems. The physical significance of our conductance results when the gegenion is a proton (or hydronium ion) is not immediately apparent. In all likelihood, transference experiments leading to information concerning the mobility of the polyion in these solutions should aid in clarifying the situation. Work on this problem is in progress.

I. Experimental Procedure

Polyacid samples A-1 and A-2 were synthesized by sulfonation of polyvinyltoluene, and sample A-3 was prepared in a comparable manner from a 1:1 copolymer of vinyltolu-

(1) R. A. Mock and C. A. Marshall, *J. Polymer Sci.*, in press.

(2) R. M. Fuoss and U. P. Strauss, *ibid.*, **3**, 246 (1948).

(3) J. R. Huizenga, P. F. Grieger and F. T. Wall, *J. Am. Chem. Soc.*, **72**, 4228 (1950).

(4) A. Oth and P. Doty, THIS JOURNAL, **56**, 43 (1952).

TABLE I

PHYSICAL CHARACTERISTICS OF SULFONATED POLYMERS

Sample designation	Base polymer type	Base mol. wt. of sulfonate[a]	Mol. wt. of polysulfonate	Volatiles in sulfonate, %	Q (mole % sulfonate)	Base equiv. wt. (g. polymer/eq. H^+)
A-3	1:1 Vinyltoluene-styrene copolymer	178.6	168,600[b]	8.22	84.49	211.2
A-1	Polyvinyltoluene	198.0	(930,000)[d]	11.77	93.22	212.4
A-2	Polyvinyltoluene	198.0	(54,000)[d]	13.16	94.02	210.6
S-1[c]	Synthesized from monomer	206.2	529,000[e]	8.80	100.00	206.2

[a] Mol. wt. of one "average" monomer unit in polymer chain. [b] Detd. by osmotic measurement. [c] Sodium salt. [d] Estimated from data for parent polymer. [e] Detd. by light scattering measurements.

ene and styrene. The latter sulfonate has been described previously.[1] Preparation and purification of the products was carried out by H. H. Roth of these laboratories. All sulfonates were somewhat hygroscopic, and contained a considerable amount of volatile matter. Heating *in vacuo* at 50° removed the volatiles, but produced a pink color in the samples. In order to avoid the possibility of degradation of the polyacids, experimental solutions were made from the undried materials, and concentrations were corrected in accordance with the results obtained from drying separate samples to constant weight.

If E is defined as the equivalent weight of titratable hydrogen per gram of polymer, then the reciprocal of E is the base-equivalent weight of the polyacid. A potentiometric titration of an aqueous polyacid solution with standard NaOH yields these quantities immediately. The mole fraction of sulfonated polymer in a sample Q is given by

$$Q = mE \qquad (1)$$

where m is the base-molecular weight (molecular weight of one chain unit) of the material. Titration results are given in Table I.

Molecular weights (number average) of the parent polymers used in preparing A-1 and A-2 were estimated from 10% toluene solution viscosities to be 930,000 and 54,000, respectively. Osmotic pressure measurements in methyl ethyl ketone solution (Fig. 1) yielded a molecular weight of 224,000 for the styrene–vinyltoluene copolymer. Also shown in Fig. 1 are osmotic data for the polysulfonate A-3 from which a molecular weight of 168,600 was computed. The "solvent" used in obtaining the latter data consisted of a 0.862 N aqueous solution of Na_2SO_4, to which had been added 0.05% Duponol ME to reduce the surface tension of the solutions. Comparison of these results indicates that the parent copolymer may have been degraded to some extent during sulfonation. Our earlier work with A-3 revealed that its ionic dissociation in water is a constant equal to 0.38, which is independent of polymer concentration and solution ionic strength at moderate to high dilutions. The limiting viscosity number for A-3 in 3.55 N HCl is 78 ml./g.

In contrast to the usage of some authors, we will reserve the symbol α to denote the degree of dissociation of a completely ionized polyelectrolyte, rather than the extent to which ionizable groups on a polymer chain are charged.

$$\alpha = \frac{\text{equiv. dissociated counterion/l. soln.}}{\text{base equiv. polyelectrolyte/l. soln.}} \qquad (2)$$

pH data for aqueous solutions of A-1 are listed in Table II. As was expected, the dissociation α, calculated with the aid of (2), was found to be essentially independent of polyelectrolyte concentration. A value of 0.44 was obtained by simply averaging the data.

TABLE II

pH OF POLYACID A-2 SOLUTIONS IN H_2O AT 25°

Concn. (base eq./l.)	pH	α
4.343×10^{-2}	1.68	0.482
3.436×10^{-2}	1.82	.441
2.596×10^{-2}	1.97	.414
1.713×10^{-2}	2.13	.432
8.708×10^{-3}	2.42	.436
2.481×10^{-3}	2.98	.422
1.155×10^{-3}	3.31	.424
H_2O	6.22	...

Sodium poly-*p*-styrenesulfonate (S-1) was prepared by polymerizing the corresponding monomer in 40% aqueous solution at 95° for three hours in the presence of 0.1% (basis monomer) $Na_2S_2O_8$. Unsaturation analysis of the reaction mixture showed essentially complete conversion after this elapsed time. The viscous solution obtained was added dropwise to a 10-fold excess of ethanol with vigorous stirring, and the resulting granular precipitate was filtered, washed with ethanol, and dried. It was again dissolved in water, and reprecipitated as above. Light scattering data for solutions of this material in 0.6902 N and 1.270 N NaCl are shown in Table III, which yield a weight average molecular weight for S-1 of 529,000.

TABLE III

LIGHT SCATTERING DATA FOR AQUEOUS NaCl SOLUTIONS OF SODIUM POLY-*p*-STYRENESULFONATE

$Z_0 = 2.15$; $P(90) = 1.667$; $M = 529{,}000$; $\lambda = 4370$ Å.; $dn/dc = 0.200$; $n = 1.342$; $H = 1.084 \times 10^{-6}$

0.6902 N NaCl			1.270 N NaCl		
Concn. $\times 10^4$ (g./ml.)	$Hc/\tau \times 10^5$	Z	Concn. $\times 10^4$ (g./ml.)	$Hc/\tau \times 10^5$	Z
66.13	6.32	1.59	52.62	4.58	1.77
56.94	5.78	1.63	34.29	4.02	1.90
40.21	4.79	1.76	20.23	3.74	1.97
22.21	4.07	1.88	10.23	3.38	1.99
9.804	3.64	2.02	7.432	3.26	2.08
6.382	3.54	2.10	3.955	3.20	2.24
3.346	3.38	2.14			

Solutions used in the conductance and pH studies were prepared in the following manner. Stock solutions were made up at a concentration of approximately 10 g. per liter by gravimetric methods. All dilutions were made from these solutions volumetrically at 25°. The solvent systems used during the course of the investigation were water, methanol, water–methanol and water–hydrogen chloride.

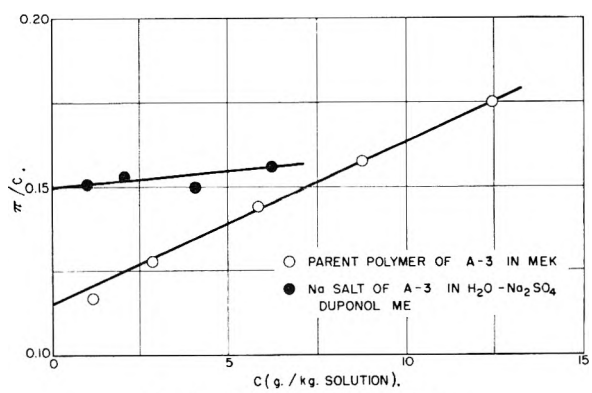

Fig. 1.—Osmotic pressure data.

Specific conductances were measured at 25 ± 0.003° with a Leeds and Northrup commercial conductivity bridge and a cell whose constant was 0.1000 ± 0.0002. Sixty-cycle alternating current at 110 volts used as a power supply was reduced to 12 volts at 60 cycles across the bridge circuit. The frequency dependence of polyacid solution conductivity was investigated with a circuit consisting of a Solu-Bridge,

a 25-volt frequency generator for a power supply, and the above cell, which permitted measurement of conductivity in the region 20 to 10,000 c.p.s. Essentially no frequency dependence over this range was observed.

II. Discussion

A. Conductance of Polyacid A-2 in Water–Methanol Solutions.—Equivalent conductances Λ of the polyacid samples were calculated by means of the equation

$$\Lambda = \frac{10^3 \kappa}{cE} \qquad (3)$$

where Λ is given in ohms^{-1} per equivalent of available hydrogen, κ is the specific conductance corrected for the solvent, and c is the polymer concentration in g. per liter of solution. Plots of log Λ *vs.* log c shown in Fig. 2 have a zero slope over the entire range of our experiments. Therefore, it appears reasonable to assume that Λ is always equal to Λ^0, the equivalent conductance at infinite dilution.

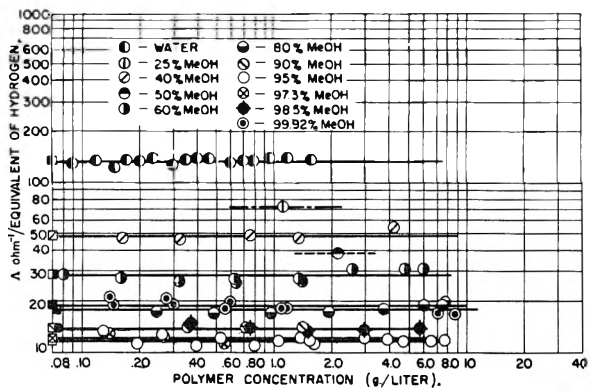

Fig. 2.—Equivalent conductance *vs.* concentration for A-2 in methanol–water systems.

A plot of Λ^0 *vs.* weight per cent. methanol in the solvent (Fig. 3) shows that the limiting conductance decreases monotonically with decreasing solvent dielectric constant (wt. % MeOH) until a minimum occurs at 95% methanol. The value of Λ^0 increases again in the region 95–100% methanol.

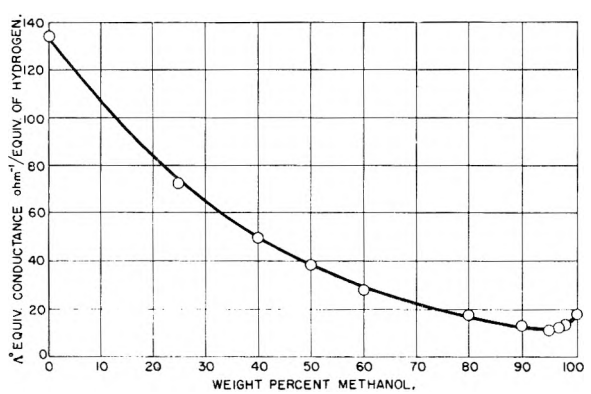

Fig. 3.—Equivalent conductance of A-2 *vs.* weight per cent. methanol in solvent.

Transference measurements of Wall and coworkers[4] with sodium polyacrylate solutions clearly demonstrate that the mobility of the large ions is sufficiently great compared to that of the sodium ions for the former to make an appreciable contribution to solution conductance. We do not have available at this time mobility data for the polysulfonic acid, which is needed to make such a comparison when the counterion is a proton. However, if it is assumed that in any solvent Λ^0 is chiefly the result of proton ion conductance, then

$$\alpha = \frac{\Lambda^0}{\lambda_H{}^0} \qquad (4)$$

where $\lambda_H{}^0$ is the limiting ionic conductance of the proton in the same medium. For aqueous solutions of A-2, $\Lambda^0 = 135$ (*cf.* Fig. 2). Introducing this value and $\lambda_H{}^0 = 350$ into (4), we find $\alpha = 0.386$, which compares favorably with the value 0.44 obtained from the *p*H measurements. It is of interest to observe that α computed from (4) for aqueous A-2 is lower than the corresponding result from *p*H data. If Λ^0 contained an appreciable contribution from the polyion conductance, one would expect α calculated from (4) to be significantly higher than the degree of dissociation obtained from *p*H results. However, the converse is apparently true, and this observation lends indirect support to the assumption of negligible polyion mobility.

In order to calculate α from polyacid conductance data in methanol–water solutions by means of (4), it is necessary to know the limiting ionic conductance of the proton in the same solvent systems. These data were not all available in the literature, and had to be obtained experimentally. Longsworth and MacInnes[5] have computed λ_{Cl} from transference and conductance measurements on 0.05 *N* solutions of NaCl and LiCl in various methanol–water mixtures at 25°. From these results we have calculated limiting ionic conductances $\lambda_{Cl}{}^0$, using the Onsager–Fuoss relation[6]

$$\lambda_{Cl} = \lambda_{Cl}{}^0 - S\sqrt{C} \qquad (5)$$

where S is the theoretical limiting slope of chloride ion conductance, and C is the concentration in equivalents per liter. For either ion (in this case Cl^-) of a 1:1 electrolyte

$$S = (\alpha^* \lambda_{Cl}{}^0 + \beta^*/2) \qquad (6)$$

where

$$\alpha^* = \frac{1.97 \times 10^6 \times 0.2929\sqrt{2}}{(DT)^{3/2}} \qquad (7)$$

$$\beta^* = \frac{28.98 \times 2\sqrt{2}}{\eta_0 (DT)^{1/2}} \qquad (8)$$

η_0 and D are the viscosity and dielectric constant of the various solvents.[7,8] Figure 4 is a plot of $\lambda_{Cl}{}^0$ *vs.* weight per cent. methanol in the solvent. The equivalent conductance of HCl in methanol–water solvents was determined experimentally, and extrapolation of plots of Λ *vs.* $\sqrt{c}$ (Fig. 5) to infinite dilution gave corresponding values of Λ^0 (Fig. 6). Then from Kohlrausch's law

$$\Lambda^0 = \lambda_H{}^0 + \lambda_{Cl}{}^0 \qquad (9)$$

and Fig. 4, values of $\lambda_H{}^0$ were obtained. The calculated results are plotted against weight per cent. methanol in Fig. 7.

(5) L. G. Longsworth and D. A. MacInnes, THIS JOURNAL, **43**, 239 (1939).

(6) L. Onsager and R. M. Fuoss, *ibid.*, **36**, 2689 (1932).

(7) E. C. Bingham, *et al.*, *Z. physik. Chem.*, **83**, 641 (1913).

(8) T. T. Jones and R. M. Davies, *Phil. Mag.*, [7] **28**, 289, 307 (1939).

TABLE IV

CALCULATION OF α FOR A-2 FROM CONDUCTANCE DATA AND THEORY

Wt. % MeOH	Dielectric constant (D)	Viscosity (cps.)	λ_{Cl}	λ_{Cl}^0	λ_H^0	Λ^0	α
0	78.5	0.8952	68.00	76.33	349.9	135.0	0.386
10.0	74.1	1.176	45.86	54.35	288.6	...	...
20.0	69.2	1.393	36.22	43.50	239.0	...	...
25.0	...	...	...	...	217[a]	72.5	0.334
40.0	59.6	1.592	30.46	37.68	167.1	49.0	.293
50.0	...	...	...	...	136[a]	39.0	.286
60.0	50.1	1.389	29.73	38.95	110.3	28.8	.261
80.0	40.1	1.027	30.82	45.20	67.8	18.2	.268
90.0	...	...	...	...	54[a]	13.5	.249
95.0	...	...	...	...	59[a]	11.7	.200
97.3	...	...	...	...	75[a]	12.2	.163
98.5	...	...	...	...	95[a]	13.4	.141
100.0	...	...	...	51.3[b]	142.2[b]	18.7	.131

[a] Interpolated values, from Fig. 4, with the aid of Kohlrausch's law and Fig. 6. [b] M. Barak and H. Hartley, *Z. physik. Chem.*, **165**, 290 (1933).

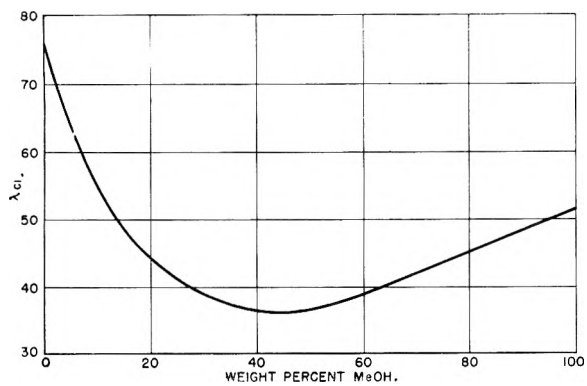

Fig. 4.—λ_{Cl} *vs.* per cent. MeOH.

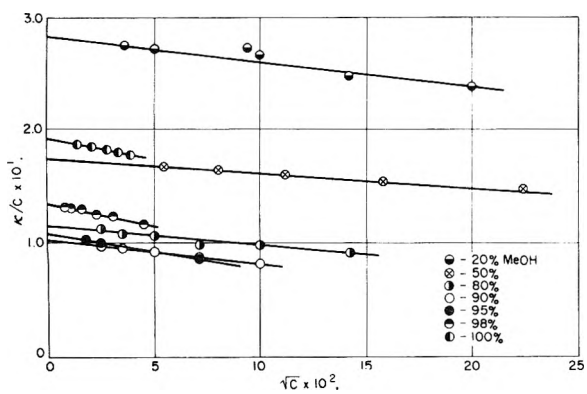

Fig. 5.—Equivalent conductance of HCl in MeOH–H_2O solutions at 25°.

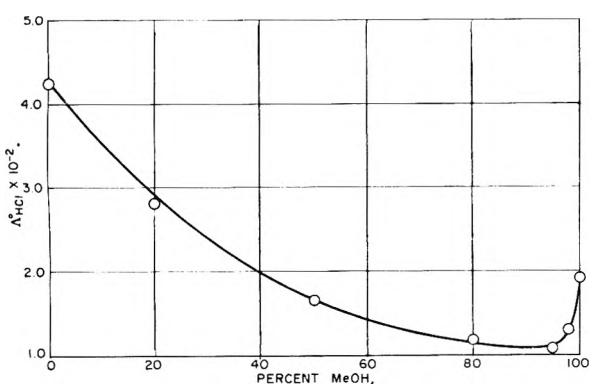

Fig. 6.—Λ^0 for HCl *vs.* per cent. MeOH in solvent at 25°.

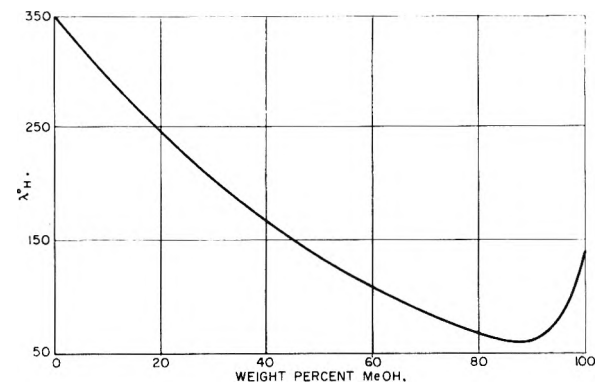

Fig. 7.—λ^0_H *vs.* per cent. MeOH in MeOH–H_2O solvent mixtures at 25°.

Introduction of these data into equation (4) together with Λ^0 values for A-2 yields α for the polyacid in the various methanol–water mixtures investigated. The calculations are summarized in Table IV, and plots of α *vs.* D and per cent. methanol, respectively, are shown in Fig. 8. α appears to be proportional to D in the regions 0–60% and 90–100% methanol content of the solvent. Between these two regions, α shows little (if any) dependence on D.

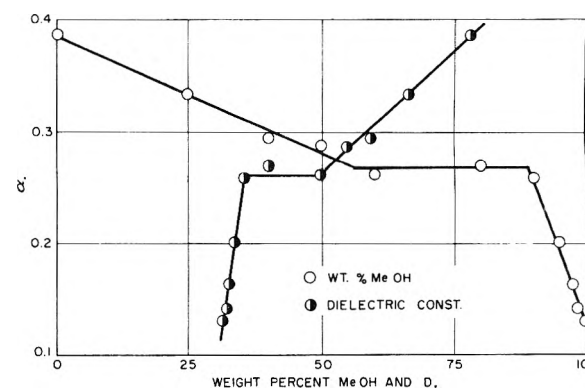

Fig. 8.—α for A-2 in MeOH–H_2O solutions at 25°.

In any solvent the degree of dissociation for "normal" electrolytes can be estimated from Ostwald's law, $\alpha = \Lambda/\Lambda^0$. If this law were to hold true for our polysulfonic acid solutions, an extrapo-

lation of conductance data to a limiting value corresponding to $\alpha = 1$ would be a necessity. However, such treatment does not appear tolerable in the light of our experimental observations of constant α over a wide range of solution ionic strengths.[1]

Our conductance, viscosity and *p*H data appear to be compatible with a molecular model in which the polymer in solution is considered to be a swollen ellipsoid as opposed to a rigid rod in the vicinity of infinite dilution. As concentration increases corresponding increases in surface charge interaction can be considered to exert a compressional force on the ellipsoid which results in a decrease in molecular size. The surface charge on such macroions remains constant throughout these changes in molecular volume, and therefore the surface charge density at moderate concentrations must be postulated as an increasing function with increasing solution ionic strength.

The concept of incomplete polyacid dissociation at infinite dilution appears to be a logical corollary to this hypothesis. The number of protons trapped within the swollen ellipsoid probably remains invariant with changing polymer concentration. Moreover, these protons should be in close proximity to sulfonate groups, with the result that the electric field inside the macromolecule is vanishingly small. As a further consequence of this model along with the assumption of negligible polyion mobility, one would anticipate at least some dependence of polyacid equivalent conductance on concentration of polymer. The fact that such dependence is not observed is a major factor opposing our speculations, which simultaneously indicates the need for further investigation of these systems.

B. Influence of Polymer Molecular Weight and Solution Ionic Strength on Polyacid Conductance.—The dependence of specific conductance on molecular weight was studied by measurements made on all three polysulfonate samples in water and on two of the samples in 95% methanol (Fig. 9). In 95% methanol, results for A-3 and A-2 are identical within the limits of experimental error.

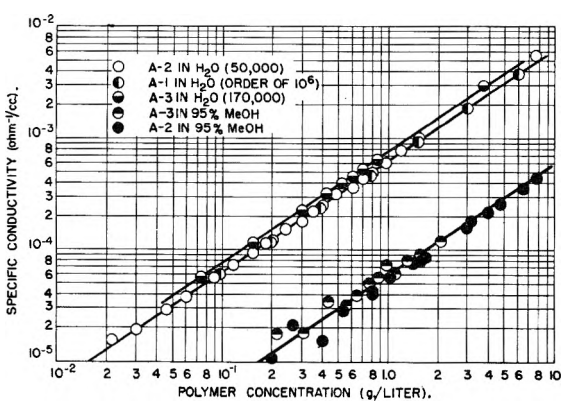

Fig. 9.—Specific conductance curves for several polyacids in H_2O and 95% MeOH at 25°.

However, A-1 and A-2 in water show nearly identical specific conductivities, while values for A-3 are slightly higher. From these somewhat anomalous data it would appear that the conductance of this polyelectrolyte is a very mild function of molecular weight.

Conductance data were obtained for solutions of A-2 in water and various concentrations of aqueous HCl in the range 1×10^{-6} *N* to 8×10^{-4} *N*. It was assumed that the contributions of the HCl and polysulfonate to the solution conductance were additive, and measured values for the HCl "solvents" were subtracted from the solution data. The resulting contributions of A-2 to κ are plotted against *c* in Fig. 10. Most of the points fall on a single line within the limits of experimental error, indicating that the equivalent conductance of the polysulfonate is unaffected by the ionic strength of the solution within this range of concentrations.

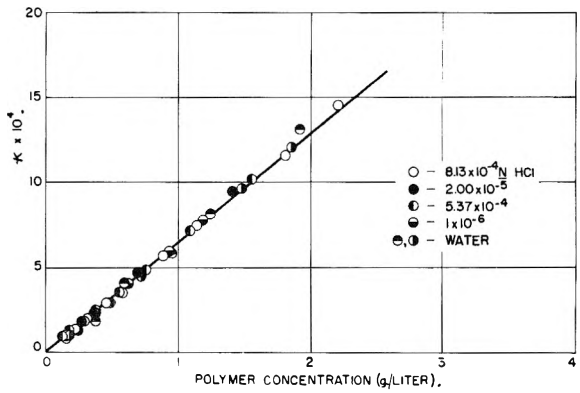

Fig. 10.—Specific conductance of polysulfonate A-2 in H_2O–HCl solutions at 25°.

C. Aqueous Solution Conductance of Sodium Poly-*p*-styrenesulfonate.—In contrast to the results described above, the equivalent conductance of sodium poly-*p*-styrenesulfonate (S-1) in aqueous solution proved to be concentration-dependent. These data, along with values previously reported by Doty and Oth[4] and by Fuoss and Strauss[2] for sodium polymethacrylate and poly-4-vinyl-N-*n*-butylpyridinium bromide can be adequately represented by the three-parameter empirical equation

$$\Lambda - \Lambda^0 = -\sqrt{C}/(A + B\sqrt{C}) \qquad (10)$$

Calculated values of *A*, *B* and Λ^0 for these three polyelectrolytes are listed in Table V and the corresponding test plots for (10) are given in Fig. 11.

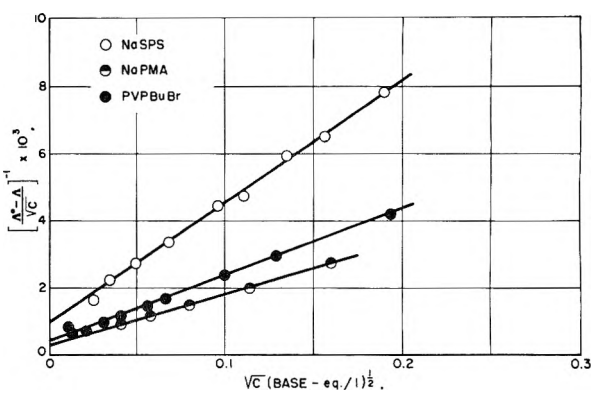

Fig. 11.—Conductance function test for several polyelectrolytes.

The weight average molecular weight calculated for S1- from light scattering data does not permit com-

TABLE V

EMPIRICAL CONDUCTANCE EQUATION PARAMETERS

Compound	Λ^0	$A \times 10^1$	$B \times 10^2$
Na PMA	100	3.10	1.53
Na SPS	100	9.90	3.60
PVP BuBr	75	4.20	1.97

parison with values obtained for the other polyelectrolytes considered here.[3,4] However, it is likely that in a given solvent the dependence of Λ on c is most strongly influenced by the strength of the polyelectrolyte (α) and the nature of its counterion, in view of the data presented for the free polyacid.

WETTABILITY STUDIES OF NYLON, POLYETHYLENE TEREPHTHALATE AND POLYSTYRENE[1]

BY A. H. ELLISON AND W. A. ZISMAN

Surface Chemistry Branch, Chemistry Division, Naval Research Laboratory

Received February 18, 1954

A study has been made of the wettability of smooth surfaces of polyethylene terephthalate, nylon and polystyrene by observing the equilibrium contact angle, θ_E, formed by a liquid drop resting on the solid surface. A variety of liquids were studied. Critical surface tensions for the three surfaces are 42.5 to 46.0 dyne/cm. for nylon, 43.0 for polyethylene terephthalate, and 32.8 to 43.3 for polystyrene. The results for nylon are compared with previous results for polyethylene to show the effect of the amide group on wettability. The results for polyethylene terephthalate are similarly compared with those for polystyrene. These comparisons show that the wettability by polar hydrogen-bonding liquids is increased by the presence of both the amide group and the ester group in the solid surface but to a much greater extent by the amide group. The wettability by organic liquids containing Cl, Br or I is less affected by the amide or ester groups as might be expected from the inability of halogenated liquids to form hydrogen bonds. Reasons are given for believing that hydrogen-bonding takes place in the wetting of nylon by water, glycerol, formamide and thiodiglycol and does not take place in the wetting of polyethylene terephthalate by these liquids. The postulated mechanism of wetting led to an experiment which showed that perfluorolauric acid could be adsorbed on nylon from *n*-decane solution rendering the nylon surface oleophobic.

Introduction

The wettability of surfaces of nylon and polyethylene terephthalate (sold under the trade name "Mylar" when in film form and "Dacron" when in fiber form) are of interest in the general study of wettability of solid surfaces because the amide and ester groups, respectively, in these two surfaces contain electronegative atoms which could take part in hydrogen-bonding at the solid/liquid interface.[2] The surface of polystyrene was included in this study for comparison since such a surface is a rough approximation to the surface of polyethylene terephthalate without the ester groups. The work on the wettability of polyethylene[3] can be used for a similar comparison in the case of the nylon surface. A parallel study of the frictional properties of these plastics has been carried on and will be reported elsewhere.[4]

Materials and Procedures

The liquids used in studying wettability were chosen to give a wide range of surface tensions and a variety of structural types. They were prepared in a high degree of purity for these wettability studies; the source and purification treatment of each have been described in a previous paper of this series.[5]

Discs of nylon 1 inch in diameter and $^1/_2$ inch thick were cut from rods of unplasticized 6,6-nylon (the linear condensation polymer of 1,6-hexamethylene diamine and adipic acid). Specularly smooth surfaces were obtained by polishing the discs with a light pressure on a Buehler polishing wheel using a clean, dry, silk polishing cloth. Presumably a flash surface heating resulted which caused the surface to melt and flow, and then to cool rapidly before crystallization occurred. These surfaces were then cleaned with a concentrated aqueous solution of the detergent Tide, were thoroughly rinsed, and finally were dried in air at 75° for several hours.

It has been shown by earlier frictional measurements on a variety of dry abraded plastic surfaces that Tide effectively degreases the surfaces and does not remain on the surface after rinsing with water.[6] This was done by observing the results of cleaning the plastic surfaces with Tide and those obtained when they were cleaned by rigorous but more time consuming cleaning procedures. This was also found to be true during wettability measurements on the same plastics.[7] In this investigation frictional measurements were also made to check the cleaning techniques and it was found that cleaning with Tide followed by thorough rinsing with distilled water produced plastic surfaces free of organic contamination.

Several types and gages of polyethylene terephthalate films were studied. The properties of this polymer (the condensation product of ethylene glycol and terephthalic acid) have been described by Amborski and Flierl.[8] Since the surfaces of these films were specularly smooth as received, it was necessary only to clean them with Tide. When the surfaces of polyethylene terephthalate were freed of electrostatic charges by using an alpha particle source, no variation in the contact angle for a given liquid was found between one gage or another, one type of manufacturing procedure or another, or one side or the other of a given sheet. Contact angles of hydrogen-bonding liquids on undischarged surfaces were lower than those reported, while those of the halogenated liquids used were the same.

Smooth surfaces of polystyrene could be obtained readily by heat casting each against the smooth surface of an acid-cleaned optically flat glass block as described in studies of other plastics.[3]

The solid/liquid contact angles were measured with the goniometer described earlier.[9] The equilibrium advancing contact angles of the various liquids of interest were obtained by gently placing a drop on the surface and adding small increments of liquid to the drop until the advancing

(1) Presented before the Division of Polymer Chemistry, 125th Meeting, American Chemical Society, March 23–April 1, 1954, Kansas City, Missouri.

(2) A. H. Ellison, H. W. Fox and W. A. Zisman, THIS JOURNAL, **57**, 622 (1953).

(3) H. W. Fox and W. A. Zisman, *J. Colloid Sci.*, **7**, 428 (1952).

(4) R. C. Bowers, W. C. Clinton and W. A. Zisman, "The Friction and Lubrication of Nylon," to be published.

(5) H. W. Fox and W. A. Zisman, *J. Colloid Sci.*, **5**, 514 (1950).

(6) R. C. Bowers, W. C. Clinton and W. A. Zisman, *Lubrication Engineering*, **9**, 204 (1953).

(7) A. H. Ellison and W. A. Zisman, THIS JOURNAL, **58**, 260 (1954).

(8) L. E. Amborski and D. W. Flierl, *Ind. Eng. Chem.*, **45**, 2290 (1953).

(9) W. C. Bigelow, D. L. Pickett and W. A. Zisman, *J. Colloid Sci.*, **1**, 513 (1946).

TABLE I

WETTABILITY OF HIGH POLYMERS STUDIED (20°)

Liquids	Surface tension, γ_{LV}°, dynes/cm.	Nylon (6,6) θ_E, deg.	Nylon (6,6) $\gamma_{LV}^{\circ}(1+\cos\theta_E)$, ergs/cm.²	Polyethylene terephthalate θ_E, deg.	Polyethylene terephthalate $\gamma_{LV}^{\circ}(1+\cos\theta_E)$, ergs/cm.²	Polystyrene θ_E, deg.	Polystyrene $\gamma_{LV}^{\circ}(1+\cos\theta_E)$, ergs/cm.²
Water	72.8	70	97.7	81	84.1	91	71.6
Glycerol	63.4	60	95.1	65	85.1	80	73.2
Formamide	58.2	50	95.6	61	86.4	74	74.2
Thiodiglycol	54.0	38	96.6	46	91.5	62	79.4
Methylene iodide	50.8	41	89.2	38	90.8	35	92.4
Aroclor 1242	45.3	19	88.1	17	88.6	21	87.6
α-Bromonaphthalene	44.6	16	87.4	15	87.7	15	87.7

contact angle reached a maximum and a reproducible value.[5] Very often, especially with liquids having contact angles below 50°, no increase in the contact angle resulted from addition of more liquid to the drop. In working with the halogenated liquids on polystyrene, the initial contact angle is the one reported since the surface was attacked soon after contact was established. The contact angle could be made to increase by adding liquid to the drop on the attacked surface, but when the drop volume reached a certain value, the contact angle would fall when the periphery of the drop became larger than the attacked area. Then the liquid would advance over the unattacked area with the initial angle.

The maximum contact angle reported for water on nylon was obtained by plotting cosine of the contact angle *vs.* time and extrapolating to zero time. This was necessary because water rapidly penetrates the surface of nylon. Water penetrates the surface of polyethylene terephthalate also, but at a much lower rate[10] so that the contact angle for water on it could be obtained in the usual manner.

Results

It was expected that the surfaces of nylon and polyethylene terephthalate would be more wettable than those of the hydrocarbon polymers polyethylene and polystyrene due to the contribution of the amide groups of nylon and the ester groups of polyethylene terephthalate. Thus, a greater variety of liquids would be expected to spread readily on these two surfaces. This was found to be true, for all liquids with surface tensions below about 40 dynes/cm. exhibited zero contact angles on smooth surfaces of nylon and polyethylene terephthalate. However, the number of pure and stable liquids having surface tensions above 40 dynes/cm. is limited; therefore, a series of only seven liquids was used for observing wettability as a function of liquid surface tension.

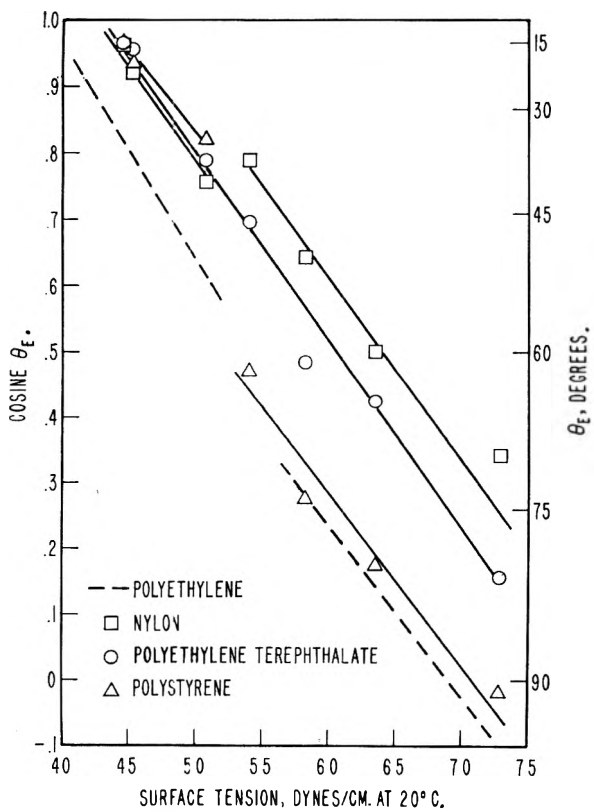

Fig. 1.—Liquid surface tension *vs.* cosine of the contact angle for several liquids on surfaces of high polymers studied.

A summary of the results obtained will be found in Table I which is arranged with liquids in the order of decreasing surface tension (γ_{LV}). Values of the equilibrium contact angle, θ_E, are reported for each liquid on the three plastic surfaces. Approximate values of W_A, the work of adhesion, were calculated from the Young–Dupré equation $W_A = f_{SV}^{\circ} + \gamma_{LV}^{\circ}(1+\cos\theta_E)$ assuming that f_{SV}°, the free energy of immersion of the solid in the vapor, was negligible.[5]

As we have found before,[3,5,11-14] in general θ_E decreases as γ_{LV}° decreases for a variety of liquids on a given surface. Table I shows this to be true in this study also with only one exception; methylene iodide exhibits a higher contact angle on nylon than does thiodiglycol. Such a situation can result if the solid/liquid interfacial tension (γ_{SL}) of the liquid giving the lower angle is much smaller than that of the liquid giving the higher angle.

Strongly hydrogen-bonding liquids (water, glycerol, formamide and thiodiglycol) have nearly the same work of adhesion for the nylon surface. But W_A for polyethylene terephthalate and polystyrene decreases as γ_{LV}° increases (see Table I); this behavior is usually observed at high values of γ_{LV}°.[3] Each of the halogenated liquids listed in Table I had nearly the same value of W_A on all three plastic surfaces. But W_A for the hydrogen bonding liquids on nylon is greater than that for the halogenated liquids; the reverse is true for these liquids on polystyrene and polyethylene terephthalate.

Figure 1 shows cos θ_E as a function of γ_{LV}°. In past publications[3,5,11-13,15] we have shown that this relation is linear for each homologus series of liquids

(10) P. W. Morgan, *Ind. Eng. Chem.* **45**, 2296 (1953).

(11) H. W. Fox and W. A. Zisman, *J. Colloid Sci.*, **7**, 109 (1952).

(12) E. G. Shafrin and W. A. Zisman, *ibid.*, **7**, 166 (1952).

(13) F. Schulman and W. A. Zisman, *ibid.*, **7**, 465 (1952).

(14) H. W. Fox, E. F. Hare and W. A. Zisman, *ibid.*, **8**, 194 (1953).

(15) E. F. Hare, E. G. Shafrin and W. A. Zisman, THIS JOURNAL, **58**, 236 (1954).

studied, and for non-homologous liquids the graphical points collect along a straight line or within a narrow rectilinear band.[7] In the present study of nylon, the graphical points for the hydrogen-bonding liquids and the halogenated liquids collect in Fig. 1 on two distinct straight lines. A similar situation is found for these liquids on polystyrene. However, the data for polyethylene terephthalate plot on only one straight line.

In Fig. 2, the relation between $\gamma_{LV}^{\circ}(1 + \cos \theta_E)$ and γ_{LV}° is shown for the three plastics studied here. Included for comparison are some of the results for surfaces of smooth polyethylene and single crystals of *n*-hexatriacontane.[3] Using the hydrogen-bonding liquids, W_A increases in the order: hexatriacontane, polyethylene and polystyrene, polyethylene terephthalate, and nylon; using the halogenated liquids, the order is hexatriacontane, polyethylene, nylon, polyethylene terephthalate and polystyrene. It is interesting to note also that like the results for hexatriacontane, the data for polystyrene and nylon separate into two distinct curves. The points for the halogenated liquids fall on the higher W_A *vs.* γ_{LV}° curve for polystyrene and hexatriacontane, and the points for the hydrogen-bonding liquids fall on the higher W_A curve for nylon. Evidently the liquids falling on the upper curves have smaller values of γ_{SL} than liquids of the same surface tension falling on the lower curves.[3] Thus the halogenated liquids on polystyrene have low values of γ_{SL} due to their solvent action while on nylon the liquids with lower γ_{SL} are those which can form hydrogen bonds with the amide groups. The leveling off of the W_A curve at high values of γ_{LV}° as given here by nylon has been observed previously for these same liquids on fluorinated polymers.[11]

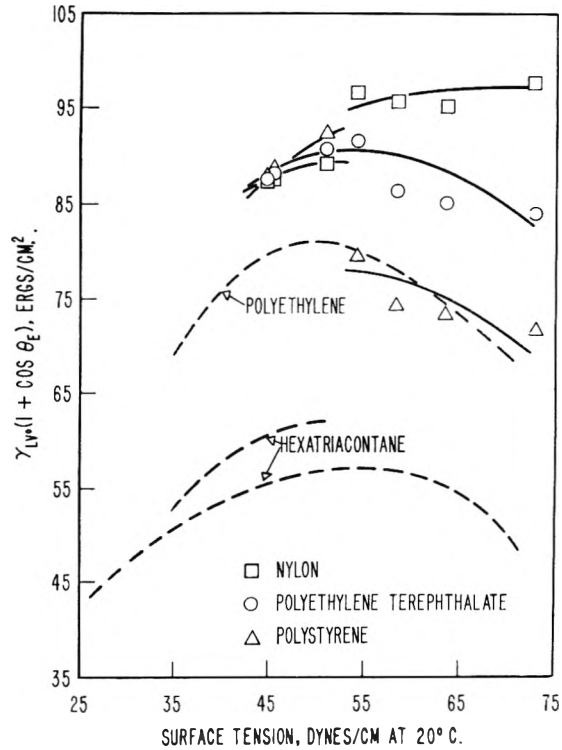

Fig. 2.—Liquid surface tension *vs.* $\gamma_{LV}^{\circ}(1 + \cos \theta_E)$ for several liquids on surfaces of high polymers studied.

Discussion

The presence of amide groups in a surface, otherwise aliphatic hydrocarbon in composition, results in increased wetting by hydrogen-bonding liquids but has less effect on the wetting by the three halogenated liquids studied. This is evident in Fig. 1 when the results for polyethylene are compared with those for nylon and it is seen that the shift in the lines for hydrogen-bonding liquids is more than double the shift for halogenated liquids.

The wettability of polyethylene terephthalate by hydrogen-bonding liquids is greater that that of polyethylene due to the presence of the ester groups and the benzene rings. As a first approximation, the effect of the benzene rings is shown by the greater wettability of polystyrene than of polyethylene (see Fig. 1). This increase could have been predicted from the findings of a study on aromatic surfaces.[14]

In polystyrene the benzene ring is partly buried in the surface since it exists as a substitution on the principal chain of the polymer. Therefore, only a slight increase in wettability is caused by the aromatic rings. In polyethylene terephthalate, the benzene rings are in the principal chain, are more exposed at the surface, and hence a greater increased wettability results. The effect of the introduction of the ester groups is to cause an additional increase in wettability by all hydrogen-donating liquids. Evidence is given below for believing that only the ether oxygen of the ester group is exposed in the surface with the result that the full increase in wetting due to an ester group does not occur.

Although the halogenated liquids behave essentially the same on the three surfaces, the cosines of the contact angles of these liquids on polystyrene are higher than normal due to their solvent power for hydrocarbons. Thus in Figs. 1 and 2 the graphical points for the hydrogen-bonding liquids and those for the halogenated liquids on polystyrene do not fall on the same line. Nylon and polyethylene terephthalate exhibit a much greater resistance to the solvent action of the halogenated liquids, and hence the contact angles of these liquids are normal or nearly so. We have defined normal wetting behavior as that resulting from forces of adhesion at the solid/liquid interface of the order of van der Waals forces.[2]

It has been shown that polyethylene terephthalate films are much less permeable to moisture than are those of polystyrene.[10] This and the fact reported here that the former resists attack by the halogenated liquids while the latter does not, can be explained by considering the surface composition of these two polymers. It has been reported recently[16] that in stretched polyethylene terephthalate films such as used here, the polymer chains are not only oriented in the direction of drawing but also the benzene rings all lie in a plane oriented normally to the surface of the film. Because of this planar structure the cohesional forces between benzene rings in neighboring chains can act to create a very close-packed array of polymer chains which

(16) R. Miller and H. Willis, *Trans. Faraday Soc.*, **49**, 433 (1953).

are highly resistant to moisture permeability and attack by the halogenated liquids used here. In polystyrene such alignment of benzene rings is sterically hindered, which causes the plastic to be softer, more permeable than polyethylene terephthalate, and attacked by the halogenated liquids.

In Figs. 1 and 2 the graphical points for the hydrogen-bonding liquids on polyethylene terephthalate fall on the same line as the points for the halogenated liquids. This would indicate that the hydrogen-bonding mechanism does not operate in the wetting of this plastic. Further consideration of surface composition results in a plausible explanation. The reference to molecular orientation quoted earlier[16] also shows that the C=O bond of the ester group is perpendicular to the surface of the plastic. A ball model of polyethylene terephthalate shows that the two oxygen atoms of the ester group are on opposite sides of the chain such that only one of them can be exposed to the hydrogen-donating group of a spreading liquid. Presumably, it is the ether oxygen which is uppermost, since it would be expected to form a much weaker hydrogen-bond.

It is obvious that water, glycerol, formamide and thiodiglycol have the ability to form hydrogen bonds with secondary amide groups if there is no steric hindrance. Inspection of the ball model of the nylon chain shows that the hydrogen-donating groups of the spreading liquids could reach the amide groups in the nylon surface. The hydrogen bonds formed would account for the high values of $\cos \theta_E$ given by these liquids (see upper line in Fig. 1). Greater values of W_A for these liquids as compared to W_A values for the halogenated liquids as shown in Fig. 2, also indicate the low values of γ_{SL} resulting from hydrogen-bonding at the solid/liquid interface.

Further evidence for believing that the hydrogen-bonding mechanism is involved in the wetting of nylon by some liquids was obtained in the following manner: a drop of *n*-decane was placed on a smooth clean surface of nylon and, of course, it spread rapidly. A second drop of *n*-decane which was saturated with perfluorolauric acid (10^{-5} mole per cent.) was placed on top of the thin film of decane left by the first drop. In less than one minute, the *n*-decane drew together to form a sessile drop with a contact angle of about 40°. This behavior can be explained by adsorption of an oriented monolayer of perfluorolauric acid on nylon through hydrogen-bonding of the acid groups to the amide groups in the surface. The contact angle of 40° is to be compared with that of 70° exhibited by a drop of *n*-decane on a close-packed film of perfluorolauric acid adsorbed on platinum foil.[15] On nylon, the spacing of the amide groups is such that a close-packed film of perfluorolauric acid cannot be expected. When the same experiment was repeated using any one of the smooth, clean plastic surfaces of polyethylene, polyvinyl chloride and polyethylene terephthalate, no sessile drops could be formed with the *n*-decane solution. Such a result was to be expected since neither polyethylene nor polyvinyl chloride offers adsorption sites for perfluorolauric acid. Even if the potential adsorption sites of polyethylene terephthalate (ester groups) were so widely spaced that the sides of the fluorocarbon chain were exposed, a sessile drop would still be formed due to the oleophobicity of a $-CF_2-$ surface.[5] The spreading observed on polyethylene terephthalate is further evidence for the correctness of the assumption made earlier, *i.e.*, that the ester groups are so oriented that the ether oxygen rather than the keto oxygen is uppermost, and that the ether oxygen atoms are unable to join in the formation of hydrogen-bonds of sufficient strength to sustain a monolayer.

In another spreading experiment on nylon, the perfluorolauric acid was replaced by a fluorocarbon (du Pont FCD-331, Perfluoro Lube Oil, b.p., 130–150° (10 mm.)) as solute. The *n*-decane did not withdraw to a sessile drop showing that the adsorption of perfluorolauric acid on nylon was by the carboxylic acid group rather than by the fluorinated chain. This would indicate that hydrocarbon acids also should adsorb, but a negative result was obtained using stearic acid as solute. This result is not conclusive since *n*-hexadecane may well spread on a monolayer of stearic acid when the layer is not close packed.[12,14] The parallel study on the frictional properties of nylon,[4] however, reports a reduction in the boundary friction for nylon on nylon when lubricated with a *n*-hexadecane solution of stearic acid. This indicated the presence of a protective film of stearic acid adsorbed on the nylon surfaces which could not be detected by the spreading experiment.

THE ADSORPTION OF FLEXIBLE MACROMOLECULES. II.

BY H. L. FRISCH AND

Department of Physics, Syracuse University, Syracuse, N. Y.

ROBERT SIMHA

Department of Chemical Engineering, New York University, University Heights, New York

Received March 8, 1954

The principal assumptions and results of the equilibrium theory previously developed are recapitulated and then extended in several directions. Adsorption of the solvent does not affect significantly the form of the isotherm. An approximate treatment of the effect of chain interference near the surface on the adsorption equilibrium is given by the solution of an appropriate diffusion equation for the chain configuration function. The magnitude of the effect increases with molecular weight. In the present approximation, larger molecular weights are still preferentially adsorbed, however to a lesser extent than in the absence of interference. The deviations from a theoretical Langmuir isotherm are also reduced, although they remain pronounced. The amount of polymer removed from solution, but not the actual surface coverage, is larger than for rigid macromolecules. Equations for multilayer adsorption are developed along the lines of the B.E.T. theory. Some comments on the interpretation of experimental data in terms of various isotherms are presented. Finally, we venture into the problem of reinforcement and make an estimate of the increment in elastic modulus arising from the extended configuration of an adsorbed chain.

I. Summary of Previous Results

In two previous communications[1,2] an equilibrium theory of adsorption from dilute solution onto a surface consisting of a regular array of active sites each accommodating one chain segment was presented. The main assumptions were: (a) consideration of a localized monolayer, (b) a treatment which operates with a lattice model on the surface and in the bulk solution, whereas chain statistics are used in the analysis of the modification of the molecular configurations in the neighborhood of the surface,[3] (c) the use of Gaussian chains as a model for the molecule in this latter analysis, (d) random placing of segments, and (e) neglect of mutual interference between chains near the surface. On this basis the probability $p(\tau)$ was obtained that the τth segment of the t consecutively numbered chain segments is deposited, provided the first one is anchored to the surface. This led to the additional assumption (f), namely, the replacement of $p(\tau)$ by an average $<p(\tau)> = p$ over τ and to $<\nu> = pt$ as the total average number of segments deposited on the surface per chain. In the derivation of the isotherm we operated exclusively with this average $<\nu>$, neglecting by assumption (f) fluctuations from chain to chain.

The important conclusion reached was that only relatively few segments are actually on the surface, since

$$p = <\nu>/t = 2\alpha/(\pi f t)^{1/2} - O(1/t) \qquad (1)$$

where f is an inverse measure of chain flexibility and $\alpha \leq 1$ the probability of a successful contact between segment and surface. Furthermore, the trapped segments are almost completely isolated from each other and separated by bridges extending into the solution and of average chain length

$$<\epsilon> \approx t/<\nu> \qquad (2)$$

Assuming (g) that the solvent is not adsorbed at all, the isotherm has in the limit $p \to \theta$, the form

$$\frac{\theta}{1-\theta} \exp(2\kappa_1\theta) = (Kc)^{1/<\nu>} \qquad (3)$$

with θ the fraction of the surface covered by adsorbed segments. Some of the assumptions made in the derivation of eq. 3 are valid for small θ so that this isotherm reduces essentially to a Freundlich isotherm. The statistical mechanical expression for the "affinity" constant K has been given (I, eq. 22).

The theory makes clear why K-constants for a high polymer cannot be obtained by extrapolation of the molecular weight dependence for low molecular fractions, and explains the observed initial steep rise of the isotherm at extremely low solution concentration c, the long region of apparent saturation and the effect of a poor solvent in favoring adsorption. Furthermore, it predicts a possible inversion of the usual temperature dependence[4] and increased adsorption with increasing chain flexibility.

The purpose of this paper is to explore the influence of some of the assumptions mentioned above, to compare various isotherms and to comment on some experimental results.

II. Solvent Adsorption

In the absence of specificity for solvent and polymer molecules, the adsorption of the two species occurs independently as long as interaction effects on the surface are small. The isotherm is then derived either by equating all corresponding partial molar free energies of solvent and solute in the two phases or more simply by Langmuir's kinetic argument. Thus if θ_L denotes the fraction of sites occupied by solvent, the equilibrium is determined by

$$(1 - \theta - \theta_L)k_1 f(c) = k_2\theta$$
$$(1 - \theta - \theta_L)k_{1L}c_L = k_{2L}\theta_L$$

The k's are rate constants for the sorption–desorption processes, $f(c) = c^{1/<\nu>}$ and c_L is the solvent concentration. Thus

$$\theta = \frac{(Kc)^{1/<\nu>}}{1 + (Kc)^{1/<\nu>} + K_{LC}c_L}$$
$$\theta_L = \frac{K_{LC}c_L}{1 + (Kc)^{1/<\nu>} + K_{LC}c_L} \qquad (3a)$$

(1) H. L. Frisch, R. Simha and F. R. Eirich, *J. Chem. Phys.*, **21**, 365 (1953).

(2) R. Simha, H. L. Frisch and F. R. Eirich, THIS JOURNAL, **57**, 584 (1953), hereafter denoted by I.

(3) A treatment based exclusively on the lattice model has been outlined by R. Ullman, paper presented at the 124th meeting of the American Chemical Society, September 6–11, 1953, Chicago, Illinois.

(4) Such an inversion, when actually observed, can be indicative of a very slow and incomplete approach to equilibrium. We are concerned here exclusively with equilibrium states.

with $K = (k_1/k_2)^{<\nu>}$, $K_L = k_{1L}/k_{2L}$. For $K_L \to 0$, the isotherm eq. 3 results, if lateral interactions are neglected, $\kappa_1 = 0$. The pure solvent adsorption does not affect the characteristic features of the polymer isotherm. The initial rise in θ is still rapid, although decreased, and saturation, $\theta = 1$, requires higher polymer concentrations. From the apparent saturation in the observed isotherms, Jenckel and Rumbach[5] deduced that the solvent does not markedly enter the picture. Now $K^{1/<\nu>}$ and K_L may be expected to be of the same order of magnitude and this deduction is applicable only for Langmuir-adsorption as considered by these authors, since $c + c_L$ = constant.

III. Chain Interference near the Surface

Equations 1 and 3 assert, for small θ at any rate, that $d\theta/dt > 0$ (see also below). The weight of polymer actually removed from the solution is proportional to

$$a = (t/<\nu>)\theta$$

and therefore $da/dt > 0$. In the limit $t \to \infty$, $a \approx$ constant$\cdot t^{1/2}$, regardless of the specific dependence of K on t. This indicates that no efficient separation with respect to molecular weight, at least for large molecular weights, can be expected. Separation of different or branched species may be possible since such differences affect the magnitude of the constant K (I, eq. 22). On the other hand, according to various observations $da/dt < 0$ above a certain molecular weight,[6] when the chains are presumably long enough to behave as more or less flexible coils. The picture developed previously suggests that this could be due to the protective action of the bridges and anchor segments on the surface which is more pronounced at higher degrees of polymerization and θ. Under such conditions, the probability p becomes a function of θ. It is necessary in this connection to examine experimentally the variation of the molecular weight dependence of the quantity a with concentration. Here we shall present an approximate extension of the theory. The results should have a bearing also on the mechanism of interaction between surface and chains in condensed systems, involved in adhesion or reinforcement.

A detailed treatment by the previous methods ought to be based on a theory of the volume effect in concentrated systems arising from the short range repulsions of the chain segments in the same as well as different molecules and modified by the presence of the solvent. We shall instead pay attention only to the reduced penetrability of the protective layer over the surface, formed by the trapped segments and the protruding bridges. This corresponds to a "repulsive barrier" E caused by short range forces between segments. The average range of this barrier, l, measured normally outwards from the surface may be considered to be of the order of an average linear dimension of a bridge, hence proportional to $<\epsilon>^{1/2}$ or, from eq. 1 and 2, proportional to $t^{1/4}$. Thus l is of the order of not more than 10 segment lengths. This estimate, of course, assumes that the bridges may be considered to be Gaussian chains. The height of the barrier E, E_0, is determined by the portion of surface sites protected at least once by the ϵ-bridges and the anchored segments. Both are obtained by orthogonally projecting the ϵ-bridges on the surface and are a function of the parameter θ. The form of $E(\theta)$ is assumed to be

$$E(\theta) = E_0(\theta)[1 - H(z - l)] \qquad (4)$$

H is the Heaviside unit function, the barrier vanishing for $z > l$. Since the total volume of segments of the average ϵ-bridges is concentrated in the region $0 < z < l$, the product $E(\theta) \times l$ depends on $<\epsilon>\theta$, that is, $t^{1/2}\theta$.

This potential changes the configurations of the chains approaching the surface, $z = z_0$. Previously the probability distribution, $W_{z_0}(x, y, z; t)$, was given by I, eq. 2. This W is a solution of a diffusion equation with a "diffusion" coefficient f. Now the diffusion is no longer free but modified by the potential E. It produces an additional "convection velocity" $-\mu$ grad E, where $\mu = f/kT$ is the equivalent of a mobility. Writing $W_{z_0}(x, y, z; t) = W_{z_0}(x, t)\, W_{z_0}(y, t) w(z, t)$, and setting $z_0 = 0$, we find that $w(z, t)$ satisfies

$$\frac{\partial w}{\partial t} = f\frac{\partial^2 w}{\partial z^2} - \frac{\partial}{\partial z}[\lambda\delta(z - l)w]; \quad z > 0, t > 0; \qquad (5)$$

where $-\lambda\delta(z - l) = \mu \operatorname{grad}_z E(\theta)$. Since it is assumed that the chain starts at $x = y = 0, z = z_0 = 0$, the boundary conditions are

$$w \longrightarrow \delta(z - z_0) \text{ as } t \longrightarrow 0$$
$$f\frac{\partial w}{\partial z} - \lambda\delta(z - l)w = 0, \text{ at } z = 0, t > 0 \qquad (6)$$
$$w, \frac{\partial w}{\partial z} \longrightarrow 0 \text{ as } z \longrightarrow +\infty, t > 0$$

$W_{z_0}(x, t)$ and $W_{z_0}(y, t)$ have been defined (see I, eq. 1a). The conditions at $z = 0$, (perfect reflection) and $z = +\infty$ ensure that w can be normalized to unity since

$$\frac{\partial}{\partial t}\int_0^\infty w dz = f\frac{\partial w}{\partial z} - \lambda\delta(z - l)w\Big]_{z=0}^{z=+\infty} \equiv 0$$

The solution of eq. 5 will be obtained as an expansion in λ. As long as the interference effect is small, this procedure will be satisfactory for all values of θ. Otherwise we are restricted to sufficiently small surface concentrations when we may expand E_0 in θ to obtain

$$E_0(\theta) = [E]<\epsilon>\theta/l + O(\theta^2) \qquad (4a)$$

where $[E]$ is the intrinsic repulsive energy per segment and independent of t. For the remainder only the value of $W_{z_0=0}(x, y, 0; t)$ is required. In the appendix it is shown that

$$W_0(x, y, 0; t) = \frac{2C^3}{(ft)^{3/2}}\left(1 - \frac{\lambda e^{-l^2/ft}}{f}\right)e^{-\rho^2/4ft} \qquad (7)$$

with $C = (2\pi^{1/2})^{-1}$ and $\rho^2 = x^2 + y^2$.

The probability $p(t)$ is given by I, eq. 3, with one modification. In eq. 1 α, the probability that if a segment touches the surface it adheres, has to be replaced by $\alpha_0(1 - \theta)$ since our treatment is correct to terms of order θ and $(1 - \theta)$ is the fraction of the

(5) E. Jenckel and B. Rumbach, *Z. Elektrochem.*, **55**, 612 (1951).

(6) For instance I. Claesson and S. Claesson, *Arkiv Kemi Mineral Geol.*, **19A**, No. 5 (1945). However see also footnote 4.

surface free of anchored polymer segments. We find with $\phi = \tan^{-1}(y/x)$

$$p(\tau) = \alpha_0(1-\theta)\int_0^{\tau}\int_0^{2\pi} W_0(x, y, 0; \tau)\rho d\rho d\phi \quad (8)$$

$$\doteq \frac{\alpha_0(1-\theta)8\pi C^3}{f^{1/2}\tau^{1/2}}\left(1 - \frac{\lambda e^{-l^2/f\tau}}{f}\right)(1 - e^{-\tau/4f})$$

The average value of $p(\tau)$ is obtained as in I, eq. 4. Thus

$$p \approx \alpha_0(1-\theta)8\pi C^3/(f^{1/2}t)[2t^{1/2} - \lambda/f\int^t c^{-l^2/f\tau}\tau^{-1/2}d\tau] \quad (9)$$

$$\approx 2\alpha_0(1-\theta)/(\pi f t)^{1/2}(1-\lambda/f)$$

$$= 2\alpha_0(1-\theta)/(\pi f t)^{1/2}[1 - [E]/(kT)<\epsilon>\theta/l]$$

since from (5), (4a), (1) and with $l = (6f<\epsilon>)^{1/2}$

$$\lambda/f = [E]/(kT)<\epsilon>\theta/l = \pi^{1/4}/(2.3^{1/2})[E]/(kT)t^{1/4}/(f^{1/4}\alpha_0^{1/2})\cdot\theta$$

The remainder of the isotherm derivation follows step by step the development in I except that the pertinent averages are now functions of the parameter θ, *e.g.*

$$<\nu> = pt = <\nu>_0(1-\theta)[1 - [E]/(kT)<\epsilon>\theta/l] \quad (10)$$

with $<\nu>_0 = 2\alpha_0 t^{1/2}/(\pi f)^{1/2}$. Equations 9 and 10 indicate an increase of the interference with increasing molecular weight and increasing chain flexibility (small f). $[E]$ is smallest in a poor solvent and increases with temperature. f is smaller at the higher temperature. The over-all dependence of the interference effect on T, however, will be a decrease with increasing T at a given θ, due to the increased thermal motion, except near the critical solubility temperature of the polymer. Thus this factor tends again to give more adsorption at the higher temperature. The terms of order λ^2 discarded in the above results contribute a term proportional to $t^{1/4}$ to the correction in p.

On substituting the value of $<\nu>$ in the isotherm I, eq. 22 and passing to the limit $p \to 0$, we obtain

$$\{\theta c^{2\kappa_1}\theta/[(1-\theta)K_1]\}^{<\nu>_0(1-\theta)(1-[E]<\epsilon>\theta/lkt)} = K_2 c \quad (11)$$

with $K_1 = j_s \exp\{x/kT - (1-\kappa_2)\}$; $K_2 = M(\text{solv})/[M(\text{segm})d(\text{solv})]\ \bar{V}^{-1}h^3/(2\pi mkT)^{3/2}$. $\bar{V}$ is the free volume per molecule of amorphous polymer, m its mass and c the concentration in weight by volume of solution. Comparing eq. 9, 10 and 11 with the corresponding quantities in I, we see that the chain interference decreases p and $<\nu>$ fairly rapidly with increasing θ. As a consequence, the isotherm, eq. 11 tends in the direction of a Langmuir isotherm, $<\nu> \to 1$. Whereas eq. 11 yields a correct limit for $\theta \to 1$, it can, of course, not be used for θ-values near unity.

To obtain the variation with molecular weight, we set $\kappa_1 = 0$ in I, eq. 22a and 11 for simplicity and find

$$(d\theta/dt)_{<\nu>_0} = \frac{\theta}{<\nu>_0[1+(Kc)^{1/<\nu>_0}]}[d\ln K_2/dt - \ln(K_2c)\, d\ln <\nu>_0/dt] > 0$$

$$(d\theta/dt) = \frac{\theta}{<\nu>[1+(Kc)^{1/<\nu>}]}[d\ln K_2/dt - \ln(K_2c)\, d\ln <\nu>/dt] > 0$$

with $K = K_1^{<\nu>}\cdot K_2$ and a corresponding definition when $<\nu> = <\nu>_0$. Both derivatives are positive, regardless of details, for instance in respect to the quantity $\bar{V}$, unless the free volume were to increase sufficiently rapidly with molecular weight, since to our degree of approximation, $\theta < 1/2$. For the difference we find, when θ is small

$$d\theta/dt - (d\theta/dt)_{<\nu>_0} \approx \theta(1-\theta)/(2<\nu>)\ln(K_2c)\lambda/[f(1-\lambda/f)] \times d\ln <\epsilon>/dt < 0; \quad (12)$$

From eq. 11, K_1 is of the order of 1–10, $K_2c < 1$. The other terms on the right-hand side of (12) are positive. This means that chain interference near the surface could, if sufficiently strong, reverse the sign of $d\theta/dt$ and lead to preferred adsorption with decreasing molecular weight because of

$$da/dt = a/t(1 - t\, d\ln <\nu>/dt + t/\theta\, d\theta/dt) \approx a/t(1/2 + t\, d\ln\theta/dt)$$

We conclude that as long as an active site can accommodate only single segments, that is, a small portion of the chain, and the sites form a sufficiently dense array on a uniform surface, the isotherm will deviate from Langmuir's type. It may ultimately approach it with increasing θ when the segment interference becomes sufficiently large. If the surface is not covered uniformly by active sites, *i.e.*, if they are surrounded by inactive ones and separated from each other by distances of the order of an extended chain length, the isotherm will follow a Langmuir equation. A similar result could occur when θ becomes quite large, and the adsorbed polymer layer ceases to behave as a two-dimensional fluid. This transition would be attained at relatively low θ-values if the ease of packing coherently the surface polymer chains into a two-dimensional lattice, the cohesional energy density and regularity of the chain are favorable. In particular polymer–surface systems exhibiting polar orienting forces should favor such a phase change. The preceding discussion would now be invalid, since steric as well as energetic hindrance of neighboring segments prevents the further deposition of a polymer chain unless it has an improbable shape, such that adsorption occurs at a single anchor. Under these conditions $<\nu> \sim pt = t(1-\theta)\ 1/t = (1-\theta)$, since a chain would be prevented from exhibiting segment flexibility; a segment adhering if and only if it is one of the t segments which has penetrated through the monolayer to the surface. With $<\nu> \sim 1$, I, eq. 22a reduces except for a small activity correction to Langmuir's isotherm.

IV. Multilayer Adsorption

So far one of the main assumptions underlying the previous theoretical consideration has been the restriction that the adsorbed polymer forms a monolayer. This restriction becomes objectionable when we wish to deal with adsorption from a concentrated solution and in possible extensions of these considerations to the formation of an adhesive bond.

Provisionally, we can imagine that the multilayer is built up by successive depositions of adsorbed segments on active sites irrespective of whether they have been previously occupied by anchor segments, as long as each site is occupied by not more than s such anchors, where s is the number

of layers. For sufficiently large Gaussian polymer chains placed randomly on uniformly distributed surface sites the previous analysis indicates that to a sufficient approximation the adsorption process is identical with the adsorption of "dissociated" segments of the macromolecule.

In deriving the isotherm valid for multiple coverage of sites we will use the simplified kinetic considerations of the B.E.T. theory in the form and notation presented in reference 7. To the usual assumptions of the B.E.T. theory (a) that the adsorption times of all layers above the first are equal (horizontal interactions are negligible), (b) that activity effects between layers can be neglected, and (c) that the solvent does not participate in the adsorption, must be added an assumption peculiar to flexible macromolecules. Namely, the whole adsorption process can be characterized by a single degree of apparent dissociation of the polymer into independent segments, *i.e.*, the average number of polymer anchors per molecule $<\nu>$ must be the average of the $<\nu>_i$'s each different and each pertaining to a given layer, i. Consequently the rate of deposition of segments is set proportional to $c^{1/<\nu>}$. Introducing this concentration dependence into the derivation in reference 7 one obtains for the total number of adsorbed segments per cm.^{2}, neglecting certain heat of mixing corrections

$$\sigma = \frac{\sigma_0 k c^{1/<\nu>}}{[q - c^{1/<\nu>}]}\left[\frac{1 - (s+1)\left(\frac{c^{1/<\nu>}}{q}\right)^s + s\left(\frac{c^{1/<\nu>}}{q}\right)^{s+1}}{1 + (k-1)\left(\frac{c^{1/<\nu>}}{q}\right) - k\left(\frac{c^{1/<\nu>}}{q}\right)^s}\right] \quad (13)$$

where k and q are constant parameters characteristic of the system and σ_0 is the number of segments which would cover 1 cm.^{2} of the surface with a unimolecular layer. The total number y of polymer chains actually removed from the solution is proportional to $(t/<\nu>)\sigma$. Replacing as usual $q^{<\nu>}$ by c_s the saturation value of the concentration at the temperature of the experiment one obtains as $s \to \infty$

$$y = tkv_m c^{1/<\nu>}/\{<\nu>(c_s^{1/<\nu>} - c^{1/<\nu>})[1 + (k - 1)(c/c_s)^{1/<\nu>}]\} \quad (14)$$

with $v_m = S\sigma_0$ where S is the surface area in cm.^{2}. The isotherm, eq. 13 possesses in general the same characteristics, except for the power of c, as the ordinary B.E.T. isotherm and is fully discussed in reference 7.

V. Comparison of Isotherms

It is instructive to compare isotherms (3) and (11) for flexible polymers with that corresponding to complete deposition on the one hand and with a theoretical Langmuir isotherm on the other. The expressions are, using the notation of eq. 11

$$\theta/(1 - \vartheta)^t = K_1^t K_2 c \text{ complete deposition} \quad (15)$$
$$\theta/(1 - \theta) = K_1^t K_2 c \text{ Langmuir}$$

The validity of the first equation is seen by considering that deposition of a molecule now requires a sequence of t empty sites, whereas the probability of desorption is still proportional to the surface concentration. This isotherm is essentially identical with the one obtained by Mackor and van der Waals[8] for rod-like molecules, as it must be. These authors have pointed out already that the amount adsorbed is considerably less, except at very small θ, than that predicted by the Langmuir isotherm. The θ-values for a coiling polymer, in turn, are smaller than those for a straight chain. In spite of the smaller surface coverage, however, the amounts $a = (t/<\nu>)\theta$, actually removed from solution, are larger, except at θ-values of the order of $<\nu>/t$ or smaller. Thus, the mode of deposition of flexible chains leads to more effective utilization of the adsorbing surface.

In several instances, measured isotherms of polymers have been fitted by means of empirical expressions of the Langmuir type.[5,6,9] Now, if our model for an active surface has any connection with reality, it has been shown that neither straight[8] nor coiling macromolecules can behave like small molecules, that is, follow Langmuir's theory. In view of the discussion at the end of Section III we conclude that this may not be applicable to adsorbents with large internal surfaces. In those instances, however, the problem of attaining equilibrium becomes particularly acute. In addition there are three points to be kept in mind. As shown in some cases by the authors themselves, they could have used Freundlich expressions equally well. Also in certain concentration ranges, all curves have similar shapes. Finally, a true theoretical Langmuir isotherm must give a pronounced molecular weight dependence of the "affinity" constant, as is indicated by eq. 15. Now Jenckel and Rumbach[5] had already concluded from their data that chains are not deposited as a whole. Theory in turn indicates that a true Langmuir isotherm requires adsorption at single points only. This might be possible with relatively short chains,[10] containing not more than a few hundred segments or at high surface concentrations, but is difficult to understand otherwise.

As an illustration of the similarity in shape we show comparative plots of two expressions. Data on a sample of polymethyl methacrylate in toluene, adsorbed on alumina at 25° are stated to have been successfully fitted by a Langmuir expression[5]

$$a = A_s Kc/(1 + Kc) = 4.26c/(0.01 + c) \quad (16.1)$$

where c is expressed in mg./10 cc. and a in mg. per 10 g. of adsorbent. Let us compare this equation with

$$a = A_s(Kc)^{1/<\nu>}/[1 + (Kc)^{1/<\nu>}] = 8.05(2c)^{0.04}/[1 + (2c)^{0.04}] \quad (16.2)$$

The values of the parameters have not been particularly chosen so as to give the closest possible agreement between the two equations. This is illustrated in Fig. 1. At extremely low c-values, less than 10^{-2} mg./10 cc., our curve necessarily rises more steeply, but thereafter approaches saturation more slowly than the former. Figure 2 shows plots

(7) J. H. de Boer, "The Dynamical Character of Adsorption," Oxford University Press, New York, N. Y., 1953.

(8) E. L. Mackor and J. H. van der Waals, *J. Colloid Sci.*, **7**, 535 (1952).

(9) E. Treiber, G. Porod, W. Gierlinger and J. Schurz, *Makromol. Chem.*, **9**, 241 (1953).

(10) For instance, the polyethylene oxides discussed by W. Heller, 27th National Colloid Symposium, Ames, Iowa, June 25–27, 1953.

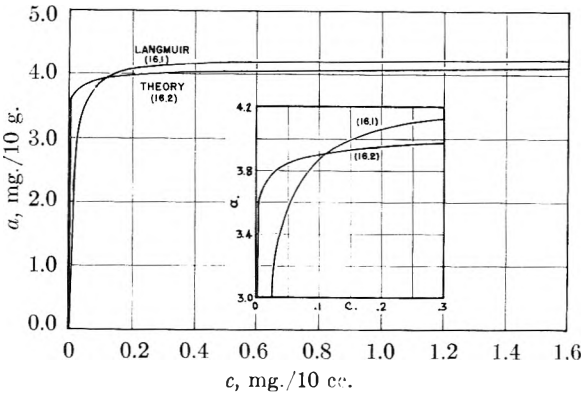

Fig. 1.—Comparison of isotherms, eq. 16.1 and 16.2.

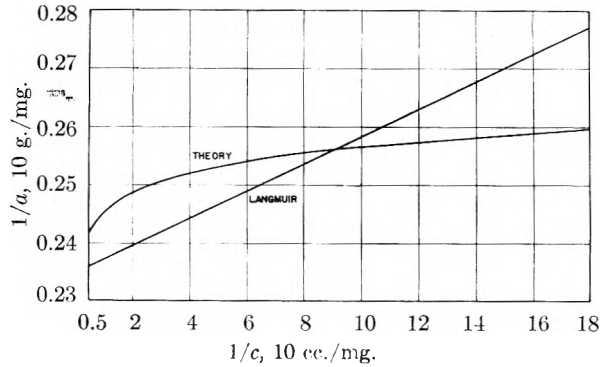

Fig. 2.—Comparison of isotherms, eq. 16.1 and 16.2 plotted as $1/a$ *vs.* $1/c$.

of $1/a$ *vs.* $1/c$. This yields a straight line for a Langmuir expression. Clearly, our formula results, in a certain c-range, also in a practically linear plot. Incidentally, in ref. 5, no graphs of $1/a$ *vs.* $1/c$ are presented.

Thus data which, within experimental error, appear as straight lines, are not necessarily indicative of an actual Langmuir isotherm. A wide concentration range, with sufficient dilution for experimental as well as theoretical reasons, must be explored and the constants of the equation determined as function of molecular weight, before the validity of a theoretical Langmuir expression 15 can be accepted. We have omitted from this discussion the κ_1-term in (3) which accounts for lateral interactions in excess over those in the bulk polymer and complicates the numerical interpretation of data.

VI. Implications for Condensed Systems

We have previously given a formal expression, eq. 13 for multilayer adsorption. On the other hand, in a rubber–filler system, for instance, hardly more than one layer will be sufficiently immobilized, so as to be considered as adsorbed on a solid particle. Accepting this and denoting again by $<\nu>$ the average number of segments per chain attached to the solid, we can formally write an isotherm as in I, eq. 22, where K is now defined as

$$K = \exp\,[<\nu>x/kT]j_s<\nu>h^3/(2\pi mkT)^{3/2}1/\bar{V} \quad (17)$$

However, it cannot be taken for granted that $<\nu>$ still obeys eq. 1. We have shown in Section III that this is certainly not the case in concentrated solutions. Yet, it seems reasonable that in the cross-linked polymer solid with its restrictions on chain mobility, the statistical analysis of I, based on Gaussian chains with no interference, is more nearly valid than in concentrated solution. We recall in this connection the success of the statistical theory of rubber-like elasticity, which has just that basis.

In thinking about the mechanism of reinforcement, the question arises to what extent adsorption, with its resulting change in chain configuration contributes to the change in physical properties, in particular to the increase in elastic modulus. One effect is the increase in the effective number of crossbonds, as stressed by A. M. Bueche. On the other hand, it has been qualitatively suggested that sufficiently small filler particles exert an orienting effect on the chain.[11] One can readily show that adsorption and bridge formation decrease the configurational entropy of a chain by an amount which is just about balanced by the energy release x per segment adsorbed. The average distance between end-points $(\bar{r}^2)^{1/2}$ is for an average adsorbed molecule given by $<\nu><\epsilon>^{1/2}l_0$ where l_0 is the length of a segment and $<\nu>$ the number of bridges. For the free coil we have instead, $t^{1/2}l_0$. Thus the adsorption process increases an average dimension by a factor $<\nu>^{1/2}$. This corresponds to an entropy decrease per chain

$$T\Delta S = 3/2kT/(tl_0^2)(r^2 - <\nu>r^2) \approx -3/2kT/(tl_0^2)<\nu>r^2$$

For an average configuration, $\bar{r}^2 = tl_0^2$, this is just of the order $<\nu>x$, considering that x is of the order of kT.

This deformation of the nearest neighbors of a solid particle produces a state of strain extending beyond the adsorbed layer. Consequently, for sufficiently low filler concentrations we may roughly write for the increase $E - E_0$ in elastic modulus

$$E - E_0 \doteq E_0 \times (\text{fraction of trapped chains}) \times g<\nu>^{1/2}$$

where $g \leqq 1$ is to account for the decay of the elastic disturbance with increasing distance from the filler particle. Denoting by N_s the total number of sites available for adsorption and by N the total number of chains, it follows that

$$(E - E_0)/E_0 = N_s\theta g/(<\nu>^{1/2}N) \quad (18)$$

Let us take then as an example 1 g. of rubber with an average degree of polymerization between crosslinks equal to 5×10^2 and 0.2 g. of filler with a surface area of 100 m.^{2} g.$^{-1}$. Assuming that each segment requires 100 Å.^{2}, we obtain $N_s = 2.10^{21}/10^2 = 2.10^{19}$, $N = 1.8.10^{19}$ and

$$(E - E_0)/E_0 \approx 1.1\theta g/<\nu>^{1/2}$$

Thus an increase in E by 10 to 20% is a reasonable figure and of the correct order of magnitude. This is all we can state. A really quantitative theory along the above lines must, of course, take into account the network structure of the polymer, as is done in the theories of rubber-like elasticity. Clearly, measurements of the entropy contribution to the elastic modulus as a function of the surface area of the filler are important in studying the mechanism of reinforcement.

(11) For instance, F. Schytil and R. Volpers, *Kolloid-Z.*, **130**, 110 (1953).

Appendix

Consider the boundary value problem given by eq. 5 and 6 and more generally $-\delta(z - l)$ replaced by a known function $h(z, l)$. We write w as a series in λ

$$w = w_0 + \lambda w_1 + \lambda^2 w_2 + \ldots$$

After substitution of this series in eq. 5, 6 and equating powers of λ we find

$$\frac{\partial w_0}{\partial t} = f\frac{\partial^2 w_0}{\partial z^2};\quad w_0 \longrightarrow \delta(z - z_0) \text{ as } t \longrightarrow 0,\ f\left(\frac{\partial w_0}{\partial z}\right)_0 = 0$$

and

$$\frac{\partial w_i}{\partial t} = f\frac{\partial^2 w_i}{\partial z^2} + Q_{i-1}(z, t),\ i \geq 1$$

$$w_i \longrightarrow 0 \text{ as } t \longrightarrow 0;\ f\left(\frac{\partial w}{\partial z}\right)_0 + h(0, l)w_{i-1}(0, t) = 0$$

with

$$Q_{i-1}(z, t) = \frac{\partial}{\partial z}[h(z, l)w_{i-1}(z, t)]$$

Denoting the Laplace transform of a function with respect to t by a bar over the symbol of the function, one finds

$$\bar{w}_0(z,p) = \int_0^\infty e^{-pt} w_0(z,t)dt = \frac{c'}{q}[e^{-q(z-z_0)} + e^{-q(z+z_0)}];$$

$$q = (p/f)^{1/2}$$

and

$$\bar{w}_1(z,p) = \frac{e^{-qz}}{2fq}\int_0^z \left\{\frac{\partial}{\partial z'}[h(z',l)\bar{w}_0(z'/p)]\right\}[e^{+qz'} + B(q)e^{-qz'}]dz' + \frac{[e^{+qz} + B(q)e^{-qz}]}{2fq}\int_z^\infty \left\{\frac{\partial}{\partial z'}[h(z',l)\bar{w}_0(z',p)]\right\}e^{-qz'}dz'$$

with

$$B(q) = 1 + h(0, l)\bar{w}_0(0, p)/fq$$

Setting $h(z, l) = -\delta(z - l)$ and passing to the limit as z and z_0 approach zero one obtains

$$\bar{w}_1(0, p) = -\frac{2c'}{qf}e^{-2ql}$$

which on inversion yields

$$w_1(0, t) = -\frac{2c'}{(\pi f t)^{1/2}}\frac{e^{-l2/ft}}{f}$$

Since we need w only at $z = 0$ to terms of order λ^2, we have

$$w(0, t) = \frac{2C}{(ft)^{1/2}}\left[1 - \frac{\lambda e^{-l^2/ft}}{f}\right] + O(\lambda^2).$$

On multiplication by $W_0(x, t)$ and $W_0(y, t)$ defined in I, one obtains the value of $W_0(x, y, 0; t)$ given by eq. 7.

New Schedule

BACK ISSUE PRICES

AMERICAN CHEMICAL SOCIETY JOURNALS

Effective January 1, 1953

Single copies or complete volumes of nearly all the ACS journals listed below may be purchased at these prices.

Journal	Current Year		Back Years			
	Member	Non-Member	Member	Non-Member	Foreign Postage	Canadian Postage
AGRICULTURAL AND FOOD CHEMISTRY	$0.40	$0.50	....	....	$0.15	$0.05
ANALYTICAL CHEMISTRY	.40	.50	$0.60	$0.75	.15	.05
Analytical Edition (I&EC)						
Volumes 1–4	....	....	1.60	2.00	.15	.05
Volumes 5–8	....	....	1.00	1.25	.15	.05
Volumes 9, et seq.	....	....	.60	.75	.15	.05
CHEMICAL ABSTRACTS, Volumes 11–44						
Numbers 1–22	....	....	1.00	1.25	.15	.05
Numbers 23 and 24	....	....	2.40	3.00*	.45	.15
CHEMICAL ABSTRACTS, Vol. 45, et seq.						
Numbers 1–22	1.00**	2.00	1.60**	2.00	.15	.05
Number 23 (Author Index)	6.00**	12.00	9.60**	12.00	free	free
Number 24 (Subject, Patent, Formula Indexes, complete)	12.00**	24.00	19.20**	24.00	free	free
CHEMICAL AND ENGINEERING NEWS	.15	.15	.15	.15	.05	free
INDUSTRIAL AND ENGINEERING CHEMISTRY	.60	.75	.80	1.00	.15	.05
Industrial Edition (I&EC)	....	....	.80	1.00	.15	.05
JOURNAL OF THE AMERICAN CHEMICAL SOCIETY, Vols. 32–73	....	....	1.00	1.25	.15	.05
JOURNAL OF THE AMERICAN CHEMICAL SOCIETY, Vol. 74, et seq.	.50	.75	.80	1.00	.15	.05
JOURNAL OF PHYSICAL CHEMISTRY	1.00	1.25	1.20	1.50	.15	.05

RATES FOR VOLUMES OF BACK NUMBERS

Journal	Member	Non-Member	Foreign Postage	Canadian Postage
ANALYTICAL CHEMISTRY (formerly Analytical Edition)	$6.00	$7.50	$0.75	$0.25
CHEMICAL ABSTRACTS				
Volumes 11–44	20.00	25.00	2.40	.80
Volume 45, et seq.	50.80**	63.50	2.40	.80
CHEMICAL AND ENGINEERING NEWS (Volumes 1–24)	2.80	3.50	2.25	.75
CHEMICAL AND ENGINEERING NEWS (Vol. 25, et seq.)	5.60	7.00	2.25	.75
INDUSTRIAL AND ENGINEERING CHEMISTRY	8.80	11.00	2.25	.75
JOURNAL OF THE AMERICAN CHEMICAL SOCIETY (Vol. 32, et seq.)	12.00	15.00	1.50	.50
JOURNAL OF PHYSICAL CHEMISTRY (Vol. 56, et seq.)	10.00	12.50	1.20	.40

(Prior Volumes—Order from Walter Johnson, 125 East 23rd Street, New York 10, N. Y.)

* Each part, when divided.

** The member discount for Volumes 45, et seq. applies only if purchase is for personal use and not for resale.

AMERICAN CHEMICAL SOCIETY

Back Issue Department

1155 Sixteenth St., N.W. • Washington 6, D. C.

MOLECULAR THEORY of GASES and LIQUIDS

By Joseph O. Hirschfelder, Charles F. Curtiss, and R. Byron Bird.

Connects equilibrium and non-equilibrium statistical mechanics . . .

This up-to-date book incorporates the many theoretical, computational, and experimental developments which have been made in the study of properties of gases and liquids during the last decade. It is designed to help you to understand the interrelationships between the various branches of statistical mechanics and thus to gain a better knowledge of the properties of matter.

The subject matter of the book . . .

. . . divides itself into three parts. The first, equilibrium properties, begins with a survey of equilibrium mechanics, which serves as the basis for the theoretical development of the equation of state. Part two, non-equilibrium properties, covers kinetic theory and the theory of transport phenomena. Wherever possible this treatment parallels the discussion given in part one. Intermolecular forces, the final section, deals with the electro-magnetic and quantum mechanical theory of the forces between molecules, atoms, ions, and free radicals.

Among the features . . .

Emphasizes physical processes and high-pressure phenomena.
Discusses both fundamental theory and applications.
Gives complete literature references.

1954. *1219 pages.* *$20.00.*

MAGNETIC COOLING

By C. G. B. Garrett, Bell Telephone Laboratories.

This book charts the progress in experiment and understanding that has occurred in the field of magnetic cooling since 1940. It gives a balanced review of the work done in England, Germany, and the United States, and outlines the problems still to be solved. One of the Harvard Monographs in Applied Science. *1954.* *110 pages.* *$4.50.*

SUPERFLUIDS, Volume II.

By the late Fritz London, formerly of Duke University. Ready in September.
Approx. 214 pages. *Prob. $6.00.*

Send for on-approval copies

JOHN WILEY & SONS, Inc., 440-4th Ave., New York 16, N. Y.